EVALUATION OF MULTILAYER INSULATION PERFORMANCE EQUATIONS AVAILABLE IN THE LITERATURE

LİTERATÜRDEKİ MEVCUT ÇOK KATMANLI YALITIM BATTANİYESİ PERFOMANS DENKLEMLERİNİN DEĞERLENDİRİLMESİ

TOYGAN ER

ASSOC. PROF. DR. ÖZGÜR EKİCİ

Supervisor

Submitted to

Graduate School of Science and Engineering of Hacettepe University

as a Partial Fulfillment to the Requirements

for the Award of the Degree of Master of Science

in Mechanical Engineering

2022

Dedicated to my family

ABSTRACT

EVALUATION OF MULTILAYER INSULATION PERFORMANCE EQUATIONS AVAILABLE IN THE LITERATURE

Toygan ER

Master of Science, Department of Mechanical Engineering
Supervisor: Assoc. Prof. Dr. Özgür EKİCİ
January 2022, 98 pages

MLI blankets are the thermal insulation materials used in cryogenics, spacecraft applications and many other sectors. In literature, there are several equations to predict the thermal performance of MLI blankets. In the content of the thesis, some of heat flux predicting equations in the literature were investigated. The accuracy and the validity of these equations were discussed by using existing in-house experimental results of 8 and 22 layer MLI blankets. In order to utilize these equations, the specifications and the parameters of MLI blankets required for these equations were defined. According to these parameters, iterative and direct numerical computing codes were generated using a commercial software to predict the heat flux results of 8 and 22 layer MLI blankets with respect to different cold boundary temperatures. Obtained heat flux results of these equations were compared with experimental steady state heat flux results to observe the accuracy of these equations. Based on the studies carried out for the thesis, it was concluded that the Layer by Layer MLI Calculation Using a Separated Mode and Doenecke equation is able to predict the heat flux through MLI blankets successfully at the cold boundary temperature of -127°C and -75°C for the MLI blankets with different number of layers. However, Modified Lockheed equation

gives unsatisfactory predictions at the same cold boundary temperatures. Obtained heat flux results of these equations were also compared with each other. Based on observations, it was concluded that the Layer by Layer MLI Calculation Using a Separated Mode and Doenecke equation gives similar results for the same cold boundary temperatures.

Keywords: MLI blanket, thermal insulation, thermal performance, predictive equations, heat flux

ÖZET

LİTERATÜRDEKİ MEVCUT ÇOK KATMANLI YALITIM BATTANİYESİ PERFOMANS DENKLEMLERİNİN DEĞERLENDİRİLMESİ

Toygan ER

Yüksek Lisans, Makine Mühendisliği Bölümü
Tez Danışmanı: Doç. Dr. Özgür EKİCİ
Ocak 2022, 98 sayfa

Çok Katmanlı Yalıtım Battaniyesi (ÇKYB) kriyojenik, uzay aracı uygulamaları ve daha birçok sektörde kullanılan ısı yalıtım malzemeleridir. Literatürde, ÇKYB'lerin ısıl performansını tahmin etmek için birçok denklem bulunmaktadır. Tez kapsamında literatürde yer alan bazı ısı akısı tahmin denklemleri incelenmiştir. Bu denklemlerin doğruluğu ve geçerliliği, deneysel sonuçları belirli olan 8 ve 22 katmanlı ÇKYB'lere ait deneysel sonuçlar kullanılarak tartışılmıştır. Bu denklemleri kullanmak için, bu denklemler için gerekli olan ÇKYB'lerin özellikleri ve parametreleri belirlenmiştir. Bu parametreler doğrultusunda, 8 ve 22 katmanlı ÇKYB'lerin deneysel kararlı durum ısı akısı sonuçlarını tahmin etmek için ticari bir yazılım kullanılarak iteratif ve doğrudan sayısal hesaplama kodları üretildi. Bu denklemlerden elde edilen ısı akısı sonuçları, bu denklemlerin doğruluğunu gözlemlemek için deneysel sonuçlarla karşılaştırılmıştır. Tez için yapılan çalışmalara dayanarak, -127° ve -75°C soğuk sınır sıcaklığına sahip ÇKYB'ler için Ayrılmış Mod Denklemi ile Katman Katman ÇKYB Hesaplaması (Layer by Layer MLI Calculation Using a Separated Mode Equation) ve Doenecke

denkleminin ısı akısı tahmininin başarılı olduğu gözlemlenmiştir. Bununla birlikte, Modified Lockheed denkleminin, aynı soğuk sınır sıcaklıklarında tatmin edici olmayan tahminler verdiği gözlemlenmiştir. Bu denklemlerden elde edilen ısı akısı sonuçları kendi aralarında da karşılaştırılmıştır. Gözlemlere dayalı olarak, Layer by Layer MLI Calculation Using a Separated Mode denkleminin ve Doenecke denkleminin aynı soğuk sınır sıcaklıkları için benzer sonuçlar verdiği sonucuna varılmıştır.

Anahtar Kelimeler: Çok Katmanlı Yalıtım Battaniyesi, ÇKYB, ısı yalıtımı, ısıl performans, tahmin edici denklemler, ısı akısı

ACKNOWLEDGEMENTS

I would like to express my gratitude to my advisor Dr. Özgür Ekici, who helped me throughout all the processes during this study. His contributions and his expertise has provided this study to be much valuable.

I would also like to thank to my colleagues for all their helps during my master studies. Their impressive backgrounds have become very inspirational for my studies and will be.

Finally, I would like to thank to my family, for their patience and support.

TABLE OF CONTENTS

ABSTRACT i

ACKNOWLEDGEMENTS v

TABLE OF CONTENTS vi

LIST OF FIGURES ix

LIST OF TABLES xi

SYMBOLS AND ABBREVIATIONS xiii

1. INTRODUCTION 1

2. LITERATURE REVIEW 3

2.1 Experimental Studies 4
2.2 Numerical Studies 7

3. MULTILAYER INSULATION 11

3.1 Heat Transfer Modes 14
3.1.1 Thermal Radiation 15
3.1.2 Solid Conduction 17
3.1.3 Gaseous Conduction 19
3.2 General Concepts on MLI Blankets 21
3.2.1 Number of Reflectors 21
3.2.2 Layer Density 21
3.2.3 Thickness Measurement 22
3.2.4 Heat Flux Measurement Methods 23

4. EXPERIMENTAL STUDIES 25

4.1 Test System 25
4.2 MLI Samples and Experimental Setup 26
4.3 Experiment 29

5. PREDICTIVE PERFORMANCE OF INVESTIGATED EQUATIONS AND DISCUSSIONS 34

5.1 Layer by Layer MLI Calculation Using a Separated Mode Equation 34

5.1.1 Theory 34

5.1.2 Modeling of an MLI Blanket Found in Literature 38

5.1.3 Comparison of Layer by Layer Method with Experimental Results 41

5.2 Doenecke Equation 47

5.2.1 Theory 47

5.2.2 Comparison of Doenecke's Equation with Experimental Results 50

5.3 Lockheed Equation 57

5.3.1 Theory 57

5.3.2 Comparison of Modified Lockheed Equation with Experimental Results 60

5.4 Comparison of Prediction Models with Each Other's 68

6. CONCLUSIONS 75

7. REFERENCES 77

8. APPENDIX 81

8.1 Appendix 1 – Layer-by-Layer Model 22 Layer MLI Blanket at Cold Boundary Layer at -127°C MATLAB Code 81

8.2 Appendix 2 – Layer-by-Layer Model 8 Layer MLI Blanket at Cold Boundary Layer at -127°C MATLAB Code 83

8.3 Appendix 3 – Layer by Layer Model 22 Layer MLI Blanket at Cold Boundary Layer at -75°C MATLAB Code 85

8.4 Appendix 4 – Layer by Layer Model 8 Layer MLI Blanket at Cold Boundary Layer at -75°C MATLAB Code 87

8.5 Appendix 5 – Doenecke Method 22 Layer MLI Blanket at Cold Boundary Layer at -127°C MATLAB Code 89

8.6 Appendix 6 – Doenecke Method 8 Layer MLI Blanket at Cold Boundary Layer at -127°C MATLAB Code 90

8.7 Appendix 7 – Doenecke Method 22 Layer MLI Blanket at Cold Boundary Layer at -75°C MATLAB Code 91

8.8 Appendix 8 – Doenecke Method 8 Layer MLI Blanket at Cold Boundary Layer at -75°C MATLAB Code 92
8.9 Appendix 9 – Modified Lockheed Model for 22 layer MLI blanket at -127°C MATLAB Code 93
8.10 Appendix 10 – Modified Lockheed Model for 8 layer MLI blanket at -127°C MATLAB Code 94
8.11 Appendix 11 – Modified Lockheed Model for 22 layer MLI blanket at-75°C MATLAB Code 95
8.12 Appendix 12 – Modified Lockheed Model 8 layer MLI blanket at -75°C MATLAB Code 96
9. CURRICULUM VITAE 98

LIST OF FIGURES

Figure 3.1: Type of Cryogenic Insulations [3] 11
Figure 3.2: Effective Thermal Conductivity of Insulations [27] 12
Figure 3.3: Multilayer Insulation [28] 13
Figure 3.4: Components of MLI Blanket [1] 14
Figure 3.5: Reflector Materials [1] 15
Figure 3.6: MLI Theoretical Heat Flow for Various Reflector Layer Emissivity and Number of Layers [29] 16
Figure 3.7: Spacer Materials [1] 17
Figure 3.8: Non-interlayer Contact Spacer [5] 18
Figure 3.9: Dacron Netting [30] 18
Figure 3.10: Effect of Layer Density on Thermal Conductivity [24] 22
Figure 3.11: Electrical Input Method [36] 23
Figure 3.12: Heat Meter Apparatus [37] 24
Figure 4.1: GÖKTÜRK-2 Thermal Vacuum Test Chamber 25
Figure 4.2: Aluminum Block Thermocouple and Heater Instrumentation 27
Figure 4.3: Thermocouple Instrumentation on MLI Blanket Surface 28
Figure 4.4: Thermocouple Layout 28
Figure 4.5: Representational View of MLI Blanket Samples 29
Figure 4.6: Experimental Setup inside TVAC 29
Figure 5.1: Representative Heat transfer Mechanism Through 4 Layer MLI Blanket 35
Figure 5.2 Layer by Layer Method Iteration Process 36
Figure 5.3: Radiative Heat Flux Between Two Surfaces 36
Figure 5.4: Variable Density MLI 38
Figure 5.5: Heat Flux Prediction for Reference MLI by the Written Code 40
Figure 5.6: Temperature Prediction at 164 K and 305 K Warm Boundary Condition 41
Figure 5.7: Experimental and Numerical Results for 8 layer MLI Blanket at -127°C Cold Boundary Temperature 43
Figure 5.8: Experimental and Numerical Results for 22 layer MLI Blanket at -127°C Cold Boundary Temperature 44
Figure 5.9:Experimental and Numerical Results for 8 layer MLI Blanket at -75°C Cold Boundary Temperature 45
Figure 5.10: Experimental and Numerical Results for 22 layer MLI Blanket at -75°C Cold Boundary Temperature 46

Figure 5.11: Experimental and Numerical Results for 8 layer MLI Blanket at -127°C Cold Boundary Temperature 50
Figure 5.12: Heat Transfer Mode Participation Percentages for 8 layer MLI blanket at -127°C..... 51
Figure 5.13: Experimental and Numerical Results for 22 layer MLI Blanket at -127°C Cold Boundary Temperature 52
Figure 5.14: Heat Transfer Mode Participation Percentages for 22 layer MLI blanket at -127°C..... 53
Figure 5.15: Experimental and Numerical Results for 8 layer MLI Blanket at -75°C Cold Boundary Temperature 54
Figure 5.16: Heat Transfer Mode Participation Percentages for 8 layer MLI blanket at -75°C 55
Figure 5.17: Experimental and Numerical Results for 22 layer MLI Blanket at -75°C Cold Boundary Temperature 56
Figure 5.18: Heat Transfer Mode Participation Percentages for 22 layer MLI blanket at -75°C..... 57
Figure 5.19: Experimental and Numerical Results for 8 layer MLI Blanket at -127°C Cold Boundary Temperature 61
Figure 5.20: Heat Transfer Mode Participation Percentages for 8 layer MLI blanket at -127°C..... 62
Figure 5.21: Experimental and Numerical Results for 22 layer MLI Blanket at -127°C Cold Boundary Temperature 63
Figure 5.22: Heat Transfer Mode Participation Percentages for 22 layer MLI Blanket at -127°C..... 64
Figure 5.23:Experimental and Numerical Results for 8 layer MLI Blanket at -75°C Cold Boundary Temperature 65
Figure 5.24: Heat Transfer Mode Participation Percentages for 8 layer MLI blanket at -75°C 66
Figure 5.25: Experimental and Numerical Results for 22 layer MLI Blanket at -75°C Cold Boundary Temperature 67
Figure 5.26: Heat Transfer Mode Participation Percentages for 22 layer MLI blanket at -75°C..... 68
Figure 5.27: Heat Flux Model Curves vs. Experimental Data for 22 Layer MLI Blanket at -127° CBT 69
Figure 5.28: Heat Flux Model Curves vs. Experimental Data for 8 Layer MLI Blanket at -127° CBT . 70
Figure 5.29: Heat Flux Model Curves vs. Experimental Data for 22 Layer MLI Blanket at -75° CBT . 72
Figure 5.30: Heat Flux Model Curves vs. Experimental Data for 8 Layer MLI Blanket at -75° CBT 73

LIST OF TABLES

Table 3-1: Accommodation Factor of Helium and Air [24] 21
Table 4-1: GÖKTÜRK-2 Thermal Vacuum Test Chamber Specifications 26
Table 4-2: Power Inputs at Steady State Cases 30
Table 4-3: Steady State Temperature Data for 8 Layer MLI Blanket 31
Table 4-4: Steady State Temperature Data for 22 Layer MLI Blanket 32
Table 5-1: Gas Conduction Parameters for Air 37
Table 5-2: MLI Blanket Parameters [6] 39
Table 5-3: Layer by Layer Parameters of 8 and 22 Layer MLI Blankets 42
Table 5-4: Predicted and Experimental Heat Flux Values for 8 layer MLI Blanket at -127°C Cold Boundary Temperature 43
Table 5-5: Predicted and Experimental Heat Flux Values for 22 layer MLI Blanket at -127°C Cold Boundary Temperature 44
Table 5-6: Predicted and Experimental Heat Flux Values for 8 layer MLI Blanket at -75°C Cold Boundary Temperature 45
Table 5-7: Predicted and Experimental Heat Flux Values for 22 layer MLI Blanket at -75°C Cold Boundary Temperature 46
Table 5-8: Correction Factor of f_N 48
Table 5-9: Correction Factors for f_p 49
Table 5-10: Doenecke Parameters for MLI Blankets 49
Table 5-11: Predicted and Experimental Heat Flux Values for 8 layer MLI Blanket at -127°C Cold Boundary Temperature 51
Table 5-12: Predicted and Experimental Heat Flux Values for 22 layer MLI Blanket at -127°C Cold Boundary Temperature 53
Table 5-13: Predicted and Experimental Heat Flux Values for 8 layer MLI Blanket at -75°C Cold Boundary Temperature 54
Table 5-14: Predicted and Experimental Heat Flux Values for 22 layer MLI Blanket at -75°C Cold Boundary Temperature 56
Table 5-15 : Effect of Perforation Rate to the Radiative Heat Transfer 59
Table 5-16: Lockheed Equation Parameters for Investigated MLI Blankets 60
Table 5-17: Predicted and Experimental Heat Flux Values for 8 layer MLI Blanket at 61
Table 5-18: Predicted and Experimental Heat Flux Values for 22 layer MLI Blanket at -127°C Cold Boundary Temperature 63
Table 5-19: Predicted and Experimental Heat Flux Values for 8 layer MLI Blanket at 65
Table 5-20: Predicted and Experimental Heat Flux Values for 22 layer MLI Blanket at -75°C Cold Boundary Temperature 67

Table 5-21: Comparison of Heat Flux Results of Investigated Models for 22 Layer MLI Blanket at -127°C 70
Table 5-22: Comparison of Heat Flux Results of Investigated Models for 8 Layer MLI Blanket at -127 71
Table 5-23: Comparison of Heat Flux Results of Investigated Models for 22 Layer MLI Blanket at -75°C 73
Table 5-24: Comparison of Heat Flux Results of Investigated Models for 8 Layer MLI Blanket at -75°C 74

SYMBOLS AND ABBREVIATIONS

Symbols

A	Surface area [m^2]
C_g	Gas conduction empirical constant
C_r	Thermal radiation empirical constant
C_s	Solid conduction empirical constant
C_2	An empirical constant to provide a representative fit for Dacron fiber
$delX$	Actual thickness [m]
f	Relative density of the spacer material
f_N	Correction factor for the number of layers
f_A	Correction factor for the size of the blanket
f_P	Correction factor for the perforation rate
k	Thermal conductivity [$\frac{W}{mK}$]
k_{eff}	Effective conductivity [$\frac{W}{mK}$]
k_s	Solid conductivity of spacer material [$\frac{W}{mK}$]
M	Molecular weight of a gas [amu]
N	Number of layers
N_s	Number of reflector layer
$\bar{N}$	Layer density [Layer/cm]
q	Heat flux [$\frac{W}{m^2}$]
q_{gas}	Gas conduction heat flux [$\frac{W}{m^2}$]
q_{rad}	Radiative heat flux [$\frac{W}{m^2}$]
q_{sol}	Solid heat flux [$\frac{W}{m^2}$]
q_{total}	Total heat flux [$\frac{W}{m^2}$]
P	Pressure [mbar]
R	Gas constant

R_{gas}	Radiative thermal resistance $[\frac{m^2K}{W}]$
R_{sol}	Conductive thermal resistance $[\frac{m^2K}{W}]$
R_{rad}	Radiative thermal resistance $[\frac{m^2K}{W}]$
Q	Heat transfer rate [W]
s	Emissivity of surfaces
T	Temperature [K]
T_i	Temperature of incident gas [K]
T_e	Temperature of emitted molecules [K]
T_w	Wall temperature [K]
t	Thickness [m]
T_h	Warm boundary temperature [K]
T_c	Cold boundary temperature [K]
T_m	Mean temperature [K]
$\propto_1$	Accommodation factor of inner cylinder
$\propto_2$	Accommodation factor of outer cylinder
$\propto$	Overall accommodation coefficient
λ	Mean free length [m]
σ	Stefan-Boltzmann constant $[\frac{W}{m^2K^4}]$
γ	Specific heat ratio
ε	Emissivity
ε_{eff}	Effective emissivity
τ	Optical thickness

Abbreviations

CBT	Cold Boundary Temperature
DAM	Double Aluminized Mylar
DAK	Double Aluminized Kapton
DGK	Double Goldized Kapton
IR	Infrared
MLI	Multilayer Insulation
SN	Silk Net
TVAC	Thermal Vacuum Chamber
VD-MLI	Variable Density Multilayer Insulation

1. INTRODUCTION

Thermal insulation is defined as the reduction of heat exchange between the subject and the other objects in contact and the subject's radiative environment. The amount of heat transfer is proportional to the temperature difference between the objects in contact. Even more, the amount of heat transfer is proportional to the fourth power of temperature difference between the object and its environment. Therefore, thermal insulation becomes even more crucial for the applications where extreme temperature differences must be protected.

Cryogenics is defined as the behavior of materials below the threshold of -150°C. Cryogenic liquids are used in various industries from medical applications to space applications. Also, space itself is another environment where there exist temperature extremes. The temperature in deep space is below 4 K. Moreover, there are principal forms of environmental heating on orbit which are direct sunlight, sunlight reflected from Earth (albedo), and infrared (IR) energy emitted from Earth. While these heating elements causes temperature rise of any material in space, the objects lose heat due to deep space temperature. The purpose of thermal design of satellites is to maintain the temperature of each hardware within its acceptable limits in space environment where temperature varies from -250°C to +300 °C [1].

In order to store and handle cryogenic fluids and protect the spacecrafts from temperature extremes of space, efficient insulation techniques are required. One of those techniques to lower the heat leak is Multilayer Insulation (MLI) concept. MLI is a passive thermal control element to prevent excessive heat gain and heat loss of objects. MLI blankets consist of alternating reflector layers to minimize radiative heat transfer and a separator material with low conductivity to minimize the thermal contact between reflector layers. This concept is one of the most efficient thermal insulation which is used in vacuum environment such as space where there is no heat transfer due to convection.

In order to evaluate the insulation effectiveness of MLI blankets, there are several methods to experimentally observe the performance of MLI blankets. Also, there are plenty of thermal performance prediction methods which are used to predict the heat leak through MLI blankets by using some specifications of blankets as parameters. In order to meet the thermal design criteria of spacecrafts, accurate thermal performance prediction is necessary.

In this study, the aim is to evaluate the thermal performance of MLI blankets with the existing prediction methods. For this reason, a brief explanation was given for the cryogenic insulation and MLI blanket concepts. Heat transfer mechanism through MLI blankets were explained and discussed. Then, a comprehensive research was carried out in order to evaluate heat transfer prediction equations used in this thesis. In the literature review section, major of experimental research related to this study were discussed. Also, several numerical research was investigated to discuss the use and validity of prediction equations. Thereafter, three different prediction equations were utilized to predict the heat transfer rate of 8 and 22 layers MLI blankets which are experimentally investigated and discussed in chapter 4. To be able to use these prediction equations, the specifications and the parameters of MLI blankets required for these equations were defined. According to these parameters, iterative and direct numerical computing codes were generated using a commercial software to predict the experimental steady state heat flux results. Validity and accuracy of these methods were compared against experimental results and against each other in chapter 5. Finally, concluding remarks and future work were given at the end of this study.

2. LITERATURE REVIEW

Thermal performance of MLI blankets were investigated by many researchers in many studies both experimentally and numerically especially as MLI method became a highly studied topic after 60's. These studies consider mostly the following assumptions for heat transfer mechanisms through MLI [2] since the heat transfer modes of MLI blankets have complex relationship with each other;

i. Optically thick layers ($\tau << 1$)

   A material is accepted to be optically thick if the photon incident on material cannot pass through the material without absorption. For optically thick reflector materials, the radiosity of the boundary surfaces can be neglected, therefore, thermal radiation depends on the optical properties of the medium between the boundary surfaces [3]. Research indicate that vapor deposited aluminized layers exhibit transmissivity. Moreover, at lower temperatures, long wavelength radiation can penetrate the layers through quantum tunneling effect [2].

ii. One dimensional heat transfer

   Thermal resistance through MLI blankets is much higher than the lateral thermal resistance of the blankets. Temperature differences at the edge of blankets and center of blanket causes a lateral heat transfer [4]. Neglecting this effect yields simpler calculations for MLI blankets.

iii. Isothermal reflector layers

   As discussed above, isothermal layer assumption provides neglection of a lateral heat transfer contributor to simplify the calculations.

iv. Negligible gas conduction

   Amount of gas conduction varies with changing interstitial pressure in MLI blankets. However around $<10^{-5}$ mbar, the gas conduction becomes a minor contributor comparing radiation and solid conduction.

v. Separable heat transfer modes

   Solid conduction and thermal radiation become independent from each other by the assumption of optically thin separator material

vi. Steady state

vii. Diffuse radiation

viii. Thin film assumption to neglect the temperature difference between inner and outer side of reflector layers

ix. No seams, tapes or etc. to contribute heat transfer

As expressed in [5], seam, tape and Velcro applications alters the performance of MLI blankets. However, in order to simplify the calculations, these applications are neglected.

Numerical investigations were based on numerical studies of heat transfer modes and empirical relationships obtained by experimental studies. Obtained equations can predict the rate of heat transfer through an MLI with a limited precision. Because of the combined heat transfer mechanism through MLI and its structural complexity, the thermal performance of MLI is not straightforward and requires a careful evaluation. So beside numerical investigations, there are plenty of experimental studies carried out using different MLI blanket configurations.

2.1 Experimental Studies

In Hedayat et. al.'s [6] work, a 45-layer variable density MLI have been wrapped around a cylindrical tank and the thermal performance characteristics of the MLI have been investigated and compared with constructed Modified Lockheed Model and Layer by Layer method. The test was conducted at a cold boundary temperature of 20 K. Heat flux through MLI is measured where warm boundary temperatures are 164 K, 235 K and 305 K. Heat flux through MLI blanket predicted with the layer-by-layer model and modified Lockheed equation are within 5 and 8 percent of the measured data, respectively where warm boundary temperature is 305K. However, at the warm boundary temperature of 164 K, the predictions with were obtained by Modified Lockheed equation and layer-by-layer equation are 30 and 34 percent below the measured heat flux values respectively. Also, heat leak predictions with respect to warm boundary temperature values have been given for 30, 60 and 75-layer variable density MLI's.

Moeini et.al [7] experimentally investigated performance of 20 layer MLI in a thermal vacuum test chamber. In this experiment, temperature dependent effective emissivity of MLI evaluated for 3 different boundary conditions. Also,

validity of Cunnington-Tien correlation is assessed to be able to predict the thermal performance of this MLI. The author defined that, depending on the power inputs for the heaters used in the experiment, the error between test results and Cunnington-Tien correlation was between 4% and 21%. The author also stated that the correlation became accurate where heat flux through the MLI blanket was lower.

Krishnaprakas [8] compared 4 different empirical model with experimental data for various MLI blanket configurations. In this work, conductance model, effective emittance model, conduction-radiation model and Cunnington-Tien model were constructed and the thermal performance of 10 different MLI blankets were compared with these models. It has been found that the Cunnington and Tien model estimates heat flux sufficiently accurate for spacecraft MLI design purposes.

Spradley et al. conducted experiments for two sizes of tank calorimeters which are 15 L and 225 L. Various MLI systems were investigated with the cold boundary temperature of 4.2 K and warm boundary temperature of 30 K to 130 K at 15 L calorimeter. Heat rate of MLI systems were, investigated which are consisting of 9 layers with double aluminized Mylar (DAM) and double goldized Mylar (DGM) radiation shields and for silk net (SN) and dacron net spacer materials. Experimental observations on the 255 L calorimeter were carries out by only using 37-layer MLI blanket consisting of DAM and SN. Testing was conducted with warm boundary temperature from 40 K to 100 K. Obtained data were compared with an existing data which was for an MLI blanket consisting of DAM shields separated by 2-SN layers with layer densities in between 18 to 50 layers/cm. The comparisons showed DAM/3-SN MLI blanket performed better than predictions obtained by the Lockheed equation. The DAM/5-SN and the DAM/3-Dacron MLI blankets performed two to three times worse than predicted heat flux values [9].

Thermal performance of four different multilayer insulations have been evaluated using double guarded flat-plate calorimeter where cold boundary temperature was hold at 320°F and at vacuum pressure less than 10^{-6} torr. Specimen MLI's

consist of 10 layers with double aluminized Kapton (DAK) / Nomex HT-287, Double Goldized Kapton (DGK) / Nomex HT-287, DGK/Nomex HT-96 and DGK / Dacron B4A. Thermal performance of these MLI were investigated for different compressive pressures between 10^{-4} psi and 10^{-1} psi. The thermal conductivity results were obtained as a function of compressive pressure. The results showed that the MLI composite with Dacron B4A separator provides lower conductivity values. It is also shown that the thermal conductivity of Nomex HT-96 is significantly higher than Dacron B4A. Goldized reflector has slightly lower conductivity than aluminized reflector when used with Nomex HT-287 separator. The thermal conductivity increases with the increasing chamber pressure [10].

Thermal performance of 3 different MLI configuration with silk net were obtained by using a boil-off calorimeter at cold boundary temperature of 78 K and warm boundary temperatures of 293 K, 305 K and 325 K. The experimental data were obtained at high vacuum level (10^{-6} torr) and low vacuum level (10^{-3} torr). Test specimen configurations were consisting of one 20-layer DAM separated by two silk net layers, 20-layer DAM separated by one layer of silk net and 10-layer DAM separated by one layer of silk net. Obtained data from experiments were compared with the predicted heat fluxes by Lockheed Martin Flat Plate equation for the silk net configuration. The differences between predictions and experimental data were between 15% and 40%. Obtained data from this experiment were also compared with a reference data in which the same configurations were experimentally investigated for Dacron spacer material. The comparison showed that heat flux performance of silk net performs 2 times better than Dacron netting even considering the small differences due to layer density and thicknesses [11].

Perforation effect on heat transfer have been researched by Deng et. al. [12]. The author experimentally investigated the effects of different perforation rates at different vacuum pressure levels using test platform. Heat flux values of perforated MLI's for different perforation rates were obtained. By analyzing the heat flux values of perforated MLI blankets, the optimized perforation rate was found to be 0.39% for a 50 layer MLI blanket for a layer density of 25 layer/cm.

Four different MLI blankets consisting of different materials was tested at warm and cold boundary temperatures at 293 K and 77 K respectively. The experimental results were compared with Modified Lockheed Method. The heat flux differences between predicted values and experimental data for layer densities of 20, 25 and 40 layers/cm are within 23%, 20% and 39% for number of layers from 40 to 70, respectively [13].

Thermal performance of 5 different MLI blankets were investigated experimentally by testing on cryostat calorimeter. The effect of perforations and seams on thermal performances were investigated for 10-layer MLI blanket. Also, heat flux characteristics of 5-, 10- and 20-layer blankets were investigated. The experimental results were also compared with layer-by-layer model. The experimental results showed that the low percent open area (0.01%) perforations contributed to approximately 5% worse thermal performance which was slightly greater than the uncertainty of the calorimeter where the experiment took place. Also, the seam has been shown to have no apparent effect on thermal degradation to the test blankets. The experimental and model results were shown to be different between 1.3% and 34% [14].

Uncertainty of MLI blankets were studied experimentally by testing 5 identical blanket coupons with 25 layers and 5 identical blanket coupons with 10 layers. The aim of the experiment was to investigate the repeatability of manufacturing of same blankets and to investigate the installation uncertainties. The experimental results showed that the repeatability of 25-layer MLI blankets was between ±8.4% whereas the repeatability of installation of the same blanket was shown to be ±8.0%. Also, the 10-layer MLI blankets performed a repeatability between ±15% and ±25% [15].

2.2 Numerical Studies

In 1970, Cunnington and Tien [3] build a mathematical expression in which the heat transfer through MLI is introduced as a combination of solid conduction and radiation. In this study, gas conduction due to residual gas in MLI assumed to be negligible when the operating pressure is below 10^{-6} torr. Also, reflector layers are assumed to have a negligible thermal resistance since the thermal conductivity of reflector layers are much higher comparing to separators.. By

utilizing this equation, thermal performance of MLI can be predicted for three types of insulation systems which are as follows:

- Mylar reflective shields coated on both surfaces with aluminum. The reflective shields are crinkled and separated by a 0.6-mil thick borosilicate glass fiber paper-type material.
- Smooth Kapton reflective shields coated on both surfaces with aluminum with the 0.6-mil thick spacer material.
- Smooth Mylar coated on both surfaces with aluminum and separated by an open silk net material.

By utilizing this equation, thermal performance of MLI can be predicted in wide range of temperature within a 20% accuracy. In this work, radiation and conduction terms are considered separable as shown by Wang and Tien [16]. The final heat transfer equation presented in this work expresses the heat flux through MLI in terms of shield emissivity, compression pressure, shield and spacer thickness, and number of interfaces. Shield emissivity and spacer conductivity are expressed as temperature dependent by some coefficients.

In another study of Cunnington and Tien [17], the effect of perforation on reflective shields have been investigated and assessed. The aim of this paper is to analyze the heat exchange of MLI with perforated shield with different fractional open areas. This works shows that the perforation significantly degrades the performance of MLI system proportional to fractional open area of reflector layers which can be result in up to 1.31 time more heat flux in radiative exchange.

Another important study has been published by Keller and Cunnington [18]. In this work, various reflectors and spacer materials have been investigated and mathematical models were developed using experimental heat transfer data. Heat transfer modes of solid conduction, radiation and gaseous conduction have been investigated and quantified for different cases. Using this mathematical method, heat flux predictions can be made for different boundary temperatures, number of layers, layer densities, and interstitial gas pressures. Also, different

perforation rates have been investigated. Experimental heat flux values were correlated with the prediction results within ±8 percent.

Hedayat et. al. [6] modified the existing Lockheed equation and used conductivity function provided by McIntosh instead of the existing functions provided for silk net and tissuglas materials. So that, Lockheed equation is modified for MLI blankets where dacron netting is used as separator material. New equation was used in order to predict the heat flux through an MLI blanket used for a cryogenic tank. Modified Lockheed Equation were found to have an accuracy of 5% to 34% with respect to experimental measurements.

Although the Lockheed model can predict the heat fluxes with an acceptable accuracy and becomes an industry standard, yet it doesn't lend itself to changes in separator materials, construction differences such as the edge sewing or heat transfer differences at low temperatures. Thus, Ross reformulated Lockheed equation to allow these considerations in heat transfer predictions through MLI blankets [19].

Doenecke [20] came up with a new equation which determines the effective emissivity (ϵ_{eff}) of MLI. In this study, data from many experimental studies were used to develop a new equation for prediction of thermal performance of MLI blankets. Obtained equation can be used by using determined correction factors by the author for MLI blankets with different number of layers, reflector perforation rates and blanket areas.

McIntosh [21] developed a model called Layer by Layer MLI Calculation Using a Separated Mode Equation which predicts the heat transfer through the MLI operating between 4K and 80K. This model considers all heat transfer modes as separated. In this model, thermal resistance between each layer can be calculated and thus, temperature of each layer can be found. So, using a mathematical software, temperature distribution, contribution of heat transfer modes and total heat transfer through MLI can be obtained.

Lixing Gu [22] used McIntosh's layer by layer method in order to evaluate the thermal performance of MLI for liquid hydrogen storage tanks for a wider temperature range which is between 20K and 300K. In addition to McIntosh's equation, Gu introduced temperature dependent emissivity and gas conductance instead of using constant values as in McIntosh's work for these temperature ranges.

Based on energy balance, a model was created to calculate the temperature field of perforated MLI blankets by Li [23]. Based on created model the effect of the MLI blanket parameters such as layer density, reflector emissivity and perforation rate on the thermal performance of MLI blankets has been investigated. Also, the model was validated by experimental data which was obtained 77K and 300K boundary temperatures. The temperature differences between the created model and experimental values were in 7%. Also, the effective thermal conductivity of experimental and model data was found to be at most 36%.

Literature review showed that there are many numerical and experimental studies to understand the characteristics of MLI blankets. Experimental studies were carried out to understand the effect of different parameters of MLI blankets such as number of layers, separator material, boundary temperatures etc. On the other hand, the numerical equations were created using physic-based heat transfer equations or empirical approaches to predict the behavior of MLI blankets. However, these equations are able to predict the heat flux through MLI blankets with limited accuracies. Also, accuracy of these models shows differences depending on the specification of MLI blankets. Therefore, validation of these equations under different conditions are essential. For this aim, three different equations were selected for the prediction of thermal performance of two different MLI blankets, whose heat flux characteristics were already determined experimentally. The heat flux predictions of these models were evaluated and validated using the experimental data.

3. MULTILAYER INSULATION

Cryogenic insulation is crucial for the areas of rocketry, space exploration programs, superconducting technology and liquid helium technology and many other areas where cryogenic matters are the key components. Cryogenic insulations are divided into two category which are non-evacuated and evacuated insulations. Non-evacuated insulations are porous materials such as foams, powders or fibers. Evacuated insulations are divided into three categories which are simple vacuum, evacuated porous insulation and multilayer insulation. Representative illustrations of these insulations are shown in Figure 3.1.

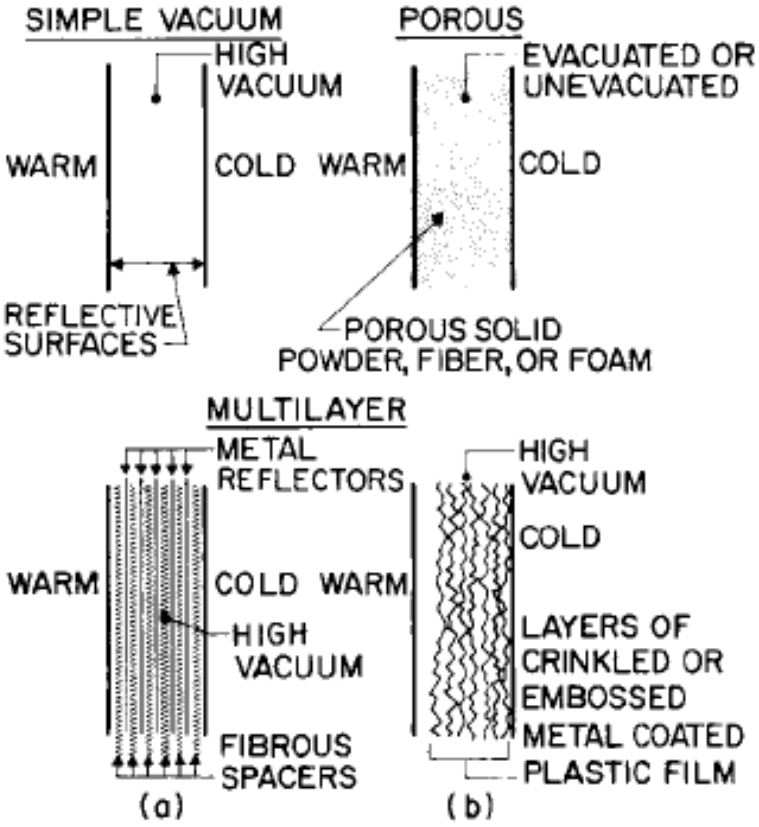

Figure 3.1: Type of Cryogenic Insulations [3]

James Dewar was the first to use vacuum insulation by using double-walled glass vessel with a high vacuum in between the walls. The importance of vacuum insulation is that the vacuum can almost eliminate two heat transfer modes which are gaseous conduction and convection [24]. However, a perfect packing of multiple reflector shields without contact was not possible. Peterson developed Multilayer Insulation (MLI) concept in 1958 [25]. His method of using glass wool sheets between aluminum foil shields, which reduced the evaporation of cryogenics in vessel by the factor of 20, raised a great interest for this application

[26]. Therefore, many research were carried out on MLI concept. Especially as the space exploration has gained pace in 1960's. The thermal conductivity of MLI concept compared to other insulation types are shown in Figure 3.2.

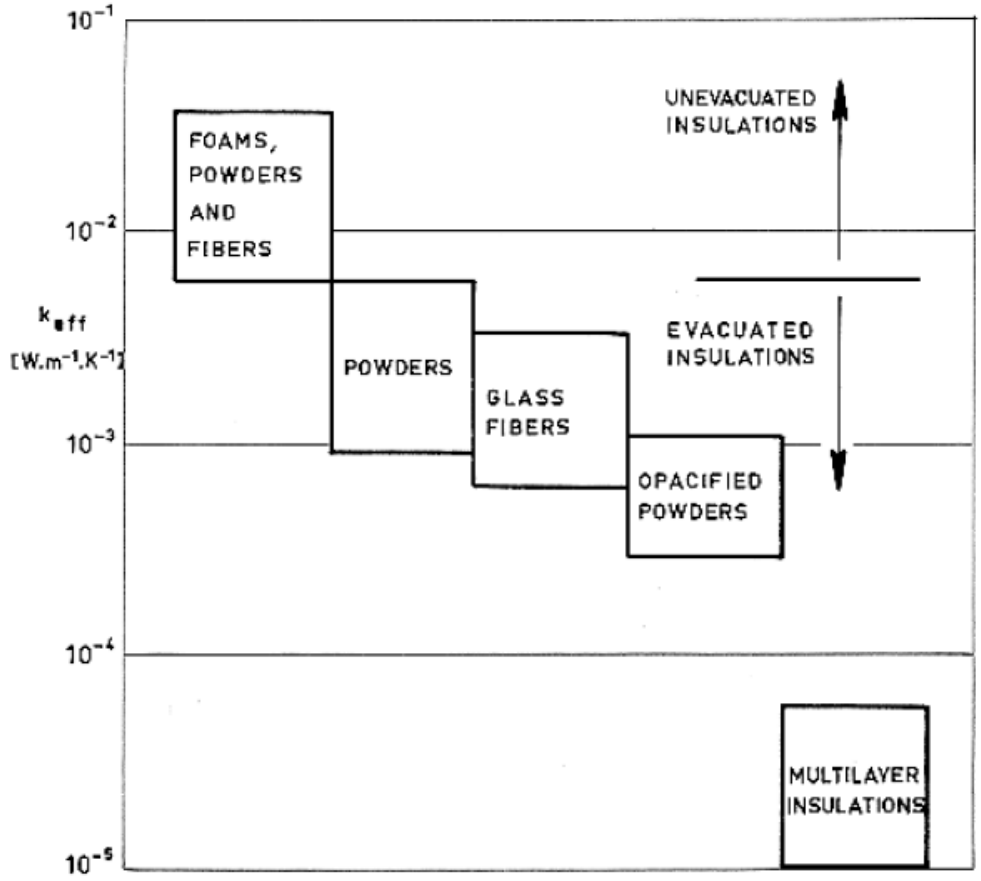

Figure 3.2: Effective Thermal Conductivity of Insulations [27]

MLI blankets are the passive thermal control elements used in spacecraft applications and cryogenic pipelines. MLI blankets prevent excessive cooling and excessive heat gain of spacecraft components by creating a radiative barrier between its external and internal surfaces. MLI is still accepted to be the most effective thermal insulation applied on spacecrafts even it was invented in the beginnings of 1900's. MLI is employed in both high-temperature applications and cryogenic insulation conditions. MLI blankets have extensive applications in storage of cryogenics, transfer at cryogenic lines, and thermal protection processes. The insulation material used in MLI, their arrangements, and thus heat transfer characteristics shows differences according to the requirements of application area.

MLI blankets consist of multiple reflector layers and netting spacers. Reflector layers reflect a large percentage of the radiation received from the neighboring warmer reflector layer. Depending on the using area, reflector layers can be perforated or non-perforated. Perforation is needed where outgas of the MLI blanket is desired. Therefore, perforation also decreases the gas conduction heat transfer through the MLI. Netting spacers are used in order to avoid direct contact between shields and so that thermal shorts are eliminated as much as possible. Low-conductivity spacer materials are used in order to minimize the solid conduction through the spacer material. A representative MLI blanket sample is shown in Figure 3.3.

Figure 3.3: Multilayer Insulation [28]

Heat transfer of MLI is a combination of radiation, solid conduction and at high pressures, gaseous conduction. Higher thermal insulation efficiency is obtained as these heat transfer forms are minimized. Radiative heat transfer can be minimized by simply adding more reflective layers. Solid conduction due to spacers can be minimized lowering the density of spacers between reflective surfaces as much as possible. Gaseous conduction can be minimized by allowing

the insulation to vent to space by perforation holes on reflector surfaces. In order to keep the spacers and reflectors together, fixing elements like seams and tapes are used. So that, depending on the manufacturing method, the structure and composition of MLI blankets may show differences. Components of MLI blankets are shown in Figure 3.4.

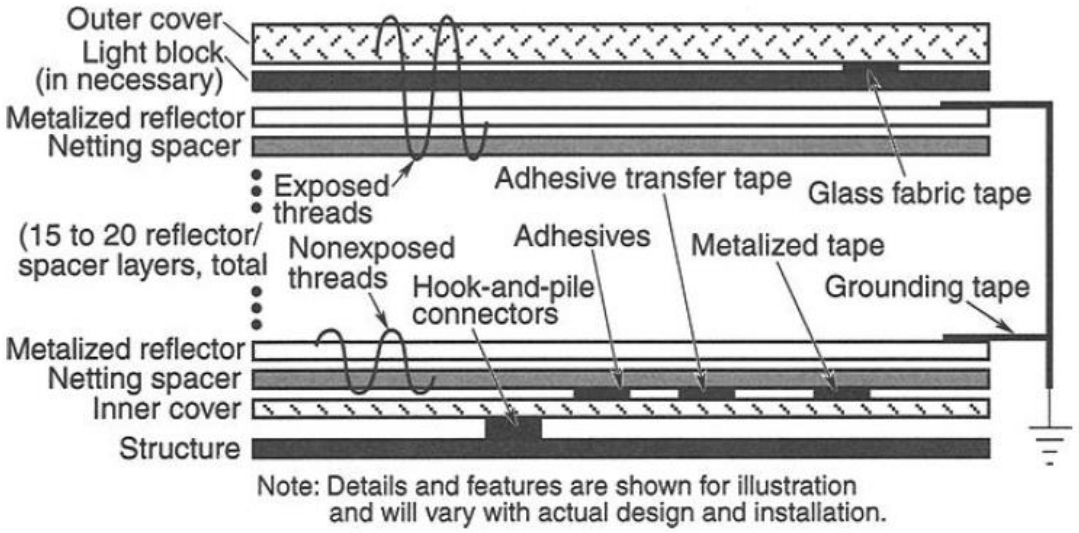

Figure 3.4: Components of MLI Blanket [1]

Some of the factors influencing the MLI performance are given below:

i. Number of reflector layers
ii. Size of blanket
iii. Foldings
iv. Spacer type
v. Fixing methods such as sewing, taping etc.
vi. Blanket compression
vii. Reflector perforation

3.1 Heat Transfer Modes

As mentioned earlier in the chapter, the heat transfer through MLI consists of solid conduction, radiation, and gaseous conduction. The aim of this section is to give a brief explanation to these heat transfer modes to understand the physics of the heat transfer through MLI blankets.

3.1.1 Thermal Radiation

Radiative heat transfer occurs due to electromagnetic waves emitted and absorbed by the materials. Whenever there is a temperature difference between two materials there exists radiative heat transfer due to this phenomenon. The main purpose of MLI is to reduce the heat transfer due to thermal radiation. For example, in Earth's orbit, spacecrafts were exposed to very high solar radiations due to sun whose heat flux is 1357 W/m^2. On the other hand, the spacecrafts lose heat due to deep space temperature which is around 4K. In order to minimize the heat transfer due to radiation under these extremes, MLI blankets consisting of low emissivity reflector layers are employed. Specifications of some reflector materials are given in Figure 3.5.

Material	Aluminized Kapton	Goldized Kapton	Aluminized Mylar	Polyester	Teflon
Description	Single or double aluminized	Single or double goldized	Double aluminized	Single or double aluminized	Single or double aluminized
Vendors	Sheldahl, Dunmore	Sheldahl	Sheldahl, Dunmore	Sheldahl, Dunmore	Sheldahl, Dunmore
Thickness, mm (mil)	0.0076–0.127 (0.3–5.0)	0.0076–0.127 (0.3–5.0)	0.0051–0.127 (0.2–5)	0.00006–0.0013 (0.25–5)	0.00003–0.0013 (0.1–5)
metal, Å	1000	750	1000	300	300
Weight, gm/cm^2				—	—
0.0051 mm (0.2 mil)			0.0007		
0.0064 mm (0.25 mil)			0.00093		
0.0076 mm (0.3 mil)	0.0011	0.0011			
0.013 mm (0.5 mil)	0.0019	0.0019	0.0017		
0.025 mm (1.0 mil)	0.0036	0.0036	0.0033		
0.051 mm (2.0 mil)	0.071	0.071	0.0066		
0.076 mm (3.0 mil)	0.011	0.011	0.0104		
0.127 mm (5.0 mil)	0.019	0.019	0.0175		
Temperature, °C					
Continuous, max/min	–250/+288	–250/+288	–250/+93[a]	260	260
Intermittent, max/min	–250/+400	–250/+400	–250/+150		
Absorptance, α (max/typ)	0.14; 0.12	0.30; 0.28	0.14; 0.12	< 0.14	< 0.14
IR emittance, ε	0.05; 0.03[b]	0.04; 0.02[b]	0.05; 0.03[c]	< 0.04	< 0.04

Figure 3.5: Reflector Materials [1]

Considering the heat transfer rate between two infinite parallel gray planes, the heat transfer equation between these two planes is given as in Eq. (1)

$$Q = \sigma A(T_2^4 - T_1^4)\frac{1}{\frac{1}{\varepsilon_1} + \frac{1}{\varepsilon_2} - 1} \tag{1}$$

MLI blankets consist of multiple reflector layers. The number of reflector layers depends on the requirements for the purpose of use. The heat transfer through

MLI blankets is inversely proportional to the number of reflector layers. For N numbers of reflector layers and two boundary shields, the heat transfer equation becomes as in Eq. (2).

$$Q = \sigma A(T_2^4 - T_1^4)\frac{1}{(N+1)(\frac{1}{\varepsilon_1}+\frac{1}{\varepsilon_2}-1)} \quad (2)$$

For an ideal case, where these reflector layers assumed to be floating on each other without touching, then the theoretical effective conductivity for MLI blankets can be calculated by using Eq. (3).

$$k_{eff} = \frac{(Q/A)t}{T_h - T_c} = \frac{\sigma t}{(N+1)(\frac{1}{\varepsilon_1}+\frac{1}{\varepsilon_2}-1)}\frac{(T_h^4 - T_c^4)}{T_h - T_c} \quad (3)$$

The ideal heat transfer rate depending on the number of reflector layers and reflector layer emissivity is shown in Figure 3.6.

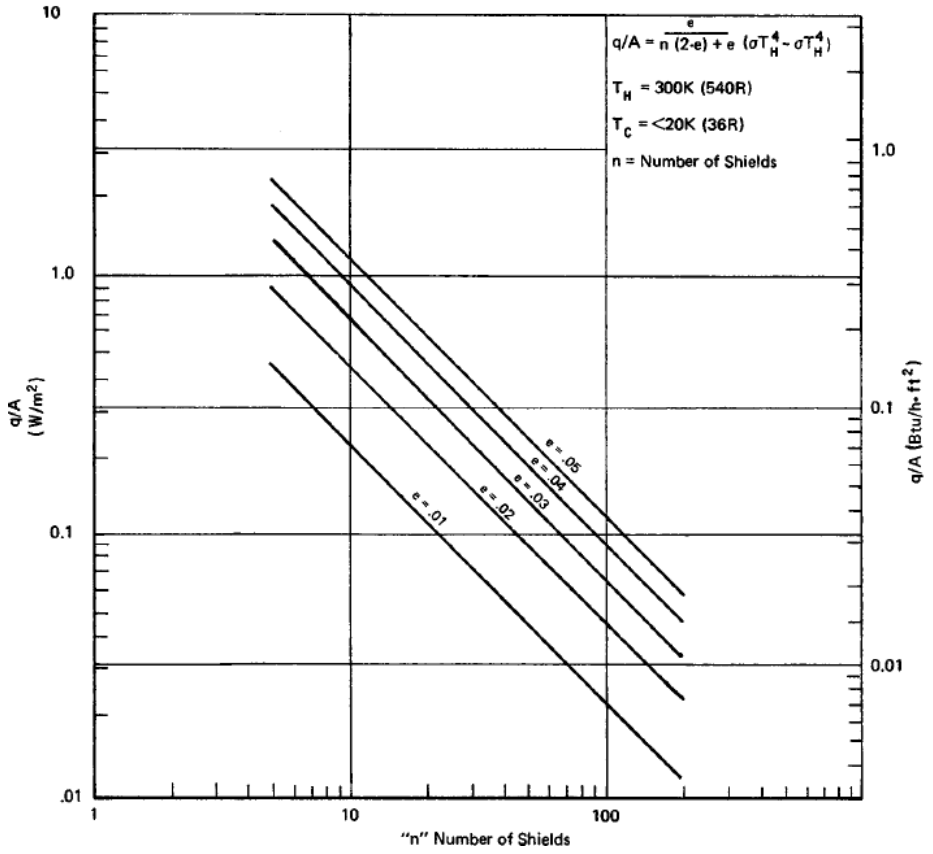

Figure 3.6: MLI Theoretical Heat Flow for Various Reflector Layer Emissivity and Number of Layers [29]

However, such heat leak rates are not attainable since it is not possible to create a floating reflector layer configuration. In order to use many reflector layers in MLI blankets, reflector layers are separated using different methods.

3.1.2 Solid Conduction

In between reflector layers, fiber or powder separator materials are introduced with the aim of:

i. Avoiding radiation tunneling
ii. Decreasing the contact area between metallized shields [27].

Solid conduction through solid components of the insulation often constitutes the dominant mode of heat transfer in MLI blankets [3]. Separator materials are selected from low thermal conductivity materials to decrease the solid conductivity between parallel adjacent reflectors. Name of some common spacer materials and thermal properties of these materials are given in Figure 3.7.

Material	Dacron Netting	Nomex Netting
Description	100% polyester fabric mesh[a]	100% Nomex aramid fabric mesh[b]
Vendors	Apex Mills	Stern & Stern Textiles, J.P. Stevens
Thickness, mm (in.)	0.16 ± 0.01 (0.0065 in. ± 0.0005)	0.16 ± 0.01 (0.0065 in. ± 0.0005)
Construction		
Meshes/cm^2	7.8 ± 1.2	7.9 ± 1.2
Denier filaments	40	40
Weight, gm/m^2	6.3 ± 0.85	6.3 ± 0.85
Burst strength, kg/cm	5.625	5.625
Temperature range, °C	–70 + 120 continuous	–70 + 120 continuous
	–70 + 177 intermittent	–70 + 177 intermittent

Figure 3.7: Spacer Materials [1]

Conduction heat transfer is governed by the Fourier law. Same heat transfer mechanism can be applied for determination of heat transfer due to solid conduction through MLI blankets. Solid conduction can be reduced by increasing thermal resistances to conductive heat flow, and from the Fourier law, it can be deduced that this can be achieved by:

i. Using low conductivity materials
ii. Increasing the length of heat flow path
iii. Decreasing the cross-sectional area of heat flow path

Considering these, there are many separator types available to use in MLI blankets. Some of these separator types are given in Figure 3.8 and Figure 3.9.

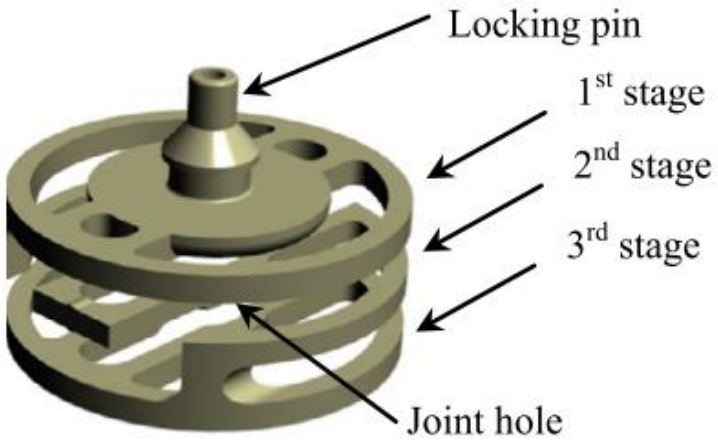

Figure 3.8: Non-interlayer Contact Spacer [5]

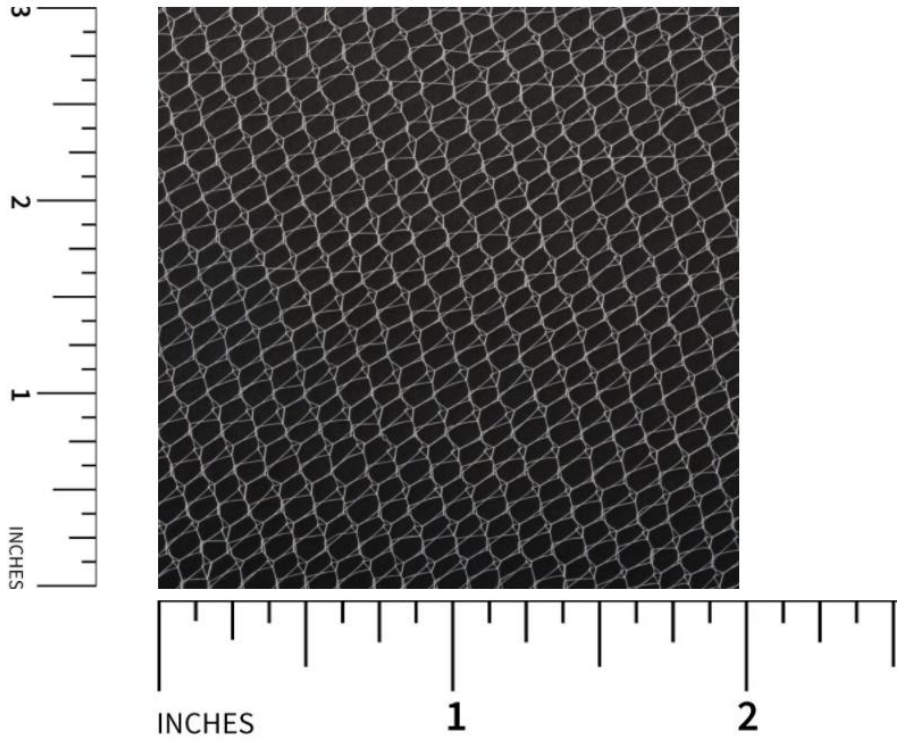

Figure 3.9: Dacron Netting [30]

i. Dacron

Polyethylene terephthalate (PET) materials are hard, stiff, strong, dimensionally stable materials. Their advantageous mechanical and thermal properties make use of them in variety of applications. Fiber form of PET is called as polyester. Polyester materials are used in MLI blankets as spacers in form of powder, sheet, mesh etc. Polyester materials can be referred as their brand names such as Mylar, Melinex Dacron etc.[31].

ii. Nomex

Aromatic polyamide (Aramid) Nomex® fiber is a member of the aramid family of fibers. Fabrics woven of Nomex® fibers are used in applications requiring excellent heat resistance. This fiber is resistant to melting and flowing at high temperatures up to 370°C [32].

iii. Silk Net

Silk net is one of the first separator materials which was used in the early use of MLI blankets. Most experimental campaigns and experimental data were obtained using silk net separator. Therefore, some of MLI performance prediction methods are still based on silk net separators. Although silk net has significantly better thermal performance comparing polyester separators, the use of polyester net became more common since cost of silk net is much higher comparing the polyester materials [11].

iv. Non-interlayer contact spacer

Conventional spacer nettings cover the whole reflector surface in order to separate the alternating reflectors from each other's. This type of spacer is placed intermittently which provides lower heat leaks since contact area is much lower than conventional spacers. The conductive path of this spacer is much higher than conventional nettings which also provides lower heat leaks.

3.1.3 Gaseous Conduction

Under atmospheric pressures, thermal conductivity of gases is independent from the gas pressure. At this pressure levels, gas conduction is described by Fourier's law since flow of the gas is in the continuum region [33]. However, as pressure gets lower, thermal conductivity becomes a pressure dependent property of the gases. At very low pressures mean free length (λ) of gases are so long that gas molecules tend to collide with surrounding surfaces rather than each other. At this pressure range (typically under $<10^{-3}$ mbar), the flow is called as molecular flow. In thermal aspect, free-molecule conduction is the point of interest for vacuum insulations and MLI blankets. At these pressures, each gas molecule transports energy from warm surface to cold surface in MLI blankets without any interruption.

Behavior of gas molecules shows differences depending on their collisions with different surfaces. Accommodation coefficient is used to express the thermal exchange of gas molecules with its surrounding surfaces. Accommodation coefficient depends both on the type of gas molecule and surface. This equation is defined by Eq. (4).

$$\propto = \frac{T_i - T_e}{T_i - T_w} \tag{4}$$

The energy accommodation coefficient is the ratio of the average energy exchanged by a gas in contact with a surface divided by the maximum energy that can be exchanged [34]. Accommodation factor becomes 1 if the temperature of the emitted molecule has the same temperature with the surface after striking at it. Whereas accommodation factor is 0 if the temperature of the emitted molecule does not change its temperature after striking at the surface.

For vacuum insulating systems, heat rate due to gas conduction was investigated by Knudsen. He obtained an equation for coaxial cylinders as in as in Eq. (5) [24].

$$\dot{Q}_{gc} = \left(\frac{\propto_1 \propto_2}{\propto_2 + \left(\frac{A_1}{A_2}\right) x(1 - \propto_2) \propto_1}\right)\left(\frac{\gamma + 1}{\gamma - 1}\right)\left(\frac{R}{8\pi}\right)^{\frac{1}{2}}\left(\frac{P}{\sqrt{T_m M}}\right)(T_2 - T_1) \tag{5}$$

This formulation became useful after Corruccini by rewriting the equation for concentric spheres, coaxial cylinders and parallel plates as in Eq. (6) [35].

$$\dot{Q}_{gc} = \left(\frac{\gamma + 1}{\gamma - 1}\right) \propto \left(\frac{R}{8\pi M T}\right)^{\frac{1}{2}} P(T_2 - T_1) \tag{6}$$

(6) is useful for defining the heat rate due to gas conduction in MLI blankets. For each specific gas, the constants are lumped into a constant and the equation can be simplified as in Eq. (7).

$$\mathrm{Q} = C_1 \propto P(T_2 - T_1) \tag{7}$$

In order to utilize this equation, thermal properties of interstitial gas inside MLI blankets and the accommodation coefficient must be defined. Accommodation coefficient is given in [24] for the gases shown in Table 3-1.

Table 3-1: Accommodation Factor of Helium and Air [24]

Temperature (K)	Helium	Air
300	0.3	0.8 - 0.9
76	0.4	1
20	0.6	-

3.2 General Concepts on MLI Blankets

Heat flux through MLI blankets can be predicted by considering those three modes of heat transfer under some assumptions. Heat flux predictions are made by using the geometrical or material properties of MLI blankets. In the following subsections, some properties of MLI blankets and measurement techniques are described.

3.2.1 Number of Reflectors

In theory, the heat flux through MLI blankets is inversely proportional to the number of reflector layers for the floating reflector shields. Therefore, adding more reflector shields should ideally decrease the heat transfer rate. However, in practical case, since there is separator material between each reflector shield, the weight of upper reflectors and separators compresses the MLI blankets. This situation degrades the thermal performance of MLI blankets as the number of reflectors are increased.

3.2.2 Layer Density

Layer density can be described as the number of layers per unit length. For most of the cases, the parameter of layer density is more important than the number of reflectors since this parameter also considers the effect of compressive effect on MLI blankets due to their weights. The heat flux through MLI blankets decreases as the number of reflector layers are increased up to some point. After that point, the heat flux starts to increase as the compression causes thermal conductivity of MLI blankets to increase. The effect of layer density is shown in Figure 3.10: Effect of Layer Density on Thermal Conductivity [24].

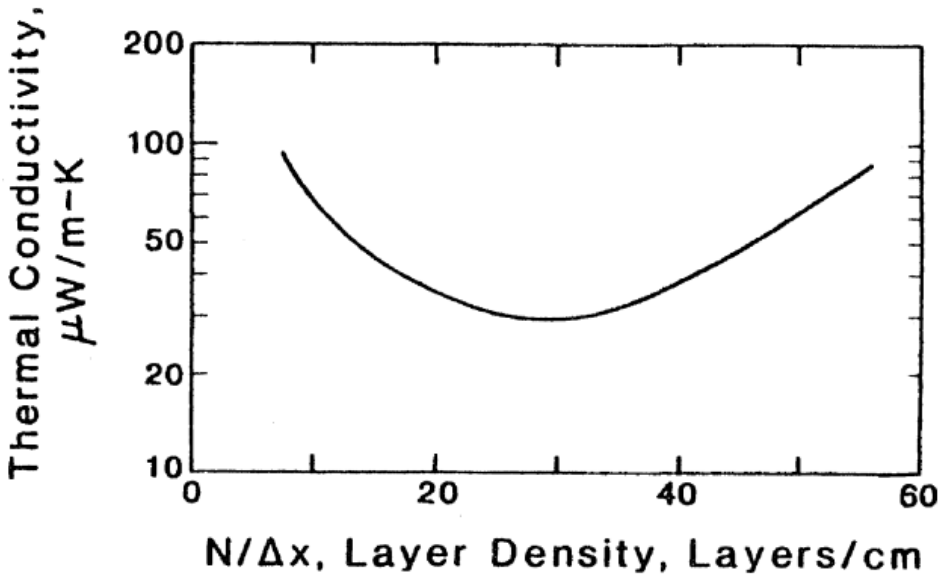

Figure 3.10: Effect of Layer Density on Thermal Conductivity [24]

3.2.3 Thickness Measurement

In order to utilize the heat flux prediction equations for MLI blankets, parameters belong to the blankets such as number of reflectors and layer density are used. Thickness of MLI is an important parameter to understand the thermal conduction of separator materials and to calculate the layer density. Therefore, thickness of MLI blankets is measured by means of different techniques. Thermal performance of MLI blankets is related to the distance of alternating layers to each other. This distance may vary due to manufacturing process, applied compressive pressure during installation and depressurization. In reference [36] two different methods were investigated and compared to each other in order to measure the thicknesses of MLI blankets accurately. First method for measuring thickness is using X-ray measurements. Using this method, 20-layer, 10-layer and 5-layer MLI blanket thicknesses were obtained from different positions. These thickness results were then compared to the second method which is needle probe penetration. A sewing needle was used in order to penetrate the MLI blankets normal to their surfaces. After penetration, the needle was rotated along its rotational axis in order to minimize its local compressive forces on MLI blankets. Then the penetration depth was measured. Needle probe penetration measurements were within +0.51 mm and -1.02 mm for the blankets with the thicknesses of 6.95mm and 20.7mm which were measured by X-ray method.

3.2.4 Heat Flux Measurement Methods

There are 4 types of experimental methods for steady state heat flux measurement through MLI blankets [4]. These are;

i. Boil-off calorimetry: Most experimental studies use boil-off calorimetry for experimental investigations for the heat flux through MLI blankets. In this technique, MLI blanket is applied over the calorimeter which is cooled by a cryogenic liquid. Then heat flux through MLI blanket is calculated using the heat of vaporization and the flow rate of a cryogenic liquid contained at saturation point.

ii. Electrical input method: Warm boundary of the MLI blanket is heated by means of electrical heaters while the cold boundary of the MLI blanket is cooled down using a cryogenic tank. As shown in Figure 3.11, a cryogenic liquid tank is thermally connected to both warm and cold boundary surface of MLI blanket. Also, electrical heaters are provided at the warm boundary of MLI blanket in order to create a temperature difference through blanket boundaries. Then by using applied power and boundary temperatures, effective emissivity value is obtained by using Stefan-Boltzmann law.

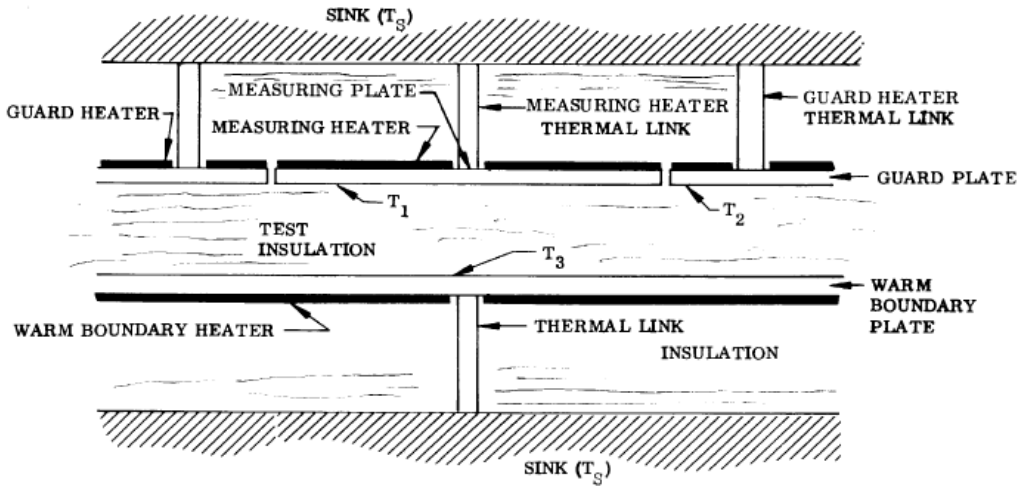

Figure 3.11: Electrical Input Method [36]

iii. Heat meter technique: This method uses constant temperature heat source and heat sinks. Between the heat source and the heat sink, MLI blanket and a heat meter is placed. At steady state, heat flux through both heat meter and MLI blanket is expected to be the same. Since the thermal conductivity of heat meter is a known property, thermal conductivity of MLI blanket is determined by means of the Fourier law. In Figure 3.12, an

apparatus to measure the thermal conductivity of MLI blankets with heat meter technique is shown.

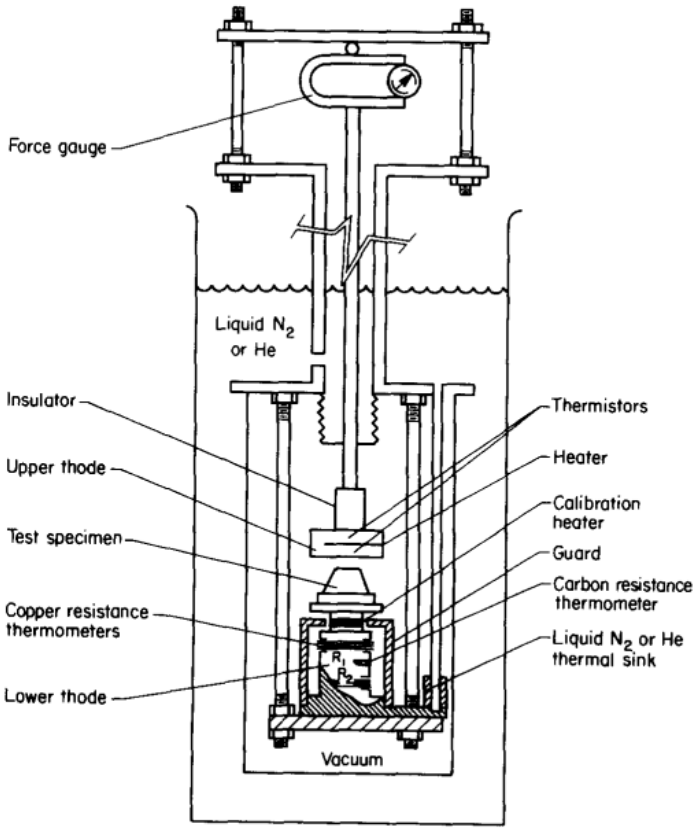

Figure 3.12: Heat Meter Apparatus [37]

iv. Temperature decay measurement: The insulation to be tested is wrapped around tube with wall thickness 't' and the wrapped tube is placed inside a vacuum chamber, supported by low conducting supports. A heater a on one side of the insulated tube is used to create heat flow along the tube. A steady state temperature profile along the insulated tube can be characterized by a decay length 'L', which results from the balance between longitudinal heat conduction along the tube wall and the transverse heat conduction through MLI.

4. EXPERIMENTAL STUDIES

4.1 Test System

The experimental studies were carried out using electrical input method which was introduced in the previous sections. Experimental tests were conducted at Turkish Aerospace Inc. by the thermal test team at GÖKTÜRK-2 Thermal Vacuum Chamber (TVAC) in between 9-12 March 2020. The TVAC is shown in Figure 4.1. The specification of the test system is shown in Table 4-1.

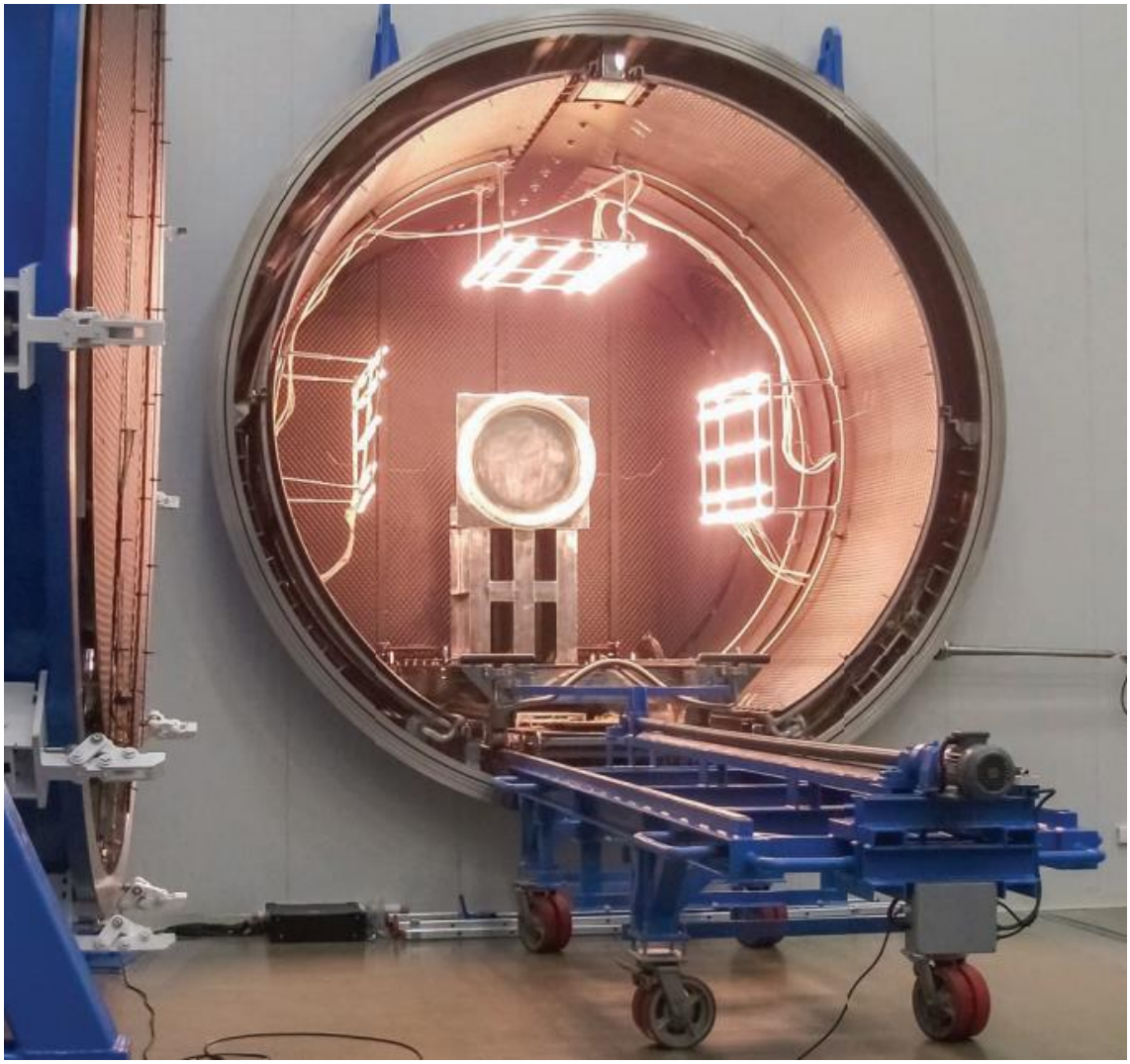

Figure 4.1: GÖKTÜRK-2 Thermal Vacuum Test Chamber

Table 4-1: GÖKTÜRK-2 Thermal Vacuum Test Chamber Specifications

Chamber Volume	4m Ø x 4.1m length
Usable Volume	2.2m Ø x 2.8m length
Vacuum Level	$<10^{-5}$ mbar
Thermal Shrouds Temperatures	-165°C - +110°C (±5°C)
Temperature Measurement	256 T-Type Thermocouples
Power Supply	50 Pieces DC (0-40V & 0-3A)
Vacuum System	Primary Vacuum System • 2 Screw Pump • 2 Root Pump Secondary Vacuum system • 1 Turbomolecular Pump • 2 Cryogenic Pump
Auxiliary Systems	Residual Gas Analyzer (RGA) Infrared Lamp Heating

4.2 MLI Samples and Experimental Setup

There are 2 MLI samples prepared for the experimental studies. MLI blanket samples consist of 8 and 22 layers of double-sided aluminum coated PET reflector which has a perforation rate of 0.84% open area and Dacron B4A netting. Prepared MLI blankets were wrapped around an aluminum block with dimension of 0.52m x 0.52m x 0.01m. On each aluminum block, there are 4 heaters instrumented on the surface to represent the temperature of the warm boundary temperatures inside the MLI blanket. The warm boundary is where the one side of the MLI blanket is relatively warmer (i.e. inner side of MLI blanket) than the other surface. The outer surfaces of MLI blankets are open to the shrouds of the TVAC whose temperatures can be controlled. The outer surface of the MLI blankets represent the cold boundary surface. The cold boundary is where the one side of the MLI blanket is relatively colder (i.e. outer side of MLI blanket) than the other surface.

In order to measure the temperatures of the aluminum block and MLI blankets, T-type thermocouples were instrumented on 8 and 22 layer MLI blanket samples. At each sample, 21 thermocouples were used to measure the temperatures. 7 thermocouples were used on the aluminum block to measure the warm boundary temperatures. 14 thermocouples were used to measure the cold boundary temperatures on MLI blankets. The thermocouples on the warm and cold boundaries were placed parallel to each other to neglect any lateral heat flux through MLI blankets. The heater and thermocouple instrumentations can be shown in Figure 4.2 and Figure 4.3. The layout of the thermocouple instrumentation is presented in Figure 4.4.

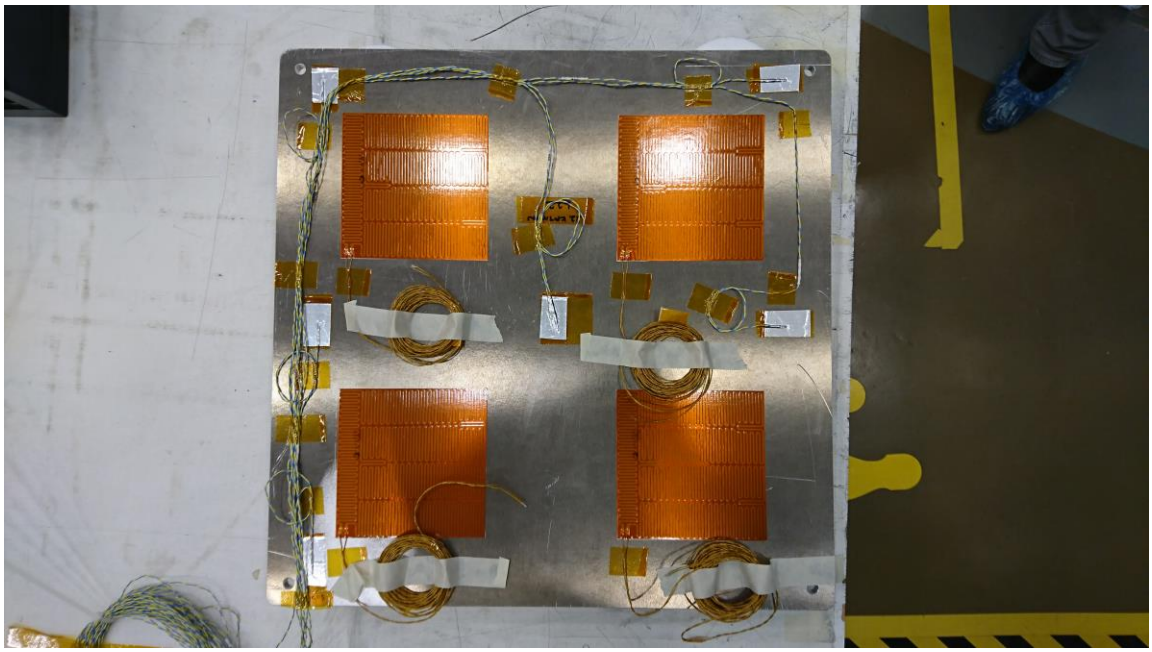

Figure 4.2: Aluminum Block Thermocouple and Heater Instrumentation

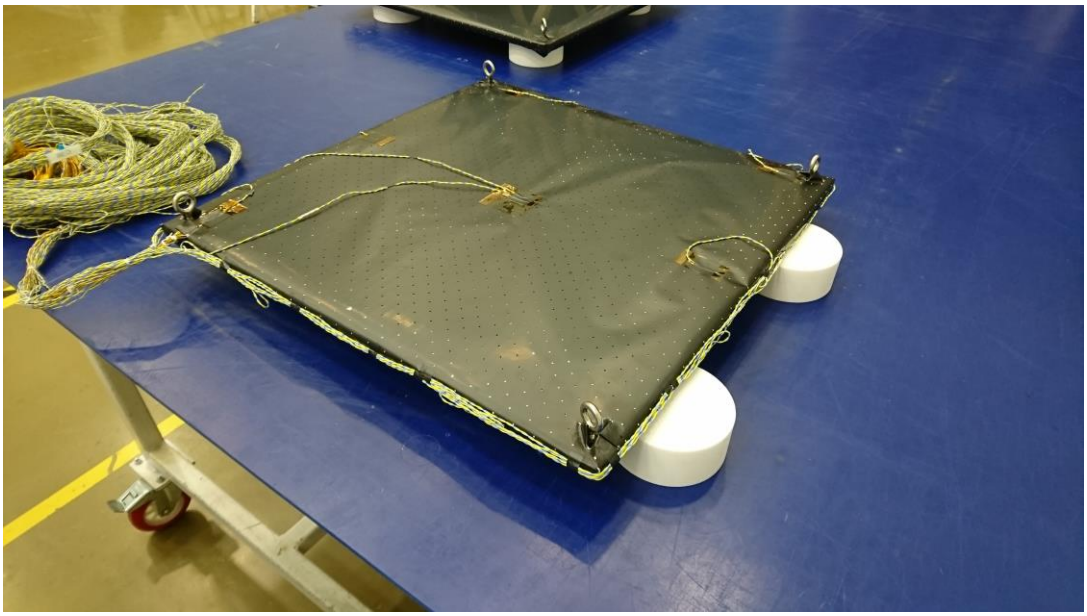

Figure 4.3: Thermocouple Instrumentation on MLI Blanket Surface

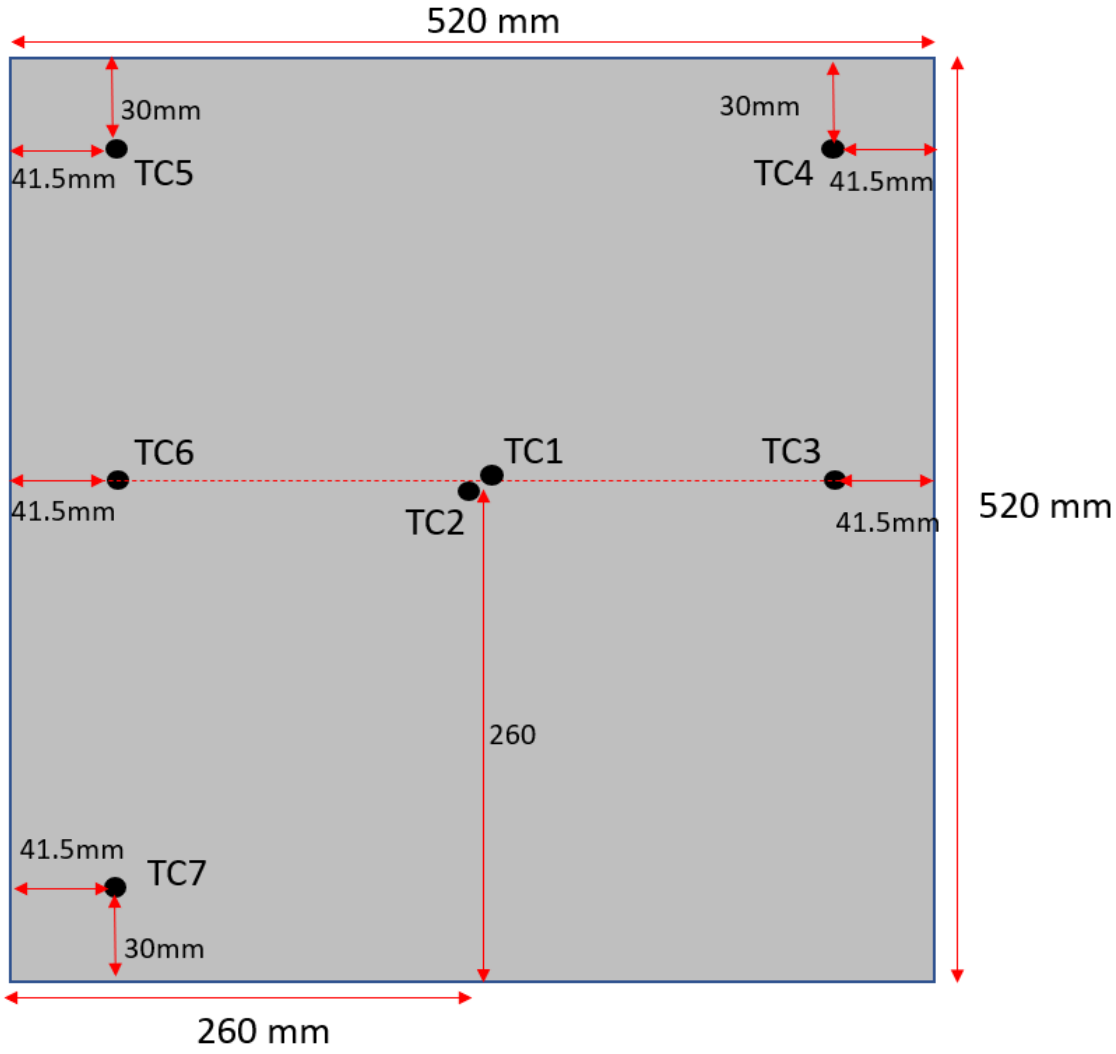

Figure 4.4: Thermocouple Layout

At each corner of aluminum block, an eyebolt was placed to hang the aluminum blocks inside the TVAC. To minimize the heat leak, a teflon insulator is used to separate the eyebolts and aluminum blocks. A representative view of aluminum blocks can be shown in Figure 4.5.

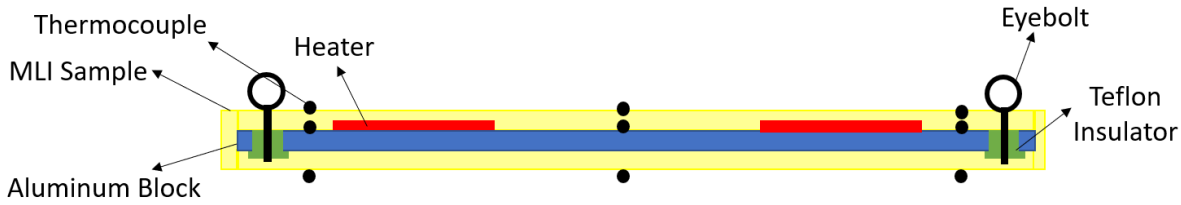

Figure 4.5: Representational View of MLI Blanket Samples

After the preparations on the aluminum block, the samples were hanged inside the TVAC by means of eyebolts using steel rope. The view of TVAC with MLI blanket samples is shown in Figure 4.6.

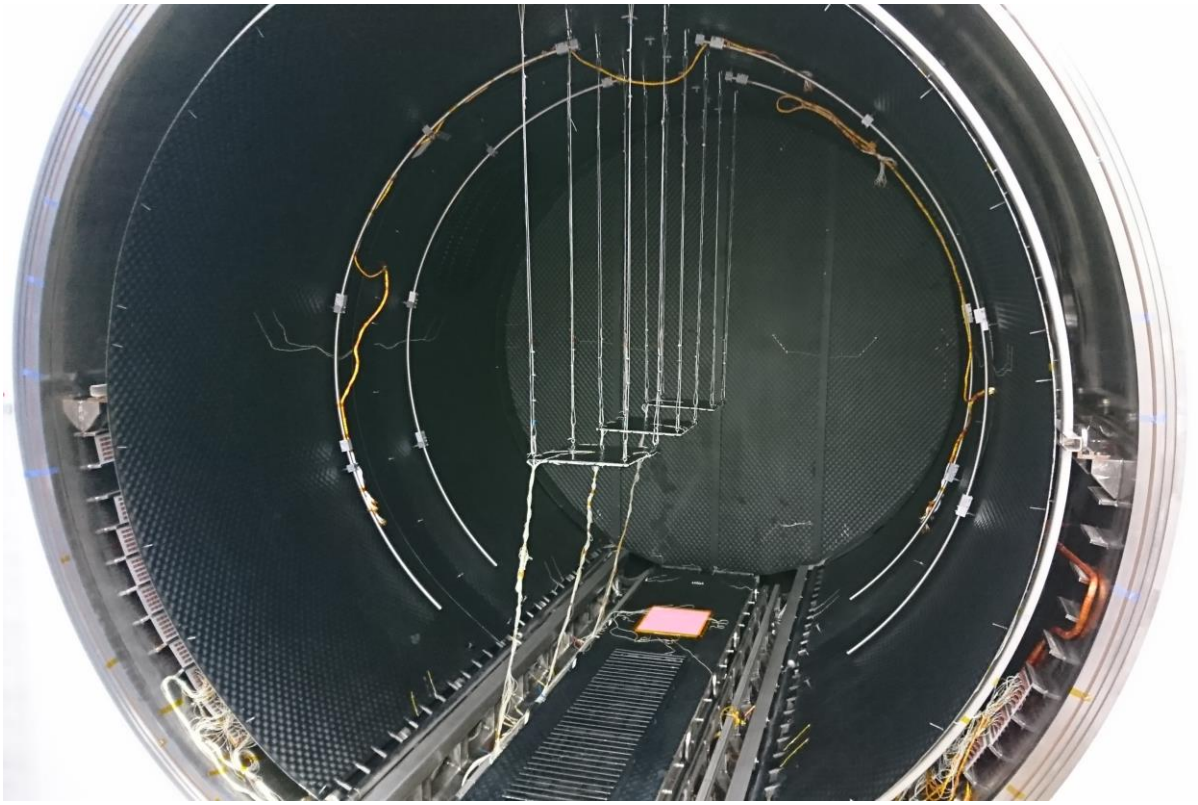

Figure 4.6: Experimental Setup inside TVAC

4.3 Experiment

The experiment was carried out by providing a vacuum environment in TVAC in order to eliminate the gaseous conduction as much as possible. The attained vacuum level was below $<10^{-5}$ mbar. Then, the thermal shrouds of the TVAC were cooled down to -160°C. At this shroud temperature, heaters on the aluminum

block were powered to adjust the warm boundary temperature. 3 different warm boundary temperatures were obtained at this shroud temperature and steady state data were recorded. Then, thermal shrouds of the TVAC were cooled down to -85°C. At this shroud temperature, 3 different warm boundary temperatures were obtained, and steady state data were recorded. At total, 6 different steady state temperature data were obtained for 6 different power inputs.

The power inputs at the cold boundary temperature at steady state is shown in Table 4-2.

Table 4-2: Power Inputs at Steady State Cases

Case No	**Cold Boundary Temperature (°C)**	**Power Input for 8 Layer MLI Blanket (W/m^2)**	**Power Input for 22 Layer MLI Blanket (W/m^2)**
1	-127	4.59	3.01
2	-127	6.02	4.57
3	-127	8.57	6.80
4	-75	3.09	1.73
5	-75	5.95	4.51
6	-75	7.62	5.68

Steady state temperature data obtained from all thermocouples at steady state configurations for each case are given in Table 4-3 and Table 4-4

Table 4-3: Steady State Temperature Data for 8 Layer MLI Blanket

Thermocouple No.	Case 1 Temp. (°C)	Case 2 Temp. (°C)	Case 3 Temp. (°C)	Case 4 Temp. (°C)	Case 5 Temp. (°C)	Case 6 Temp. (°C)
01	-19.9	7.96	30.72	-7.28	37.91	51.13
02	-19.9	7.95	30.7	-7.30	37.92	51.11
03	-20.23	7.57	30.24	-7.53	37.61	50.78
04	-20.33	7.37	30.03	-7.55	37.38	50.51
05	-20.32	7.39	30.04	-7.58	37.38	50.50
06	-20.09	7.75	30.48	-7.38	37.77	50.96
07	-20.59	7.05	29.57	-7.76	37.04	50.12
08	-128.25	-126.5	-124.98	-77.72	-76.73	-75.65
09	-128.41	-126.68	-125.1	-77.8	-76.75	-75.64
10	-117.82	-112.26	-107.16	-75.28	-76.32	-69.29
11	-113.68	-96.65	-102.16	-73.68	-68.98	-66.35
12	-116.05	-110.17	-105.83	-75.03	-71.18	-68.86
13	-120.94	-116.64	-112.75	-76.15	-73.81	-72.19
14	-107.9	-101.87	-95.46	-71.78	-65.00	-61.90
15	-113.04	-110.87	-110.9	-72.63	-72.84	-70.53
16	-114.04	-110.88	-111.7	-73.16	-72.35	-71.02
17	-107.50	-103.21	-101.7	-70.69	-68.23	-66.43
18	-108.00	-103.48	-103.25	-70.7	-68.69	-67.13
19	-108.10	-103.55	-105	-70.98	-69.31	-67.83
20	-108.50	-103.21	-104.27	-70.91	-69.10	-64.52
21	-105.49	-98.88	-99.75	-69.98	-66.87	-64.98

Table 4-4: Steady State Temperature Data for 22 Layer MLI Blanket

Thermocouple No.	Case 1 Temp. (°C)	Case 2 Temp. (°C)	Case 3 Temp. (°C)	Case 4 Temp. (°C)	Case 5 Temp. (°C)	Case 6 Temp. (°C)
01	-16.62	16.38	49.24	-10.92	50.11	62.75
02	-16.52	16.45	49.32	-10.83	50.17	62.82
03	-16.64	16.3	49.14	-10.92	50.03	62.65
04	-16.8	16.02	48.78	11.03	49.77	62.36
05	-16.96	15.88	48.51	-11.11	49.58	62.17
06	-16.96	16.34	49.13	-10.81	50.06	62.67
07	-16.93	15.9	48.55	-11.07	49.59	62.15
08	-130.51	-129.37	-128.63	-77.35	-76.90	-76.13
09	-130.67	-129.63	-128.98	-77.33	-76.91	-76.16
10	-127.86	-125.9	-123.98	-76.89	-75.96	-75.07
11	-119.32	-114.23	-109.02	-75.68	-71.90	-70.03
12	-120.71	-115.63	-110.55	-76.23	-72.51	-70.46
13	-121.6	-117.53	-112.73	-76.4	-73.43	-71.80
14	-112.14	-105.8	-99.26	-73.2	-66.98	-64.74
15	-112.4	-111.84	-111.31	-73.06	-72.58	-70.93
16	-112.3	111.81	-111.40	-72.79	-72.39	-70.75
17	-108.12	-104.92	-101.47	-71.55	-68.67	-66.66
18	105.63	-102.3	-98.65	-70.76	-67.34	-65.21
19	-105.75	-102.66	-99.20	-70.79	-67.49	-65.36
20	-106.06	-102.45	-98.39	-71.07	-67.52	-65.27
21	-103.94	-100.49	-97.05	-69.90	-66.43	-64.45

Different cold and warm boundary temperatures were obtained by applying different power inputs to the heaters on the aluminum block and by changing the

thermal shroud temperatures of the TVAC. By looking into the steady state temperatures, one can say that the temperatures on the warm boundary temperatures are homogeneously distributed while the temperatures on the cold boundary temperatures are inhomogeneous. Especially the temperature differences between the upper and lower side of the MLI blankets are much more. The reason behind it is, at the lower side of TVAC, there is a temperature unregulated area, where the temperatures are much higher. Since the thermal radiation is related with the view factor, the lower side of the MLI blankets is much warmer comparing to the upper side of MLI blanket. Also, at the middle of the outside of the MLI blanket, the temperatures are much lower since there are heat leaks at the corner of the MLI samples due to the experimental setup. These inhomogeneous temperatures at the cold boundary and small leaks due to experimental setup may have effect the prediction accuracies of the equations which will be discussed at chapter 5.

5. PREDICTIVE PERFORMANCE OF INVESTIGATED EQUATIONS AND DISCUSSIONS

Comprehensive literature survey carried out for the thesis reveals that there are several MLI heat flux prediction equations in literature. While some of these equations were created based on entirely empirical approach, some of these equations were both empirical and numerical based. The predictive accuracy of these equations was validated at limited temperature ranges since the experimental studies for these equations were carried out at certain temperatures. Also, since the experimental studies were carried out with certain materials, the validity of these equations for different materials remains unknown.

Based on literature review, three different equations were selected to predict the heat flux of MLI blankets. Layer by Layer Using a Separated Mode equation is a well-known method which predicts the performance of MLI blankets with physic-based equation. It is also the first model that uses dacron separator material in its equation. Lockheed model is a widely used empirical equations that predicts the performance of MLI blankets based on experimentally obtained data set. The studies for this model were used as the basis of international standard for MLI, ASTM C-740 [38]. In 2001, the Lockheed Model were modified such that it can also predict the heat flux of MLI blankets with dacron separator material. Doenecke investigated several papers in literature and came up with a new equation based on the experimental investigations in those papers. The data set in those papers were used to determine constants of this new equation by least square method.

5.1 Layer by Layer MLI Calculation Using a Separated Mode Equation

5.1.1 Theory

Layer by Layer MLI Calculation Using a Separated Mode Equation is McIntosh's work which is used in order to predict the temperature profile and heat flux through MLI blankets. This method considers all 3 heat transfer modes which are solid conduction due to spacer material, thermal radiation between MLI reflectors and gas conduction due to interstitial gas in MLI blankets. This method treats each heat transfer mode and each layer separated and then combined into an

equation. Considering this, the total heat flux through MLI can be written as in Eq. (8).

$$q_{total} = q_{rad} + q_{solid} + q_{gas} \tag{8}$$

This method calculates the heat transfer through MLI blankets layer by layer instead of treating MLI blankets as a bulk structure. So, (8) is written for each adjacent layer pairs. Therefore, for an MLI blanket consisting of N layers, N-1 equation is written. After all equations are written, linear temperature assumption is made for each layer for initial iteration. Depending on this assumption, new temperature distribution and heat flux values between each adjacent layer are determined. However, the spacer conductivity and reflector emissivity properties show temperature dependency. Also, the heat transfer equation is nonlinear since thermal radiation is proportional with T^4. So, resulting heat flux values between adjacent layers are different for the first iteration. However, the final heat flux values between each adjacent layer must be equal. Therefore, new iterations are made based on previously iterated temperature distribution until uniform heat flux values between adjacent layers are obtained. The heat transfer mechanism through MLI blankets and iteration mechanism for Layer by Layer equation are shown in Figure 5.1 and Figure 5.2 respectively.

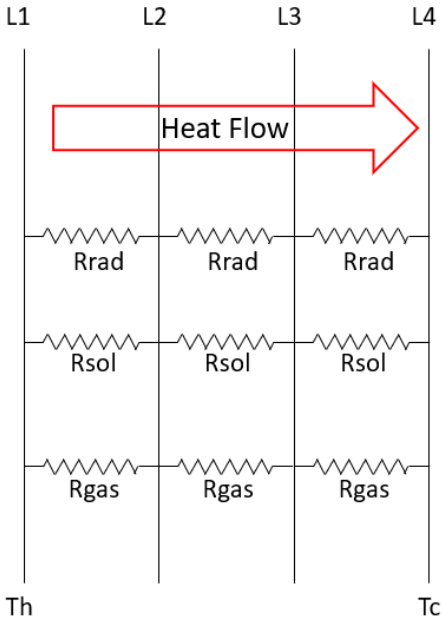

Figure 5.1: Representative Heat transfer Mechanism Through 4 Layer MLI Blanket

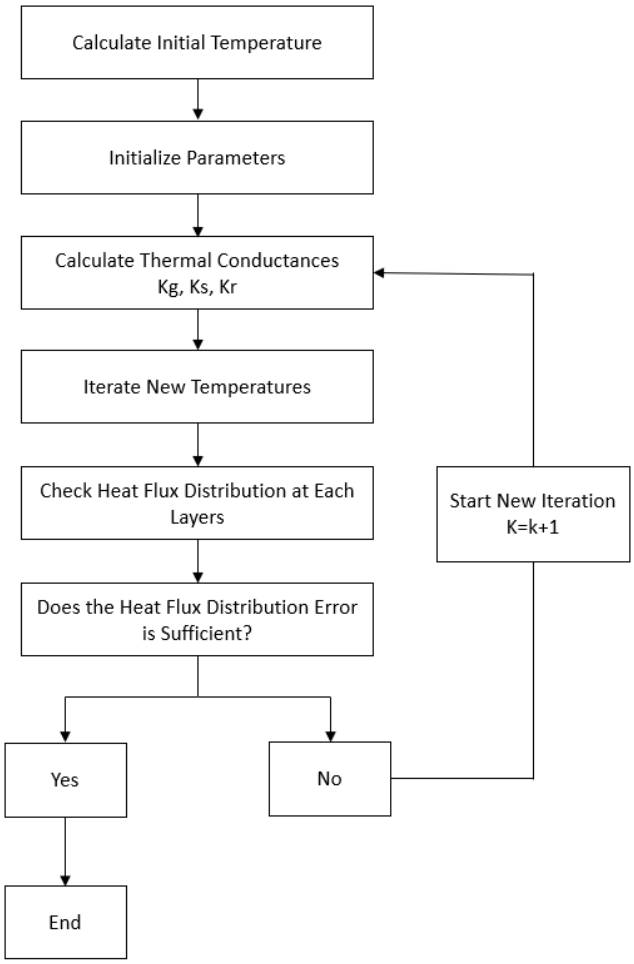

Figure 5.2 Layer by Layer Method Iteration Process

In order to calculate the heat fluxes, each heat transfer modes must be evaluated firstly. Radiative heat flux between two parallel surfaces can be represented as thermal network model as shown in Figure 5.3.

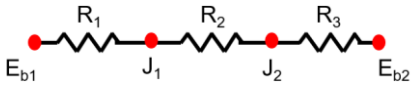

Figure 5.3: Radiative Heat Flux Between Two Surfaces

Based on the network model, the heat transfer rate between two surfaces can be written as in Eq. (9) [39].

$$q_{12} = \frac{\sigma(T_1^4 - T_2^4)}{\frac{1-\varepsilon_1}{\varepsilon_1} + 1 + \frac{1-\varepsilon_2}{\varepsilon_2}} \tag{9}$$

Considering MLI blankets with same reflector material, $\varepsilon_1 = \varepsilon_2 = \varepsilon$, then the radiative heat flux equation between each adjacent layer becomes as Eq. (10).

$$q_{12} = \frac{\sigma(T_1^4 - T_2^4)}{\frac{2-\varepsilon}{\varepsilon}} \quad (10)$$

Conductive heat transfer occurs due to temperature gradient between two bodies in contact. The rate of conductive heat transfer depends on temperature gradient between the two bodies, the area of contact and the conductive properties of these bodies. Conductive heat flux is given as Eq. (11).

$$q_c = -k\frac{dT}{dt} \quad (11)$$

In Layer by Layer equation, a parameter 'f' is added for the solid conduction term which represents the relative density of the separator material compared to solid material due to spacers have mesh structures. Also, for Dacron material separators, an empirical value C_2 is added to the solid conduction term.

In Layer by Layer equation, the conduction term is given below as in Eq. (12).

$$q_c = \frac{C_2 \, \mathrm{f} \, k_s(T_h - T_c)}{delX} \quad (12)$$

In McIntosh's work, C_2 and k values are given in Eq. (13) and Eq. (14) as follows;

$$C_2 = 0.008 \quad (13)$$

$$k_s = 0.017 + 7\mathrm{x}10^{-6}(800 - \mathrm{T}) + 0.0228 \, \mathrm{x} \, \ln(\mathrm{T}) \quad (14)$$

Gu [22] expressed the value of C_2 as temperature dependent as followed in Eq. (15) for a wider temperature range which is between 80 K to 300 K;

$$C_2 = 0.008 \, \mathrm{x} \, (-0.2005673 + 3.2843027\mathrm{x}10^{-5}T^2) \quad (15)$$

Gas conduction in Layer by Layer equation is expressed by (7) for each alternating reflector layer. Using this equation gaseous heat transfer can be found between each layer. Required parameters for the calculation of (7) are given in Table 5-1.

Table 5-1: Gas Conduction Parameters for Air

Parameter	**Constant**
C_1	1.1666
P	$5\mathrm{x}10^{-4}$
$\propto$	0.9

5.1.2 Modeling of an MLI Blanket Found in Literature

A numeric computing program (MATLAB) [40] has been used in order to develop a code to calculate the heat flux through MLI blankets by Layer by Layer MLI Calculation Using a Separated Mode Equation. To understand whether the code gives accurate results for the prediction of thermal performance of MLI blankets, the code has been first implemented for an MLI blanket, whose heat flux were determined by the same method in literature.

Reference MLI blanket in the literature [6] consists of 45 layers and a foam insulation at its cold boundary. To obtain maximum performance, the MLI blanket was designed as variable density, whose thicknesses between reflector layers are changing. For design purposes, the first 10 layers are consisting of low-density layers with 8 layers/cm. Second section of MLI blanket is medium density section consisting of 15 layers with a density of 12 layer/cm. And the final section of MLI blanket is high density section consisting of 20 layers with a density of 16 layers/cm. Taking the layer densities into consideration, the corresponding thicknesses between layers were found to be as 0.125 cm, 0.0833 cm and 0.0625 cm, respectively. Representation of Variable Density MLI (VD-MLI) is shown in Figure 5.4.

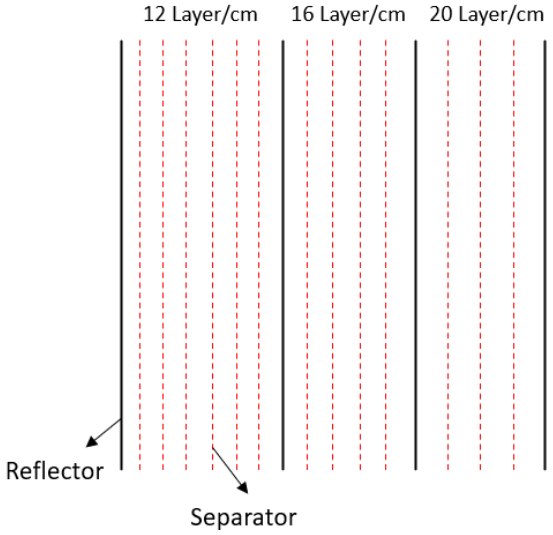

Figure 5.4: Variable Density MLI

To predict the heat fluxes for different warm boundary temperatures, some of parameters for the MLI blanket must be known. These parameters are tabulated in Table 5-2.

Table 5-2: MLI Blanket Parameters [6]

Parameter	Property
Foam Conductivity	0.000866 W/mK
Foam Emissivity	0.8
MLI Emissivity	0.03
MLI Perforation Factor	1.15
Shroud / Surroundings Emissivity	0.04
Interstitial Gas Pressure	1.33×10^{-5}
Accommodation Coefficient	0.8
Interstitial Gas Specific Heat Ratio	1.4
Empirical Spacer Conduction Coefficient	0.008
Separator Material Density	1390 kg/m^3
Separator Density/Material Density	0.0087

Based on the configuration of VD-MLI and given parameters, MATLAB was used to calculate the heat flux through VD-MLI in order to compare the created code with the literature data to validate the code for future calculations. The obtained heat flux data were compared with literature data in Figure 5.5.

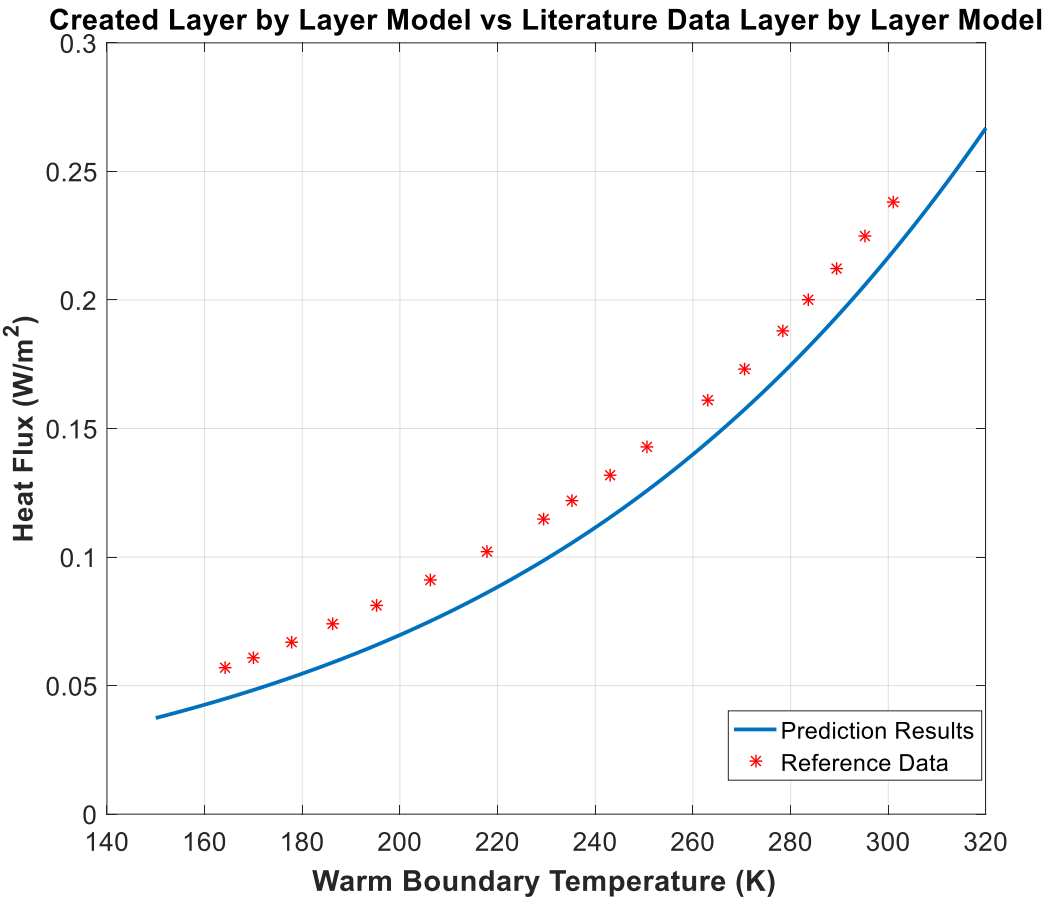

Figure 5.5: Heat Flux Prediction for Reference MLI by the Written Code

The predicted heat flux with Layer by Layer equation for reference MLI blanket in [6] and the predicted heat flux with Layer by Layer equation by the prepared code shows a discrepancy of 20% at the 160 K warm boundary temperature and 8% at the 300K warm boundary temperature. Under this condition, the predictions of layer temperatures for 164K warm boundary temperatures and 305 K warm boundary temperatures are given in Figure 5.6. As shown in Figure 5.6, the maximum temperature discrepancies at 164 K and 305 K warm boundary temperatures are around 6 K and 2 K respectively between the reference data.

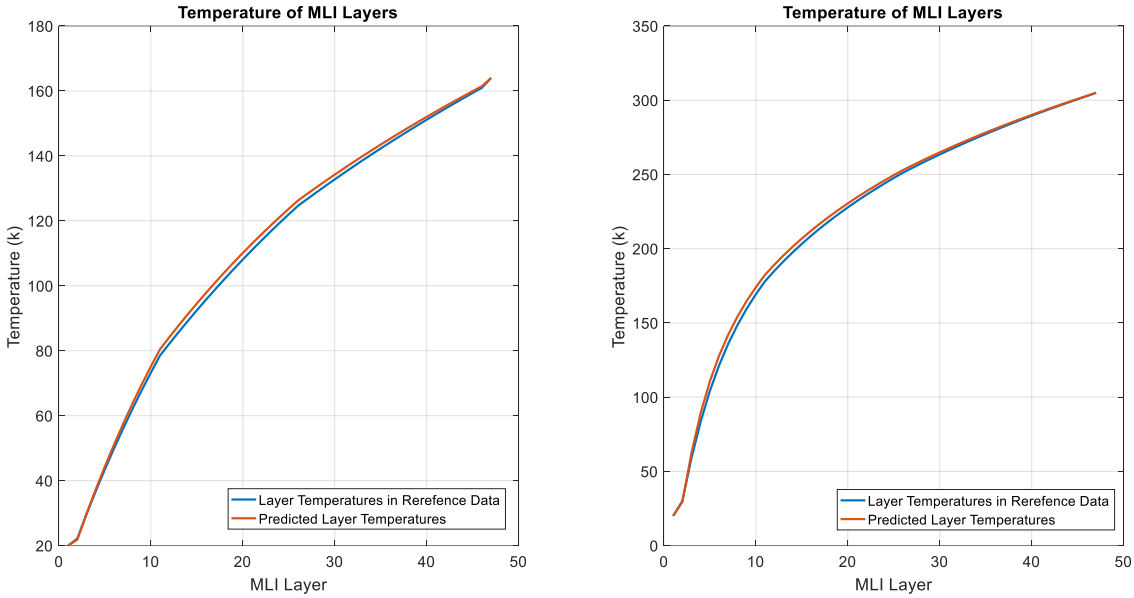

Figure 5.6: Temperature Prediction at 164 K and 305 K Warm Boundary Condition

5.1.3 Comparison of Layer by Layer Method with Experimental Results

Prepared numerical program was adapted for the experimentally investigated MLI blankets. To do this, some of specifications of spacer material had to be determined in order to use these specifications as parameters in the code. Based on the thickness measurement methods, needle probe was used in order to measure the MLI blanket thicknesses. 20 measurements were taken from different locations on each MLI blankets. The average thicknesses for 8 and 22 layer MLI blankets were found to be 2.25 mm and 4.44 mm respectively.

Another parameter required for the Layer by Layer equation is separator density. Separator density defined as the ratio of the weight of the separator to the solid density of the material of the separator. In order to define the separator density, image processing tool of MATLAB was used. By this method the separator density were found to be 11.93% per unit area. Input parameters required for Layer by Layer equation were tabulated in Table 5-3.

Table 5-3: Layer by Layer Parameters of 8 and 22 Layer MLI Blankets

Parameter	**8 Layer Blanket**	**22 Layer Blanket**
Number of Reflector Layer	9	23
MLI Blanket Thickness (mm)	2.25	4.44
Thickness Between Layers (m)	0.000282	0.000202
Separator Density (f)	0.1193	0.1193

In order to predict the heat flux by Layer by Layer equation, two different cold boundary temperatures were used as in the experimental cold boundary temperatures which are -127°C and -75°C. Based on these cold boundary temperatures, heat flux through MLI blankets were determined for warm boundary temperatures between 200 K and 350 K.

The predicted heat fluxes for experimentally investigated MLI blankets were given in Figure 5.7, Figure 5.8, Figure 5.9 and Figure 5.10. Predicted and experimental heat flux values and error between predicted and experimental heat flux values are given in Table 5-4, Table 5-5, Table 5-6 and Table 5-7.

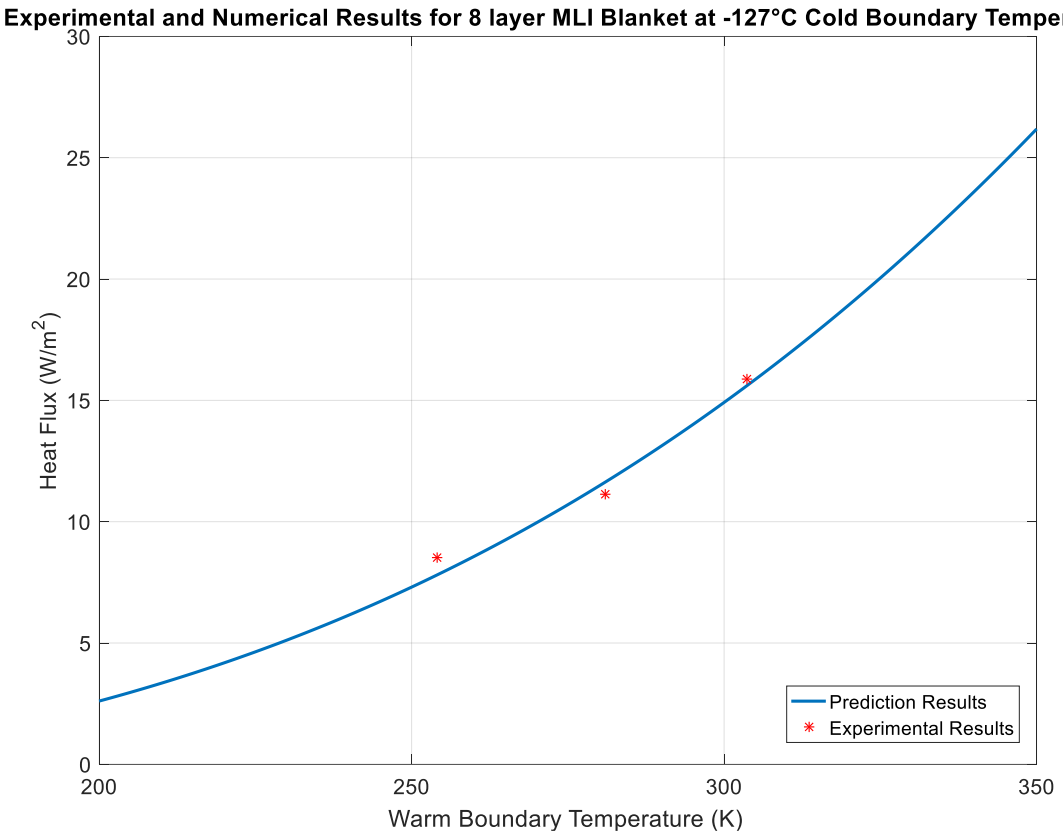

Figure 5.7: Experimental and Numerical Results for 8 layer MLI Blanket at -127°C Cold Boundary Temperature

Obtained heat flux predictions and experimental results shows very good agreement with each other for 8 Layer MLI blanket at -127°C cold boundary temperature. The maximum discrepancy between the equation and experimental data were calculated to be 8.3%.

Table 5-4: Predicted and Experimental Heat Flux Values for 8 layer MLI Blanket at -127°C Cold Boundary Temperature

Warm Boundary Temperature (K)	**Experimental Heat Flux (W/m^2)**	**Predicted Heat Flux (W/m^2)**	**Error (%)**
254	8.504	7.796	8.3
281	11.14	11.63	4.4
303.7	15.86	15.64	1.4

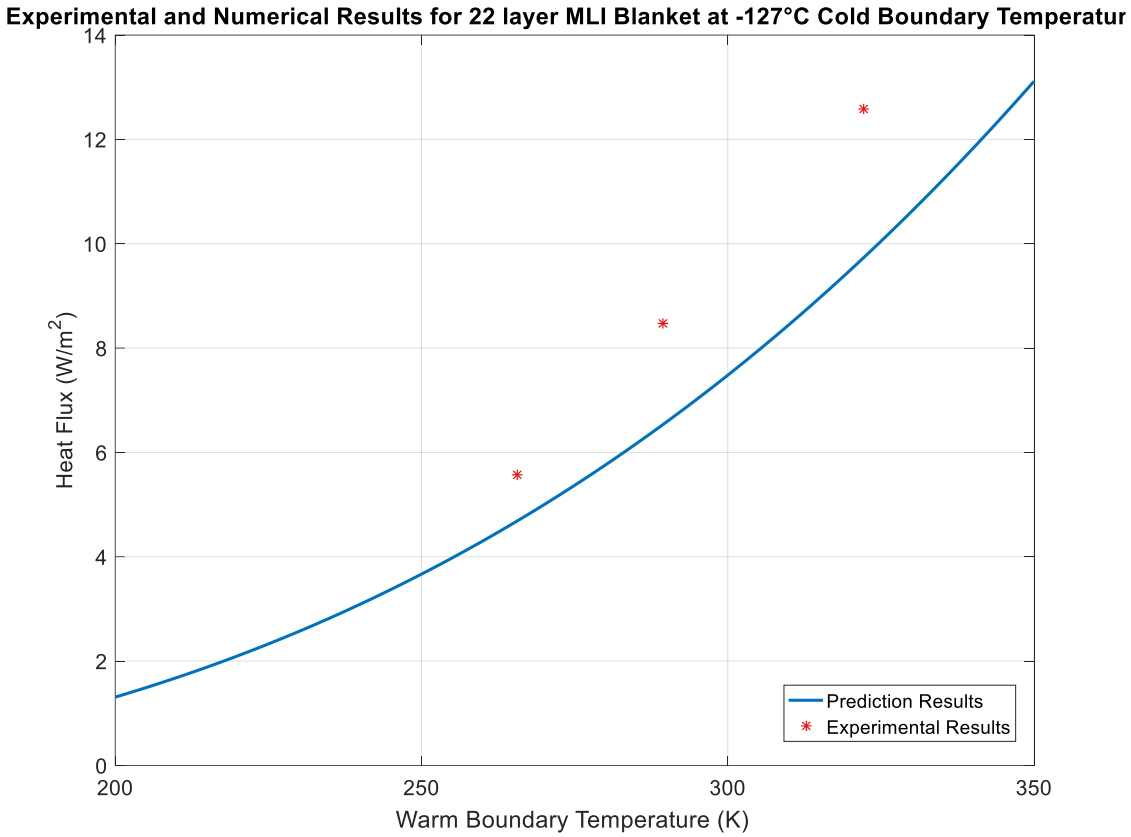

Figure 5.8: Experimental and Numerical Results for 22 layer MLI Blanket at -127°C Cold Boundary Temperature

As illustrated in Figure 5.8, obtained heat flux prediction by Layer by Layer equation is able to follow the heat flux trend obtained by experimental results. However, as the warm boundary temperature increases, the heat flux is underestimated by the equation. Unlike 8 Layer MLI blanket at this cold boundary temperature, the predicted heat fluxes are lower than experimental results for 22 layer MLI blanket. The maximum discrepancy between equation and experimental data were calculated to be 23.2%.

Table 5-5: Predicted and Experimental Heat Flux Values for 22 layer MLI Blanket at -127°C Cold Boundary Temperature

Warm Boundary Temperature (K)	**Experimental Heat Flux (W/m^2)**	**Predicted Heat Flux (W/m^2)**	**Error (%)**
256.4	5.56	4.71	15.2
289.4	8.47	6.50	23.2
322.2	12.57	9.71	22.7

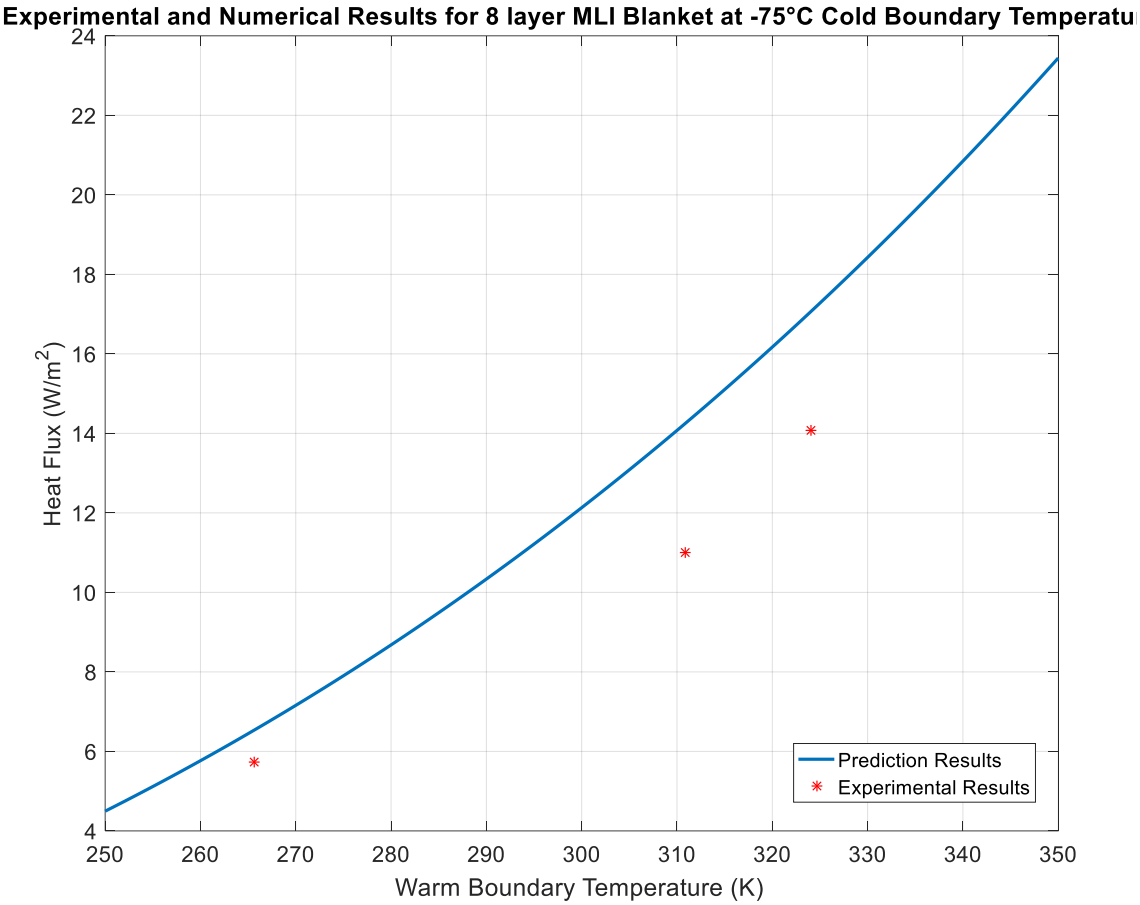

Figure 5.9:Experimental and Numerical Results for 8 layer MLI Blanket at -75°C Cold Boundary Temperature

As illustrated in Figure 5.9, obtained heat flux prediction by Layer by Layer equation is able to follow the heat flux trend obtained by experimental results. However, as the warm boundary temperature increases, the heat flux is overestimated by the equation. The maximum discrepancy between equation and experimental data were calculated to be %29.3.

Table 5-6: Predicted and Experimental Heat Flux Values for 8 layer MLI Blanket at -75°C Cold Boundary Temperature

Warm Boundary Temperature (K)	**Experimental Heat Flux (W/m²)**	**Predicted Heat Flux (W/m²)**	**Error (%)**
265.7	5.73	6.57	14.6
310.9	11.02	14.25	29.3
324.1	14.09	17.07	21.1

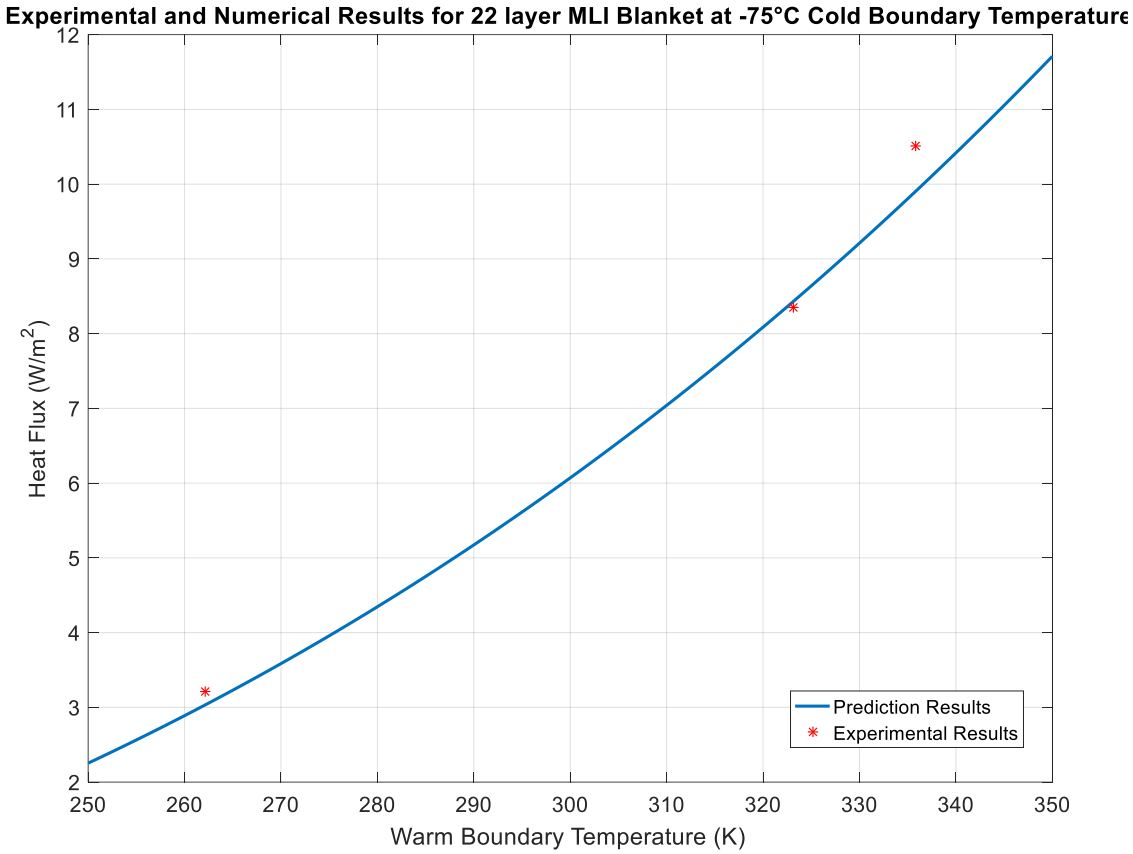

Figure 5.10: Experimental and Numerical Results for 22 layer MLI Blanket at -75°C Cold Boundary Temperature

Obtained heat flux predictions and experimental results shows very good agreement with each other for 22 Layer MLI blanket at -75°C cold boundary temperature. The maximum discrepancy between equation and experimental data were calculated to be 8.3%.

Table 5-7: Predicted and Experimental Heat Flux Values for 22 layer MLI Blanket at -75°C Cold Boundary Temperature

Warm Boundary Temperature (K)	**Experimental Heat Flux (W/m^2)**	**Predicted Heat Flux (W/m^2)**	**Error (%)**
262.1	3.21	3.02	5.9
323.1	8.35	8.42	7.0
335.8	10.51	9.91	5.7

5.2 Doenecke Equation

5.2.1 Theory

Doenecke equation considers the parameters of boundary temperatures, number of layers, blanket area and perforation rate for the prediction of MLI blankets heat flux performance. This equation was proposed for the MLI blankets of spacecrafts. Therefore, the author assumed negligible gas conduction since the interstitial pressure in space is below 10^{-4} mbar. Hence, this equation does not govern the gas conduction in heat flux predictions. In order to separate the solid conduction and thermal radiation terms, the author assumes optically thin spacer material. Thus, spacer material has no contribution in thermal radiation in total heat flux determination.

In this equation, instead of using cold and warm external blanket temperatures, mean temperature (T_m) was be used in equations. T_m can be calculated using Eq. (16).

$$4T_m^3 = \frac{T_h^4 - T_c^4}{T_h - T_c} \tag{16}$$

Heat flux due to solid conduction and radiation was given as in Eq.17 and Eq.18.

$$q_c = h(T_h - T_c) \tag{17}$$

$$q_r = \sigma \varepsilon_{eff}(T_h^4 - T_c^4) \tag{18}$$

As mentioned earlier, the heat transfer through MLI blankets can be given as either as k_{eff} or ε_{eff}. Both these expressions can be converted to each other. So, heat transfer coefficient can be converted to ε_{eff} by using Eq. (19).

$$\varepsilon_{eff} = \frac{h\,(T_h - T_c)}{\sigma\,(T_h^4 - T_c^4)} \tag{19}$$

Using Eq. (16) and Eq. (19) ε_{eff} can be rewritten as Eq. (20). This expression is used in Doenecke equation to represent the solid conduction heat flux through MLI blankets.

$$\varepsilon_{eff} = \frac{h}{4\sigma T_m^3} \tag{20}$$

The radiative heat transfer is expressed as proportional to $T_m^{0.667}$ in Doenecke equation as in many other studies. Therefore, the structure of the equation becomes as Eq. (21).

$$\varepsilon_{eff} = (C_S \frac{1}{4\sigma {T_m}^2} + C_R T_m^{0.667}) f_N f_A f_P \quad (21)$$

The experimental data of two different studies were used in order to define the coefficients of C_s and C_r. A best fit with experimental data were created by applying least square method. The resulting constants of this method were determined as 0.000136 and 0.000121 for C_s and C_r respectively.

The experimental data belongs to an MLI blanket consisting of 20 layer. Since different layer MLI blankets would have different thermal performances, the equation requires a correction factor for number of layer. Experimental data of 4 different studies were investigated to find out the effect of number of layer to the thermal performance of MLI blankets. MLI blankets consisting of 5 to 30 layer were investigated and a correction factor of f_N were derived as in Table 5-8.

Table 5-8: Correction Factor of f_N

N	**f_N**
5	2.048
10	1.425
15	1.164
20	1.000
25	0.905
30	0.841

Another considered parameter in Doenecke equation is the perforation rate of MLI blankets. Doenecke investigates the influence of perforations by considering the Gebhart factor of 3 parallel surfaces. Using Gebhart factor of those surfaces, view factor equation of perforated parallel surfaces was defined. Using derived equation, correction factor of f_P was derived for the Doenecke equation. Correction factors for different perforation rate reflectors with different emissivities were given in Table 5-9.

Table 5-9: Correction Factors for f_p

Perforation Rate (%)	f_p	
	$\varepsilon = 0.04$	$\varepsilon = 0.03$
0.1	0.756	0.704
0.2	0.783	0.737
0.5	0.865	0.837
1.0	1.000	1.000
1.5	1.133	1.161
2.0	1.266	1.322

The experimental data of two different studies were investigated to understand the effect of MLI blanket area to the heat flux. Experimental heat flux of MLI blankets between 0.5m^2 to 100m^2 were analyzed and an equation for MLI blankets with a surface area between 0.5m^2 to 3m^2 were derived. The correction factor f_A is calculated using Eq. (22)

$$f_A = 1/10^{(0.373\ logA)} \tag{22}$$

In order to predict the heat flux through MLI blankets, the correction factors were written in functions depending on their parameters. Corresponding functions are written as Eq. (23) Eq. (24) below.

$$f_N = -6.5867x10^{-7}N^5 + 6.52x10^{-5}N - 0.002543N^3 + 0.05019N^2 - 0.54191N + 3.782 \tag{23}$$

$$f_{P,e=0.03}: 0.0024558P^3 - 0.011342P^2 + 0.34P + 0.67 \tag{24}$$

For the 8 and 22 layer blankets, the parameters of f_N, f_P and f_A are presented in Table 5-10.

Table 5-10: Doenecke Parameters for MLI Blankets

Parameters	8-layer MLI Blanket	22-layer MLI Blanket
f_N	1.6023	0.9530
f_P	0.9491	0.9491
f_A	1.2577	1.2577

5.2.2 Comparison of Doenecke's Equation with Experimental Results

Using the parameters required for Doenecke's equation, a MATLAB code was written for the prediction of the MLI blankets which are experimentally investigated. Heat fluxes were determined for the warm boundary temperature interval of 200 K and 350 K at two different cold boundary temperature which are -127°C and -75°C.

The predicted heat fluxes for experimentally investigated MLI blankets were given in Figure 5.11, Figure 5.13, Figure 5.15 and Figure 5.17. Predicted and experimental heat flux values and error between predicted and experimental heat flux values are given in Table 5-11, Table 5-12, Table 5-13 and Table 5-14.

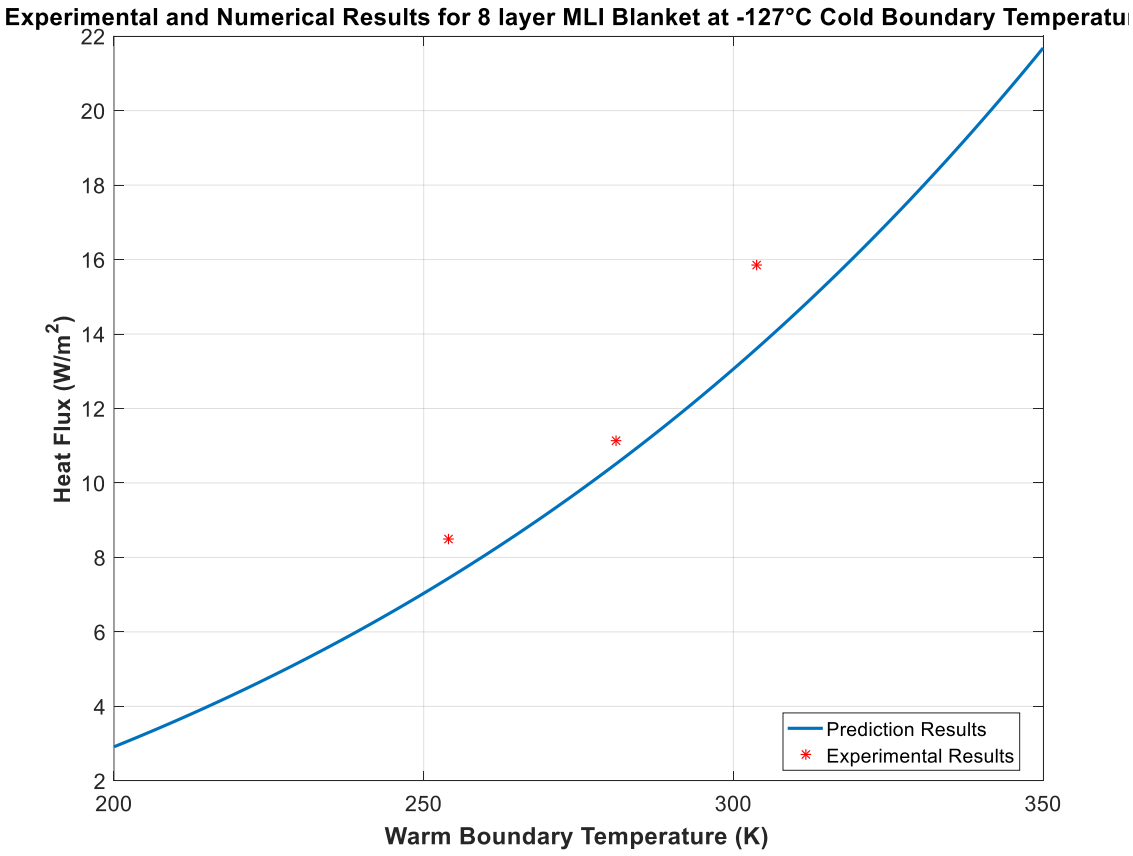

Figure 5.11: Experimental and Numerical Results for 8 layer MLI Blanket at -127°C Cold Boundary Temperature

As illustrated in Figure 5.11, obtained heat flux prediction by Doenecke equation is able to follow the heat flux trend obtained by experimental results. However, as the warm boundary temperature increases, the heat flux is underestimated by the equation. The maximum discrepancy between equation and experimental data were calculated to be %14.9. The participation of heat transfer modes in

total heat flux for 8 layer MLI blanket at -127°C is also given in Figure 5.12 in percentages.

Table 5-11: Predicted and Experimental Heat Flux Values for 8 layer MLI Blanket at -127°C Cold Boundary Temperature

Warm Boundary Temperature (K)	Experimental Heat Flux (W/m^2)	Predicted Heat Flux (W/m^2)	Error (%)
254	8.50	7.44	12.4
281	11.14	10.51	5.66
303.7	15.86	13.50	14.9

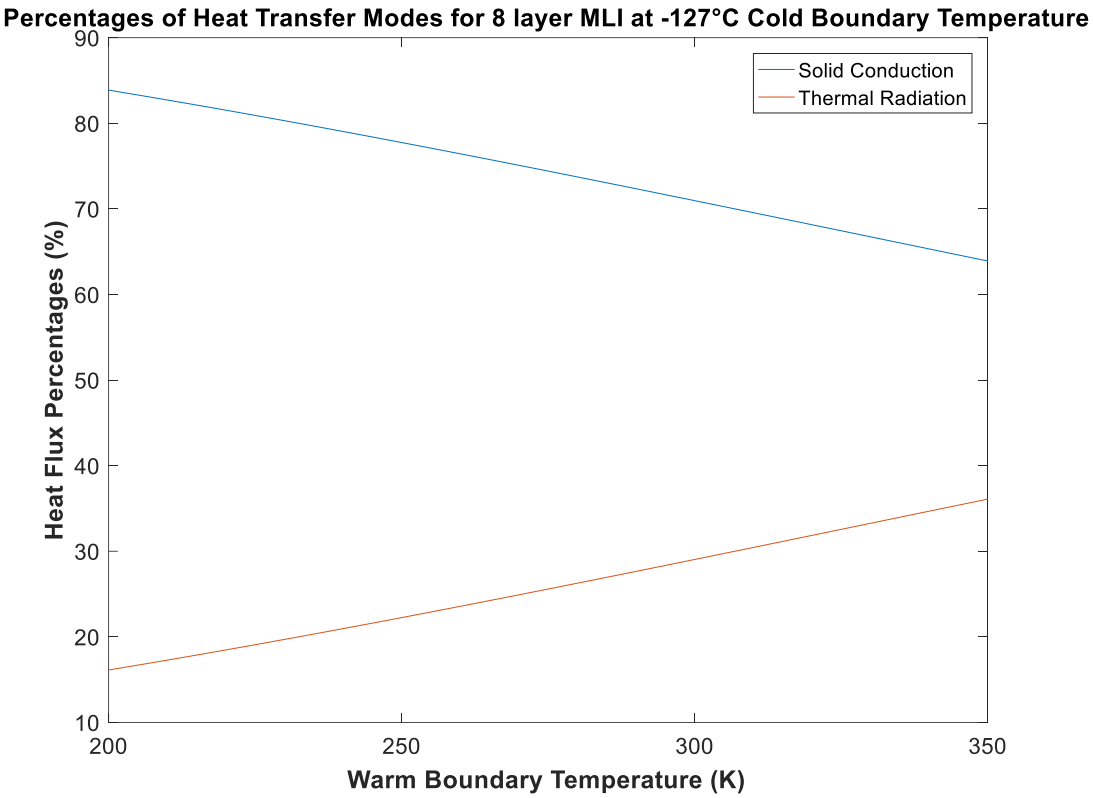

Figure 5.12: Heat Transfer Mode Participation Percentages for 8 layer MLI blanket at -127°C

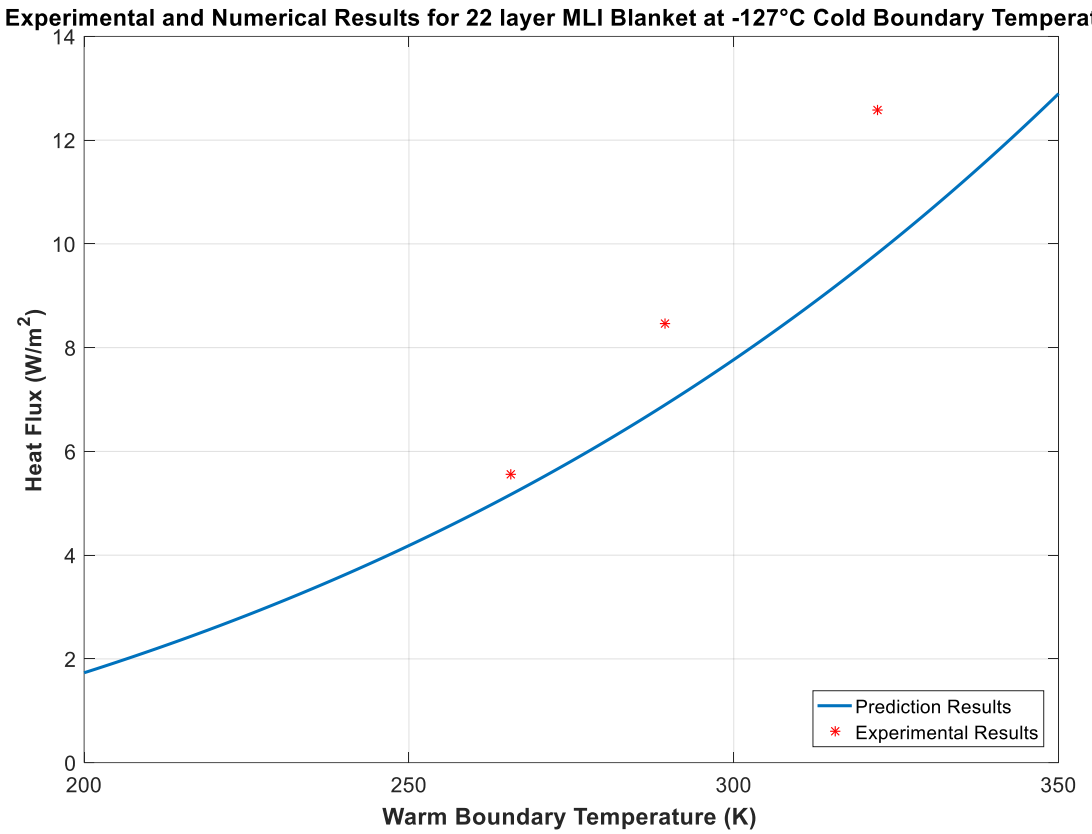

Figure 5.13: Experimental and Numerical Results for 22 layer MLI Blanket at -127°C Cold Boundary Temperature

As illustrated in Figure 5.13, obtained heat flux prediction by Doenecke equation can follow the heat flux trend obtained by experimental results. However, as the warm boundary temperature increases, the heat flux is underestimated by the equation. As the predicted heat fluxes for 8 Layer MLI blanket at this cold boundary temperature, the predicted heat fluxes are lower than experimental results for 22 layer MLI blanket. The maximum discrepancy between equation and experimental data were calculated to be 21.9%. The participation of heat transfer modes in total heat flux for 22 layer MLI blanket at -127°C is also given in Figure 5.14 in percentages.

Table 5-12: Predicted and Experimental Heat Flux Values for 22 layer MLI Blanket at -127°C Cold Boundary Temperature

Warm Boundary Temperature (K)	Experimental Heat Flux (W/m^2)	Predicted Heat Flux (W/m^2)	Error (%)
265.7	5.57	4.55	18.3
289.4	8.46	6.87	18.7
322.2	12.57	9.81	21.9

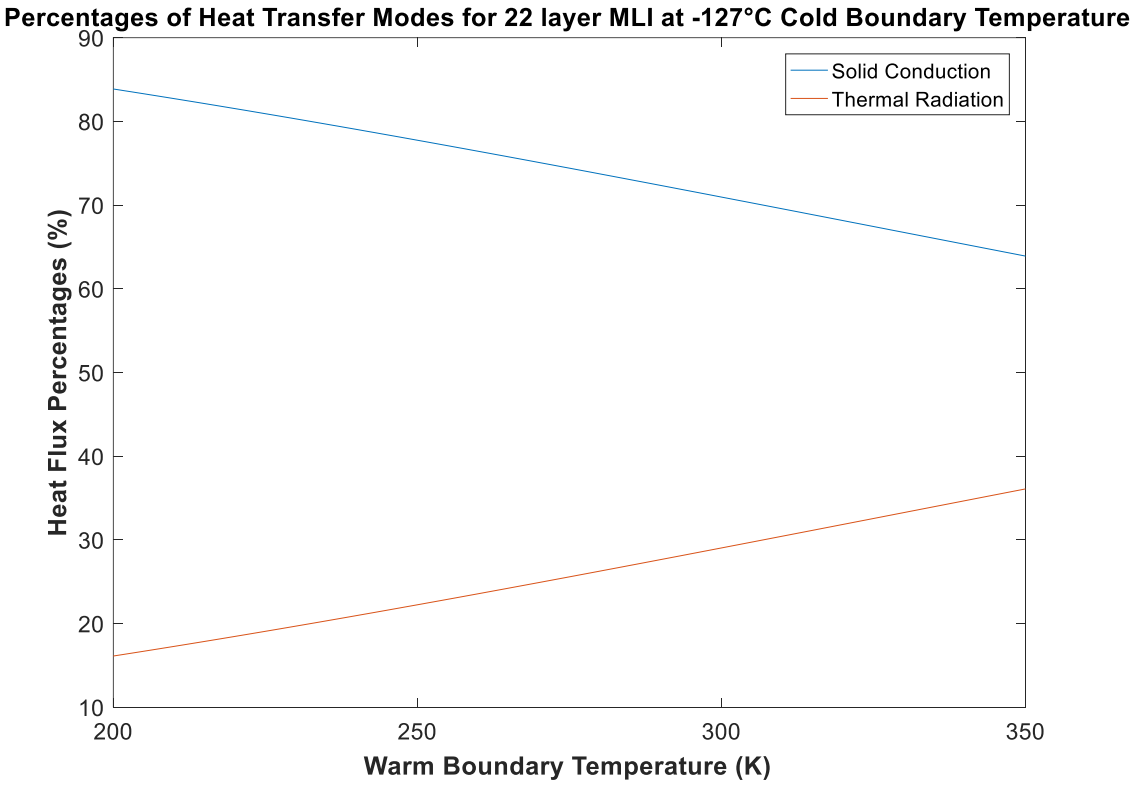

Figure 5.14: Heat Transfer Mode Participation Percentages for 22 layer MLI blanket at -127°C

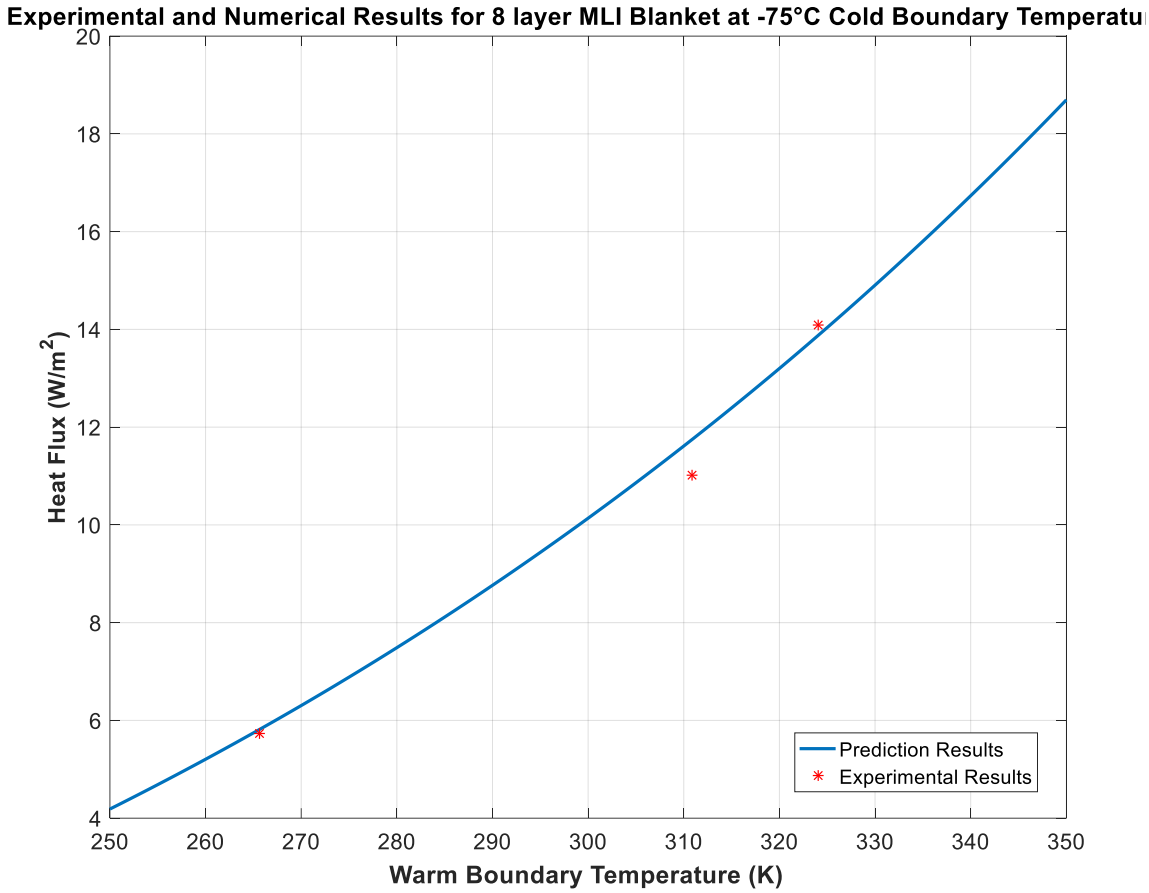

Figure 5.15: Experimental and Numerical Results for 8 layer MLI Blanket at -75°C Cold Boundary Temperature

Obtained heat flux predictions by Doenecke equation and the experimental results shows good agreement with each other for 8 Layer MLI blanket at -75°C cold boundary temperature. The maximum discrepancy between equation and experimental data were calculated to be 6.8%. The participation of heat transfer modes in total heat flux for 8 layer MLI blanket at -75°C is also given in Figure 5.16 in percentages.

Table 5-13: Predicted and Experimental Heat Flux Values for 8 layer MLI Blanket at -75°C Cold Boundary Temperature

Warm Boundary Temperature (K)	**Experimental Heat Flux (W/m^2)**	**Predicted Heat Flux (W/m^2)**	**Error (%)**
265.7	5.72	5.88	2.8
310.9	11.02	11.77	6.8
324.1	14.09	13.87	1.6

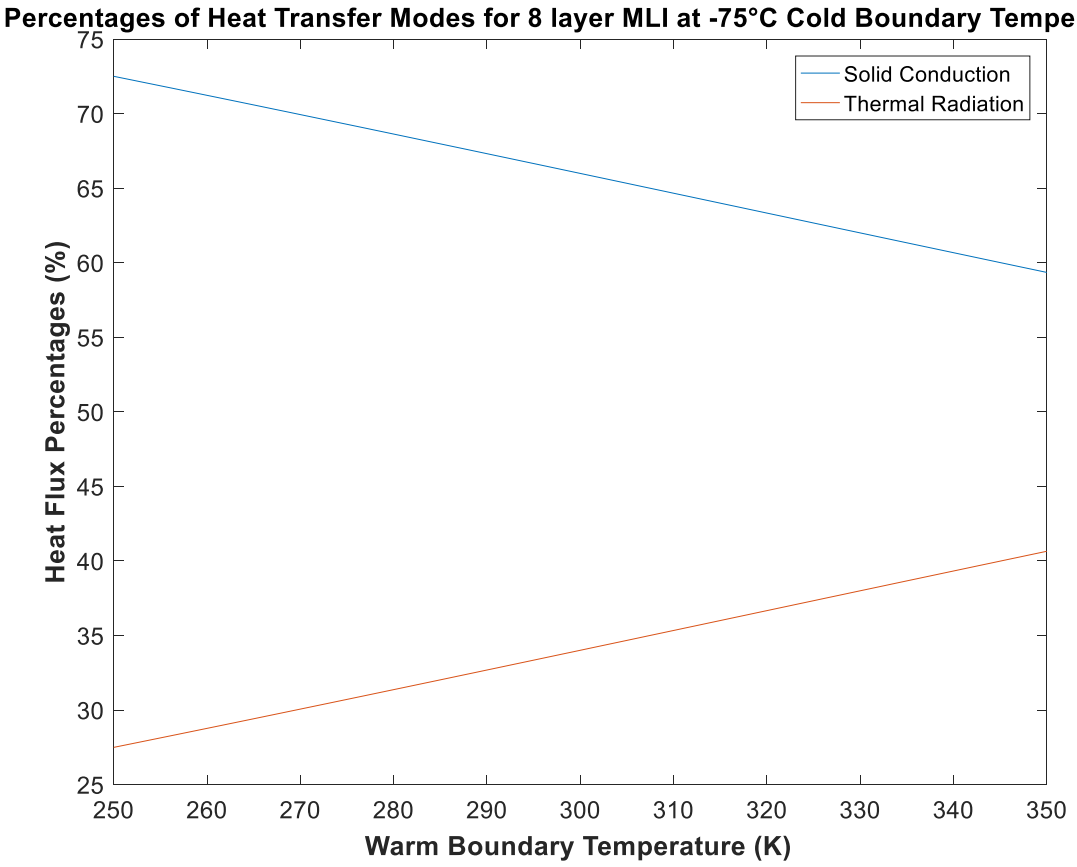

Figure 5.16: Heat Transfer Mode Participation Percentages for 8 layer MLI blanket at -75°C

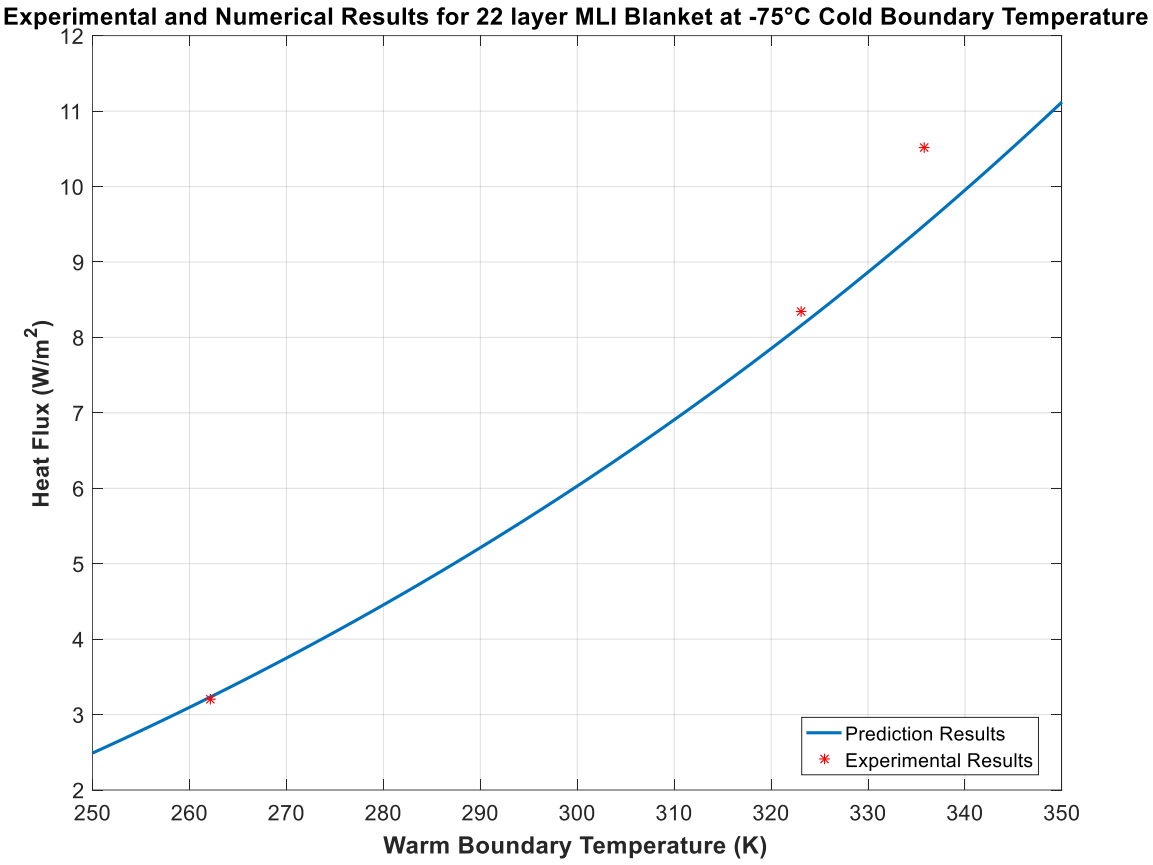

Figure 5.17: Experimental and Numerical Results for 22 layer MLI Blanket at -75°C Cold Boundary Temperature

Obtained heat flux predictions by Doenecke equation and the experimental results shows good agreement with each other for 22 Layer MLI blanket at -75°C cold boundary temperature. The maximum discrepancy between equation and experimental data were calculated to be 9.6%. The participation of heat transfer modes in total heat flux for 22 layer MLI blanket at -75°C is also given in Figure 5.18 in percentages.

Table 5-14: Predicted and Experimental Heat Flux Values for 22 layer MLI Blanket at -75°C Cold Boundary Temperature

Warm Boundary Temperature (K)	**Experimental Heat Flux (W/m^2)**	**Predicted Heat Flux (W/m^2)**	**Error (%)**
262.1	3.21	3.22	0.03
323.1	8.35	8.15	2.4
335.8	10.51	9.50	9.6

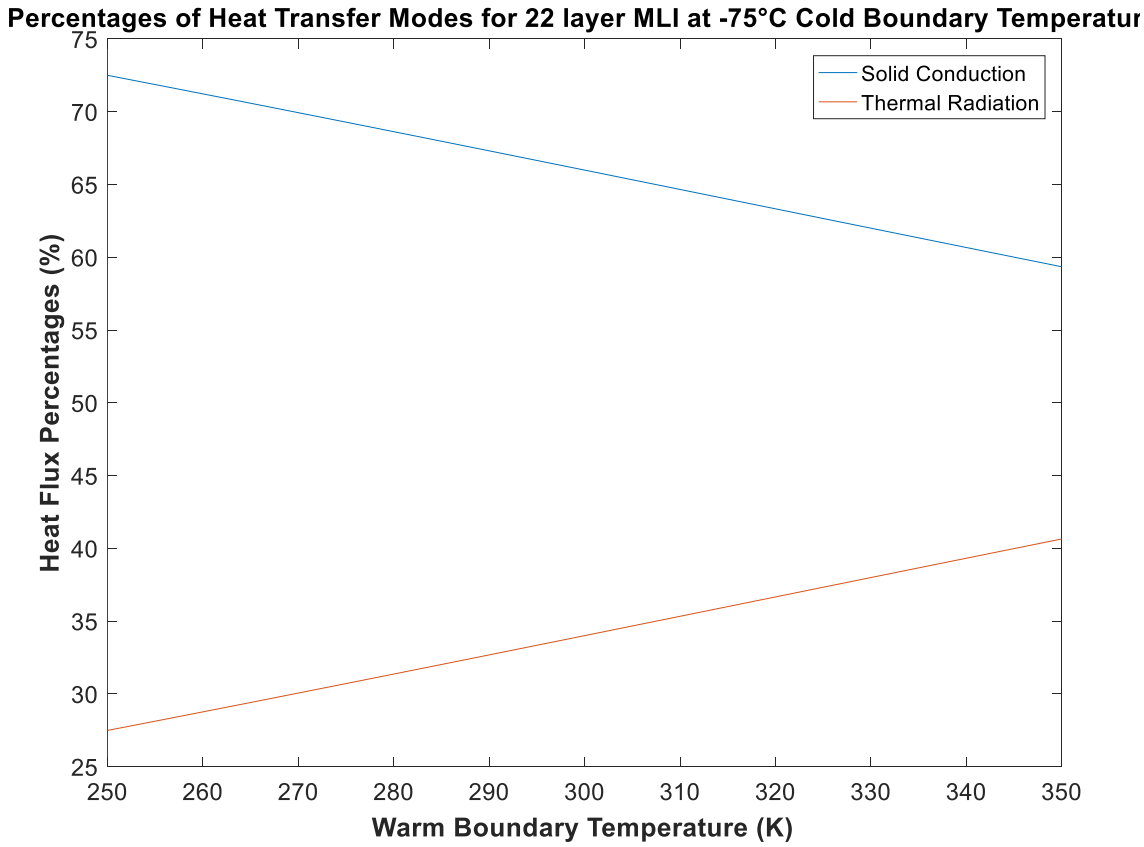

Figure 5.18: Heat Transfer Mode Participation Percentages for 22 layer MLI blanket at -75°C

5.3 Lockheed Equation

5.3.1 Theory

In the content of prediction of heat flux performance of various MLI blanket systems, several MLI blankets were investigated experimentally with respect to the variables of layer number, layer density, cold and warm boundary temperatures, reflector perforation rate and interstitial gas pressure. Obtained steady state heat fluxes were then used to create empirical equations for investigated MLI blankets. These equations were called Lockheed Models. By using Lockheed models, heat flux of these MLI blankets can be approximated with a limited accuracy. The structure of Lockheed equations is given in Eq. (25).

$$q = \frac{C_s \bar{N}^n T_m}{N_s}(T_h - T_c) + \frac{C_r \epsilon}{N_s}\left(T_h^{4.67} - T_c^{4.67}\right) + \frac{C_g P\left(T_h^{0.52} - T_c^{0.52}\right)}{N_s} \qquad (25)$$

The original Lockheed equations does not govern the Dacron material as spacer. This model was modified such that, it can also estimate the heat flux of MLI blankets with Dacron spacer materials. Therefore, solid conduction constant was adapted to the Dacron materials. Solid conduction constant C_s in Eq. (25) was changed as given in Eq. (26). With Eq. (26), the Modified Lockheed equation becomes as in Eq. (27)

$$C_s = 2.4x10^{-4}x\ (0.017 + 7\text{x}10^{-6}(800 - \text{T})) + 0.0228\ \text{x}\ \ln(\text{T}) \tag{26}$$

$$q = \frac{2.4x10^{-4}x\left(0.017 + 7\text{x}10^{-6}(800 - \text{T})\right) + 0.0228\ \text{x}\ \ln(\text{T})\ \bar{N}^{2.63}}{N_s}(T_h - T_c) + \frac{C_r\epsilon}{N_s}\left(T_h^{4.67} - T_c^{4.67}\right) + \frac{C_g P\left(T_h^{0.52} - T_c^{0.52}\right)}{N_s} \tag{27}$$

Required parameters in Eq. (27) were determined using the specifications of experimentally investigated MLI blankets. Measured thicknesses for the 8 and 22 layer MLI blankets are 2.25 mm and 4.44 mm respectively. This corresponds to a layer density of 35.47 layer/cm and 49.50 layer/cm for 8 and 22 layer MLI blankets respectively.

For DAM 1% perforated reflector materials, C_r is given as $7.07\text{x}10^{-10}$ as empirical constant in [36] However, investigated MLI blankets have 0.84% perforation rate. Thus, this constant had to be modified before using it to predict the heat flux through investigated MLI blankets. In the same reference, the effect of fractional open area to the radiative heat transfer was given. In this study, perforation rates and different patterns were investigated and contribution of these effects were compared with the non-perforated MLI blanket. The effect of perforation rate to the radiative heat transfer is tabulated in Table 5-15.

Table 5-15 : Effect of Perforation Rate to the Radiative Heat Transfer

Perforation Rate (%)	**q_r/q_{r0}**
0.26	1.09
0.55	1.17
1.07	1.31
0.48	1.13
1.23	1.23
0.99	1.23

Based on the table above, considering the perforation rates of 0.26, 0.55 and 1.07an interpolation process was carried out to find the effect of 0.84% perforation rate on radiative heat transfer through MLI blankets. The results of interpolation showed that the radiative heat transfer decreases by 1.03 times comparing to the 1% perforated MLI blanket for the 0.84% perforation rate. So, the C_r was divided by 1.03 for investigated MLI blankets.

The studies which use Lockheed equation as prediction model were carried out using helium and nitrogen gas as interstitial gas. Therefore C_g is given only for interstitial gases of either helium and nitrogen. Since the experimental investigation to be carried out with interstitial gas of air, this might lead to an error in calculations. However, since the effect of gas conduction becomes very small with increasing vacuum pressures, this effect can be neglected. So, since the experimental investigations carried out below 10^{-5} mbar, gas conduction effect in Lockheed equation is neglected.

Based on the studies for the determination of parameter constants the corresponding constants are summarized in Table 5-16.

Table 5-16: Lockheed Equation Parameters for Investigated MLI Blankets

Parameter	8 Layer MLI Blanket	22 Layer MLI Blanket
$\bar{N}$	35.47	49.50
n	2.63	2.63
N_s	8	22
C_r	6.864×10^{-10}	6.864×10^{-10}
ϵ	0.035	0.035

After the determination of parameter constants, (27) was used in numeric computing program to predict the heat transfer through 8 and 22 layer MLI blankets for -127°C and -75°C cold boundaries. Based on these cold boundary temperatures, heat flux through MLI blankets were determined for warm boundary temperatures between 200 K and 350 K. The obtained heat fluxes and experimental data were discussed in the next section.

5.3.2 Comparison of Modified Lockheed Equation with Experimental Results

Using the parameters required for Modified Lockheed Equation, a numerical program was prepared for the prediction of the MLI blankets which are experimentally investigated. Heat fluxes were determined for the warm boundary temperature interval of 200 K and 350 K at two different cold boundary temperature which are -127°C and -75°C.

The predicted heat fluxes for experimentally investigated MLI blankets were given in Figure 5.19, Figure 5.21, Figure 5.23 and Figure 5.25. Predicted and experimental heat flux values and error between predicted and experimental heat flux values are given in Table 5-17, Table 5-18, Table 5-19 and Table 5-20. The participation of heat transfer modes in total heat flux for all cases are presented in Figure 5.20, Figure 5.22, Figure 5.24 and Figure 5.26.

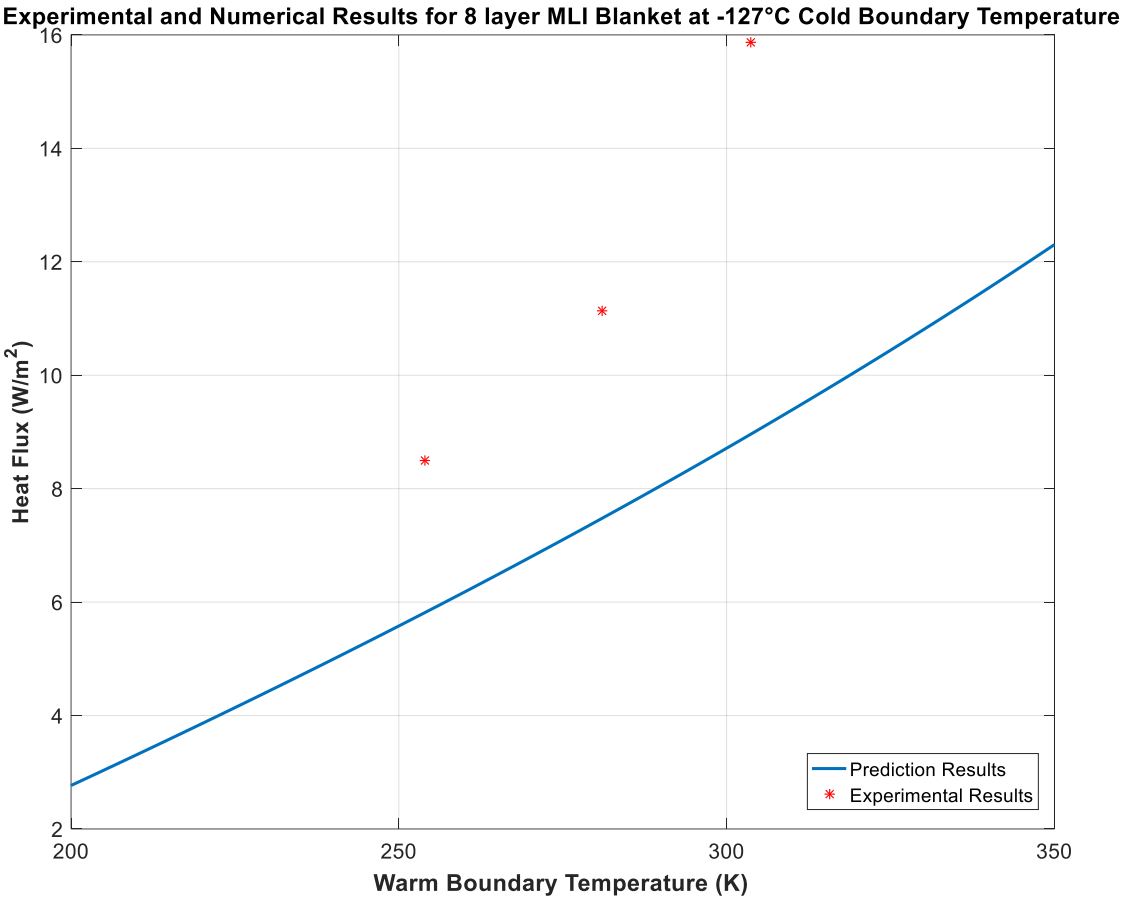

Figure 5.19: Experimental and Numerical Results for 8 layer MLI Blanket at -127°C Cold Boundary Temperature

Table 5-17: Predicted and Experimental Heat Flux Values for 8 layer MLI Blanket at -127°C Cold Boundary Temperature

Warm Boundary Temperature (K)	Experimental Heat Flux (W/m^2)	Predicted Heat Flux (W/m^2)	Error (%)
254	8.50	5.81	31.6
281	11.14	7.48	32.8
303.7	15.86	8.98	43.3

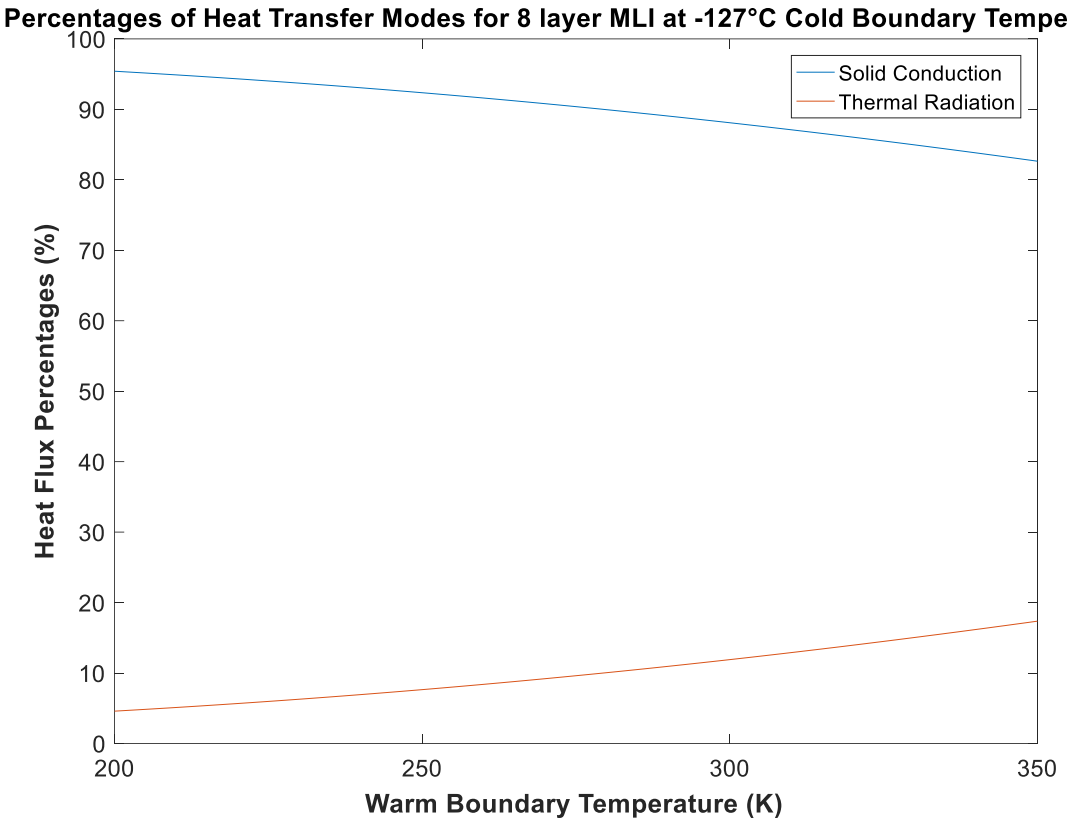

Figure 5.20: Heat Transfer Mode Participation Percentages for 8 layer MLI blanket at -127°C

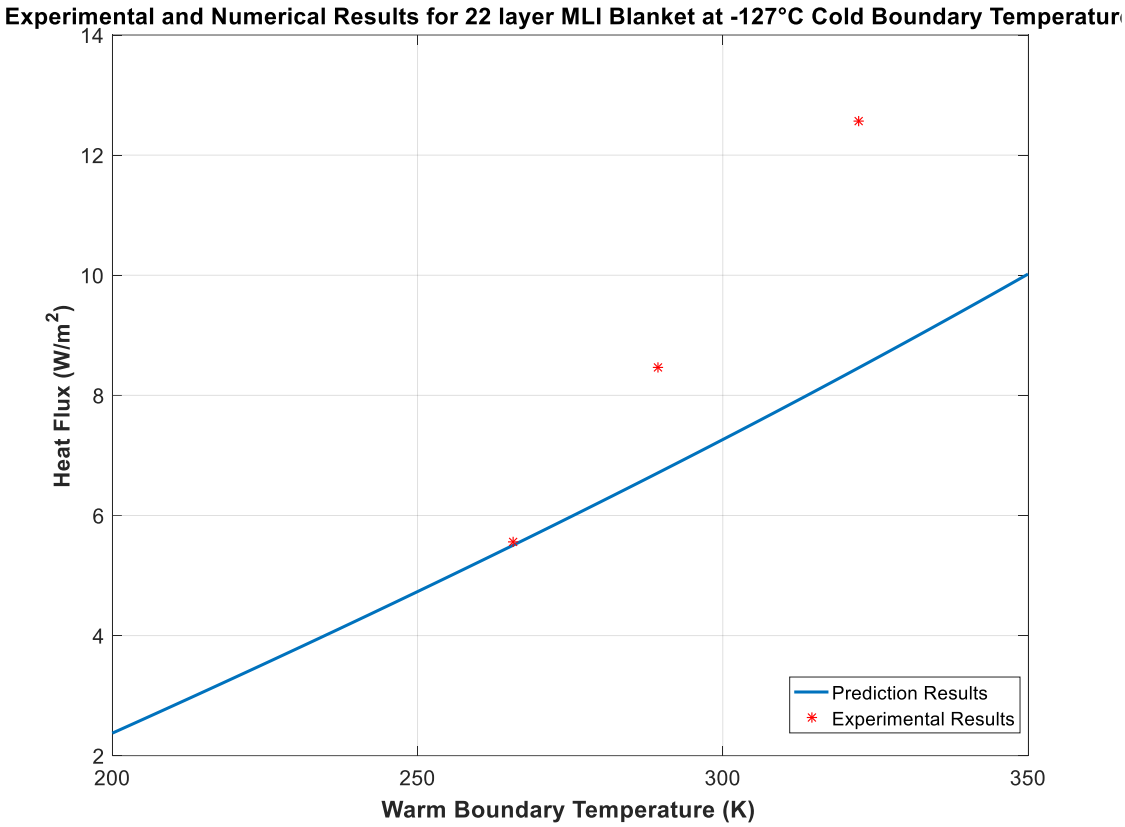

Figure 5.21: Experimental and Numerical Results for 22 layer MLI Blanket at -127°C Cold Boundary Temperature

Table 5-18: Predicted and Experimental Heat Flux Values for 22 layer MLI Blanket at -127°C Cold Boundary Temperature

Warm Boundary Temperature (K)	Experimental Heat Flux (W/m^2)	Predicted Heat Flux (W/m^2)	Error (%)
265.7	5.56	5.50	1.0
289.4	8.46	6.70	20.8
322.2	12.57	8.45	32.7

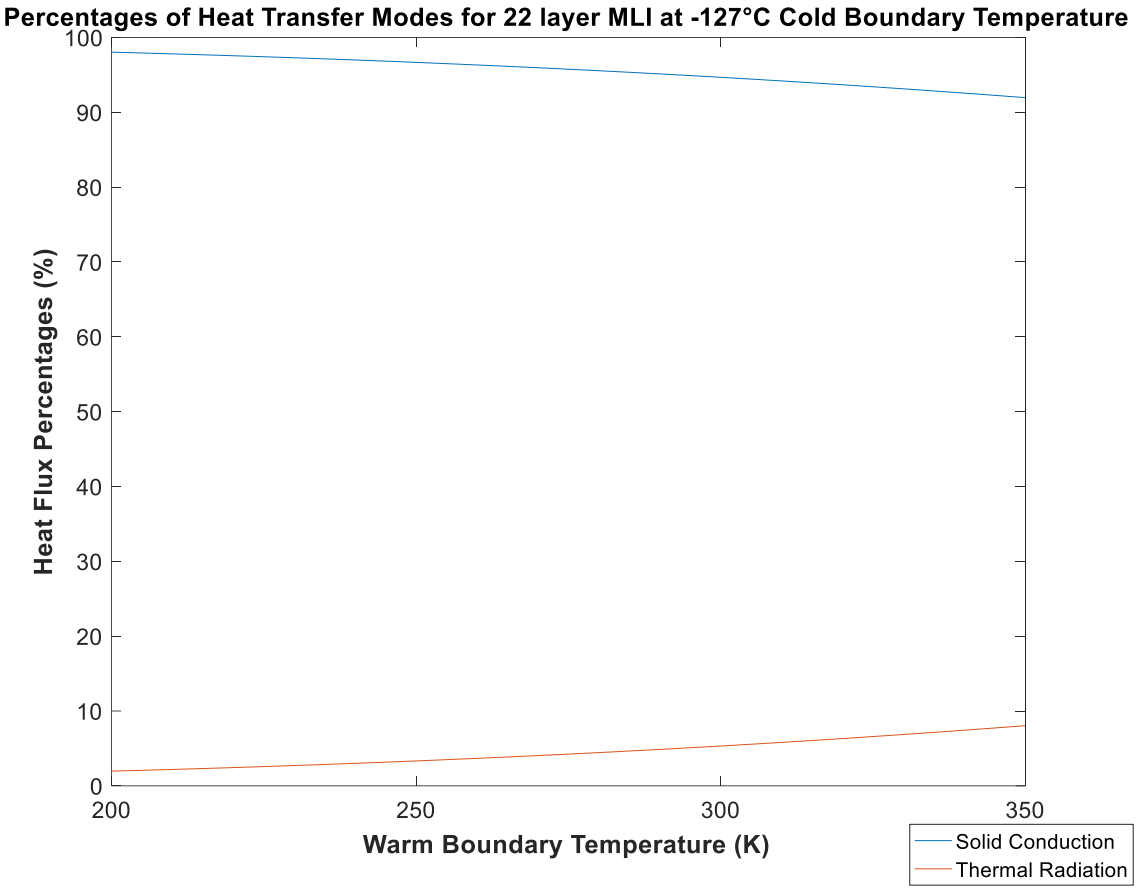

Figure 5.22: Heat Transfer Mode Participation Percentages for 22 layer MLI Blanket at -127°C

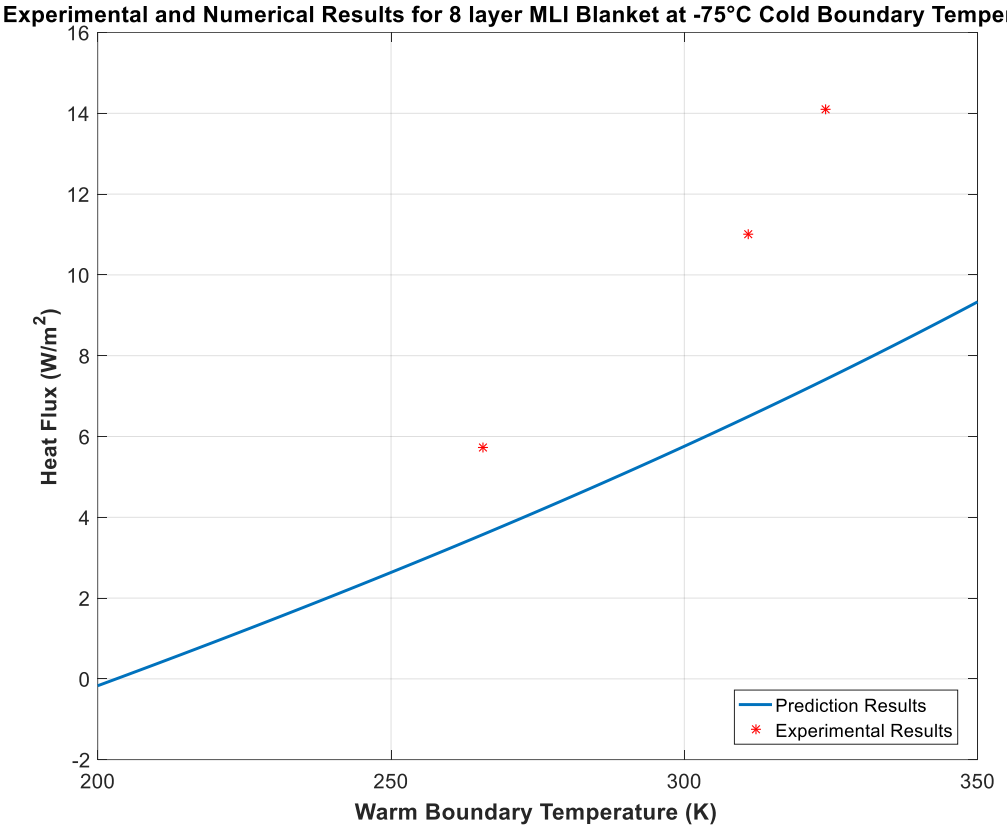

Figure 5.23:Experimental and Numerical Results for 8 layer MLI Blanket at -75°C Cold Boundary Temperature

Table 5-19: Predicted and Experimental Heat Flux Values for 8 layer MLI Blanket at -75°C Cold Boundary Temperature

Warm Boundary Temperature (K)	Experimental Heat Flux (W/m^2)	Predicted Heat Flux (W/m^2)	Error (%)
265.7	5.72	3.58	37.4
310.9	11.02	6.5	41.0
324.1	14.09	7.40	47.5

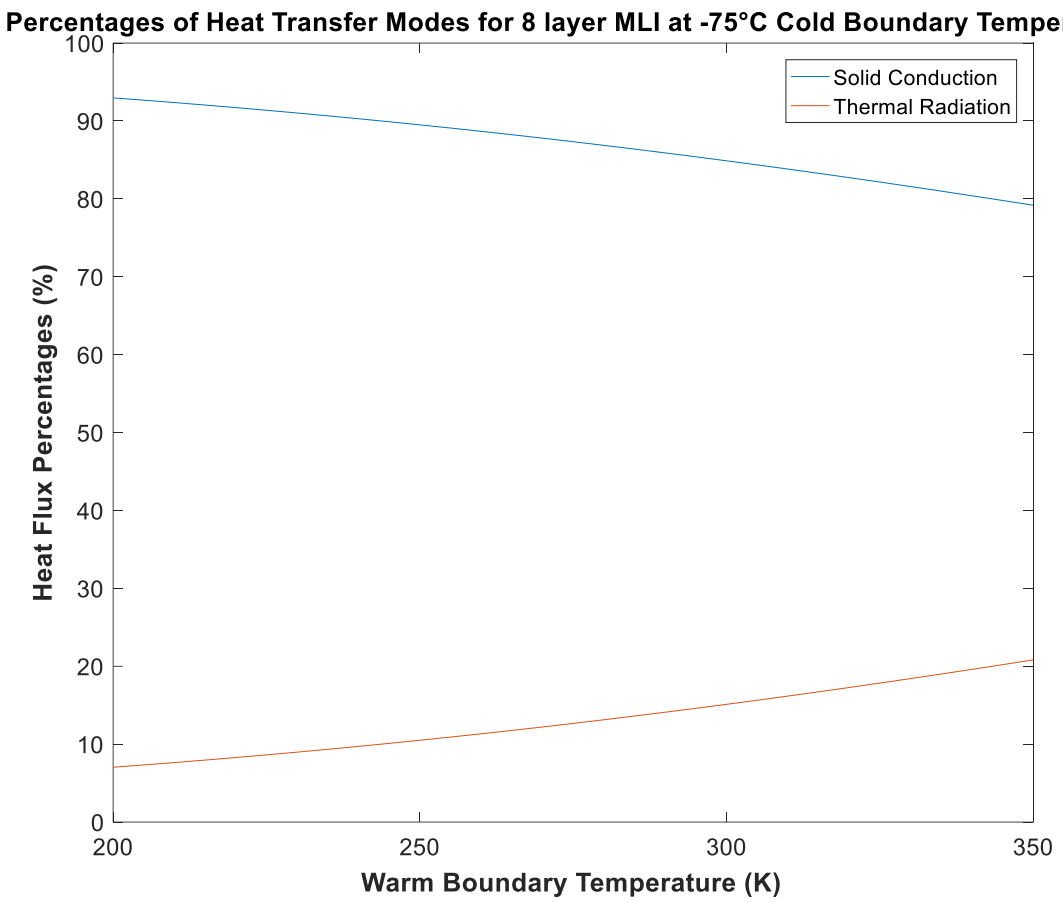

Figure 5.24: Heat Transfer Mode Participation Percentages for 8 layer MLI blanket at -75°C

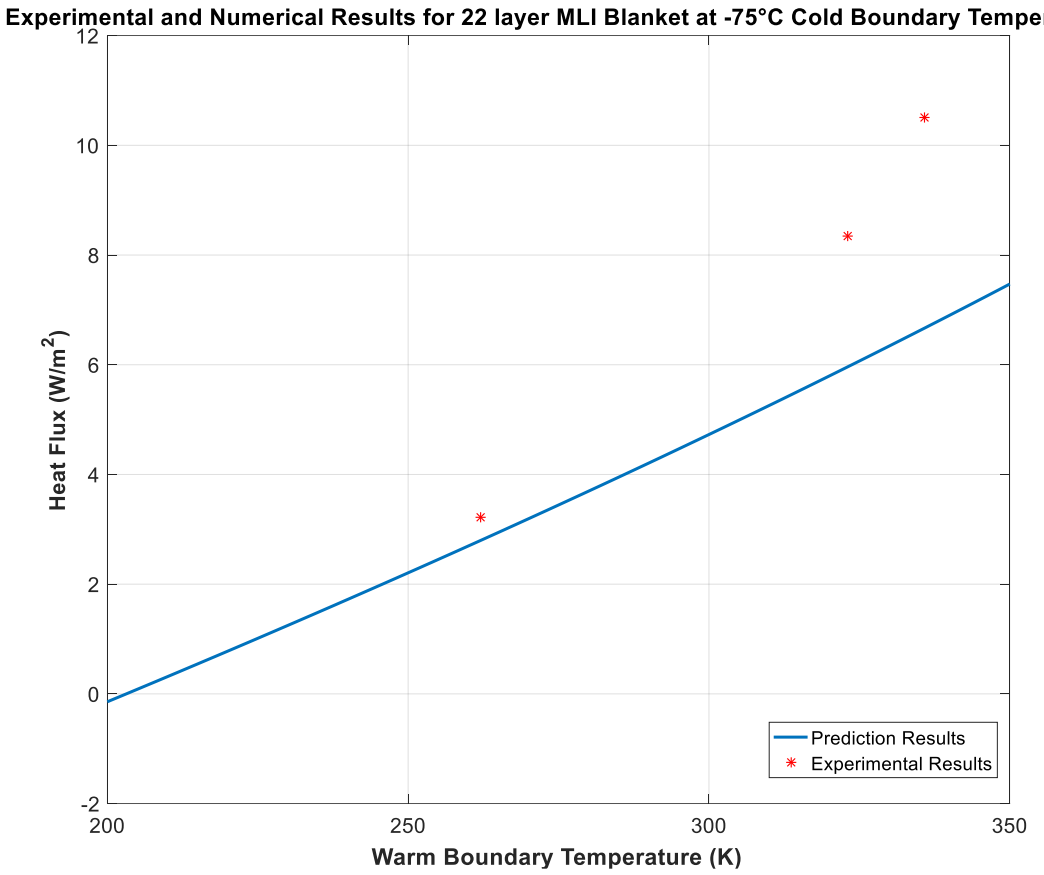

Figure 5.25: Experimental and Numerical Results for 22 layer MLI Blanket at -75°C Cold Boundary Temperature

Table 5-20: Predicted and Experimental Heat Flux Values for 22 layer MLI Blanket at -75°C Cold Boundary Temperature

Warm Boundary Temperature (K)	**Experimental Heat Flux (W/m^2)**	**Predicted Heat Flux (W/m^2)**	**Error (%)**
262.1	3.21	2.80	12.7
323.1	8.35	5.97	28.5
335.8	10.51	6.66	36.6

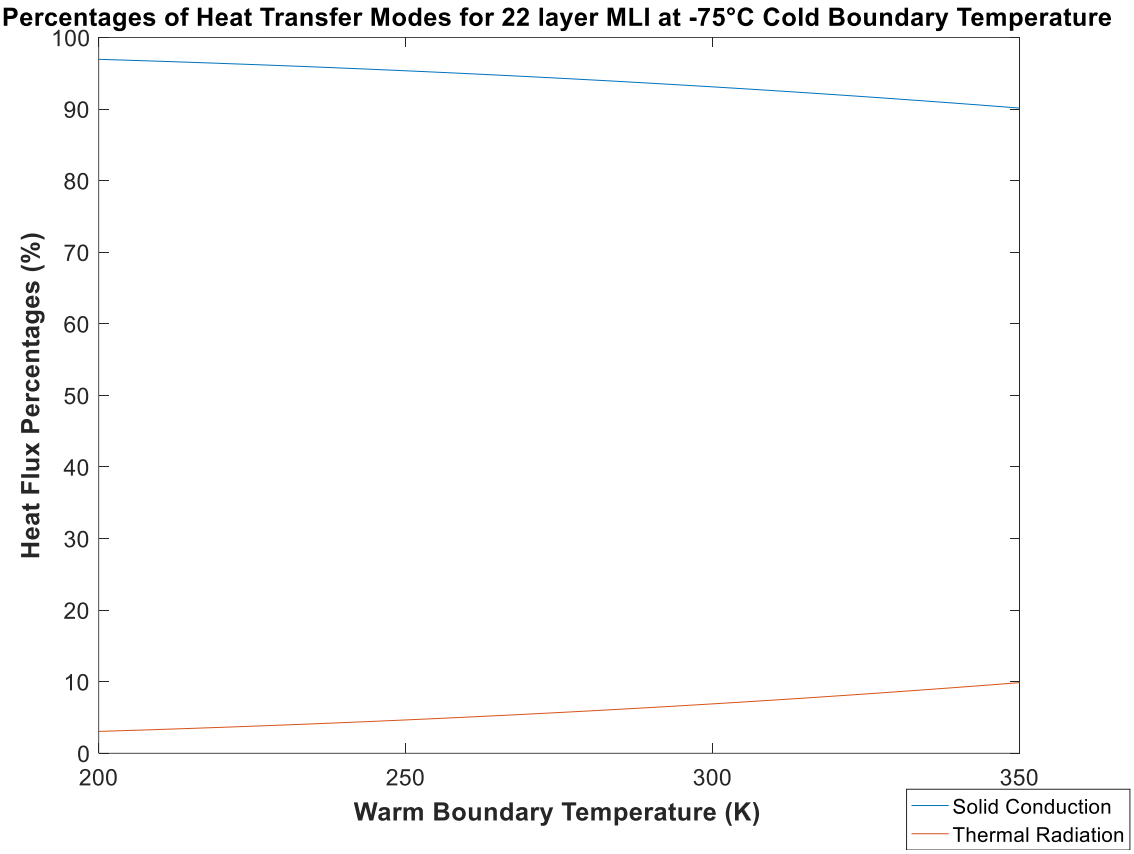

Figure 5.26: Heat Transfer Mode Participation Percentages for 22 layer MLI blanket at -75°C

Overall inspection of predicted heat fluxes by Modified Lockheed Equation and experimental heat flux results reveals that this model is unable to predict the heat fluxes at these boundary temperatures. Unlike other methods, Modified Lockheed equation predicts a linear heat flux along all warm boundary temperatures which shows that the effect of radiation is very small in this model. Both Layer by Layer equation and Modified Lockheed equation were generated for MLI blankets used below 100 K. However, the constants used in Layer by Layer equation were adapted in [22] for higher cold boundary temperatures between 20 K to 300 K. However, the constants used in Lockheed equation were not adapted for higher cold boundary temperatures. Therefore, increased prediction error in Lockheed equation might be attributed to these reasons.

5.4 Comparison of Prediction Models with Each Other's

Temperature dependent heat flux prediction results of investigated models were compared with each other in the following graphs.

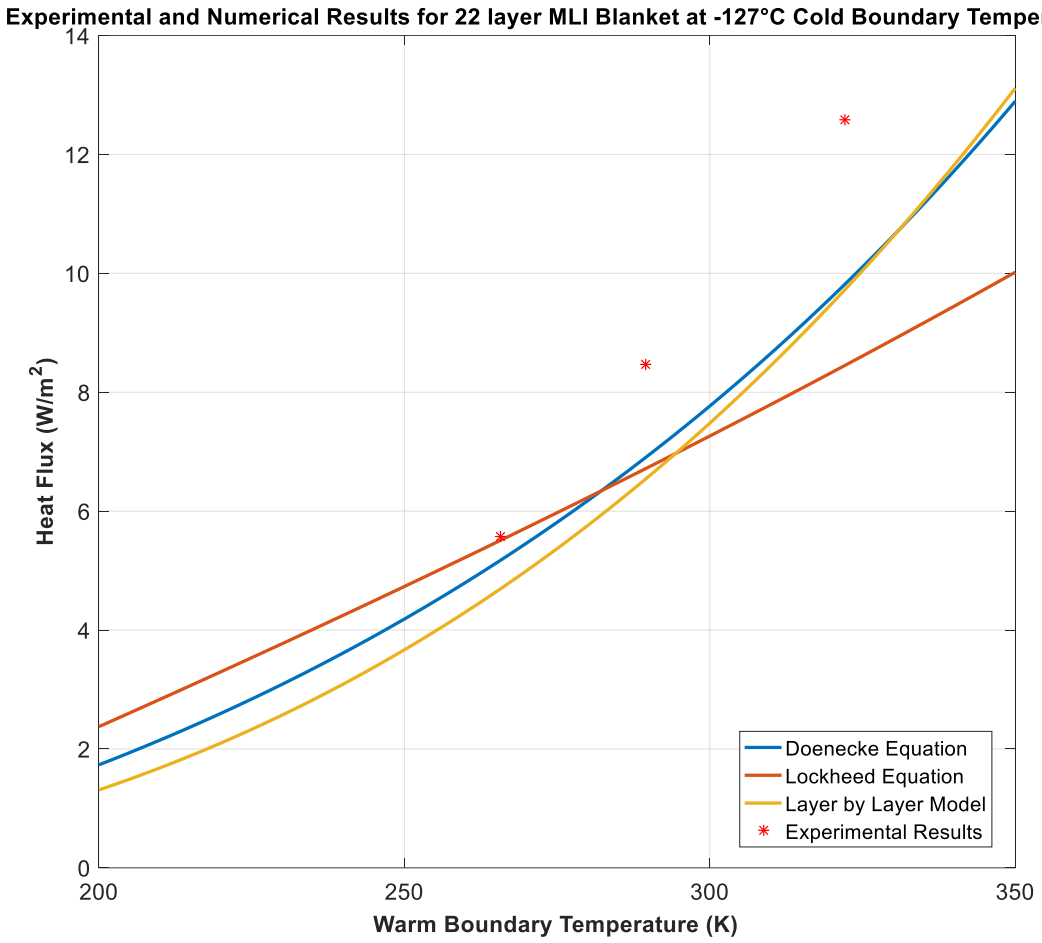

Figure 5.27: Heat Flux Model Curves vs. Experimental Data for 22 Layer MLI Blanket at -127° CBT

The heat flux prediction results of investigated models for 22 layer MLI blanket at -127°C cold boundary temperature is shown above in Figure 5.27 with experimental heat flux results. As illustrated in Figure 5.27, both Doenecke Equation and Layer by Layer equation are able to follow the trend of experimental data. However, overall inspection of heat flux data shows that the Doenecke Equation is more accurate than the Layer by Layer equation. The discrepancy of heat flux results of all three models with respect to experimental data is shown in Table 5-21.

Table 5-21: Comparison of Heat Flux Results of Investigated Models for 22 Layer MLI Blanket at -127°C

Warm Boundary Temperature (K)	Layer by Layer Model Heat Flux (W/m^2)	Doenecke Equation Heat Flux (W/m^2)	Lockheed Equation Heat Flux (W/m^2)	Experimental Heat Flux (W/m^2)
256.4	4.71	4.55	5.50	5.57
289.4	6.50	6.87	6.70	8.46
322.2	9.71	9.81	8.45	12.57

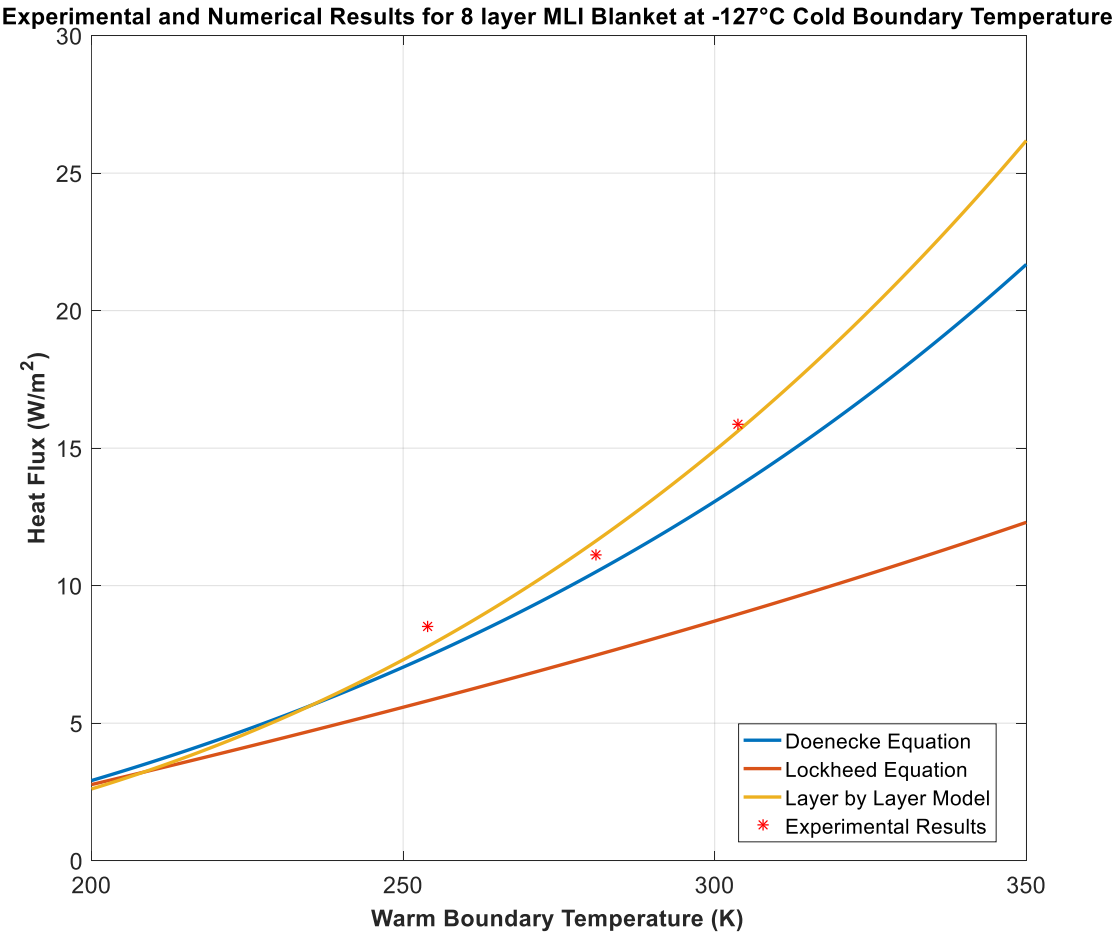

Figure 5.28: Heat Flux Model Curves vs. Experimental Data for 8 Layer MLI Blanket at -127° CBT

The heat flux prediction results of investigated models for 8 layer MLI blanket at -127°C cold boundary temperature is shown above in Figure 5.28 with experimental heat flux results. As illustrated in Figure 5.28, both Doenecke Equation and Layer by Layer equation show very good agreement with the

experimental data. However, overall inspection of heat flux data shows that the Layer by Layer equation is more accurate than the Doenecke Equation as opposed to the heat flux results of 22 layer Blanket at the same cold boundary temperature. The discrepancy of heat flux results of all three models with respect to experimental data is shown in Table 5-22.

Table 5-22: Comparison of Heat Flux Results of Investigated Models for 8 Layer MLI Blanket at -127

Warm Boundary Temperature (K)	**Layer by Layer Model Heat Flux (W/m^2)**	**Doenecke Equation Heat Flux (W/m^2)**	**Lockheed Equation Heat Flux (W/m^2)**	**Experimental Heat Flux (W/m^2)**
254	7.79	7.44	5.81	8.504
281	11.63	10.51	7.48	11.14
303.7	15.64	13.50	8.98	15.86

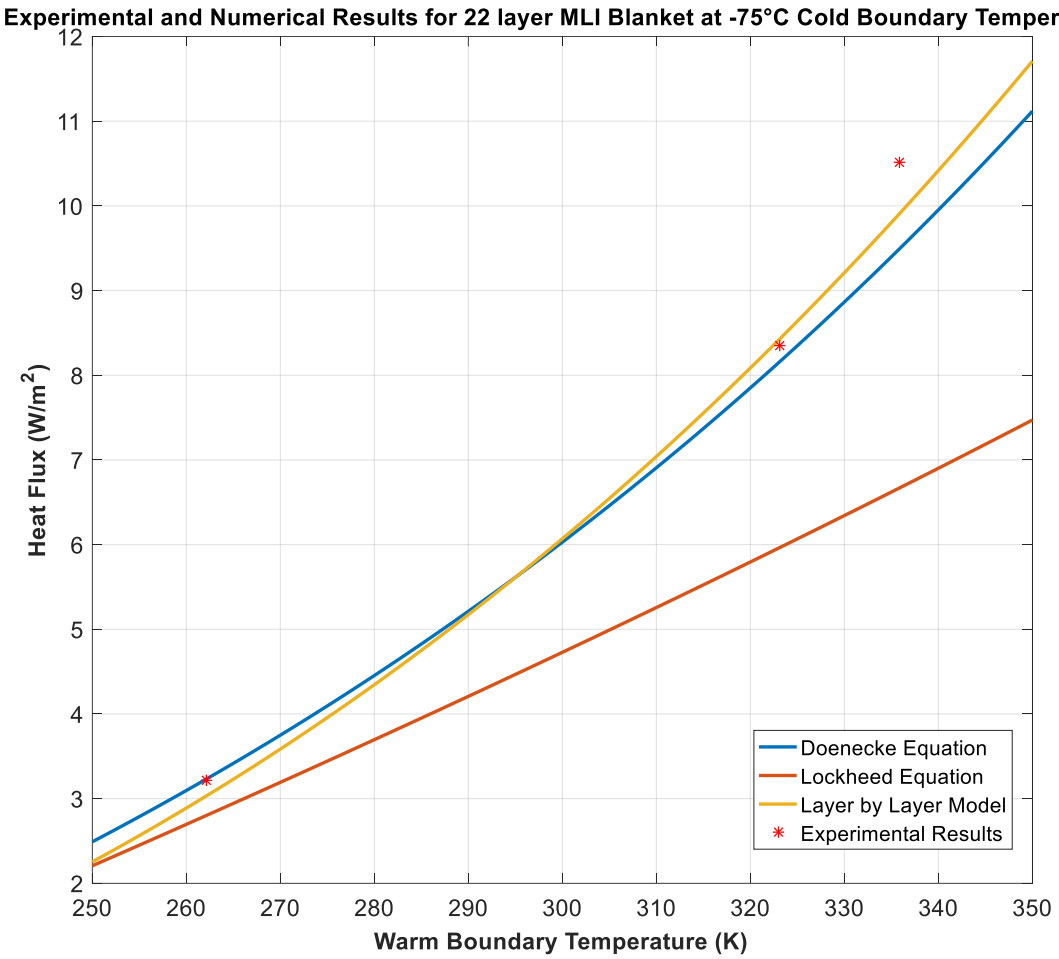

Figure 5.29: Heat Flux Model Curves vs. Experimental Data for 22 Layer MLI Blanket at -75° CBT

The heat flux prediction results of investigated models for 22 layer MLI blanket at -75°C cold boundary temperature is shown above in Figure 5.29 with experimental heat flux results. As illustrated in Figure 5.29, both Doenecke Equation and Layer by Layer equation show good agreement with the experimental data. However, overall inspection of heat flux data shows that the Layer by Layer equation is slightly more accurate than the Doenecke Equation at this cold boundary temperature. The discrepancy of heat flux results of all three models with respect to experimental data is shown in Table 5-23.

Table 5-23: Comparison of Heat Flux Results of Investigated Models for 22 Layer MLI Blanket at -75°C

Warm Boundary Temperature (K)	Layer by Layer Model Heat Flux (W/m^2)	Doenecke Equation Heat Flux (W/m^2)	Lockheed Equation Heat Flux (W/m^2)	Experimental Heat Flux (W/m^2)
262.1	3.02	3.22	2.80	3.21
323.1	8.42	8.15	5.97	8.35
335.8	9.91	9.50	6.66	10.51

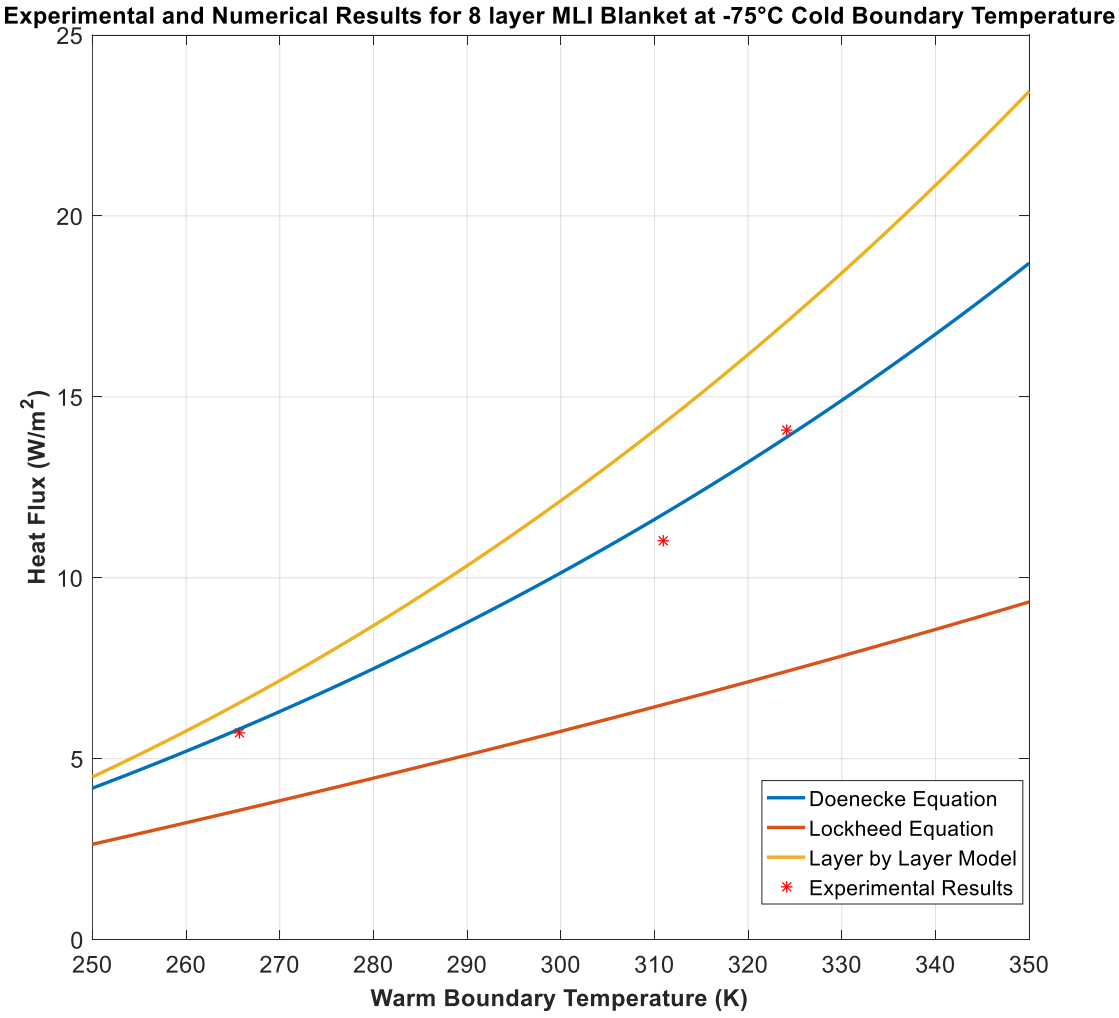

Figure 5.30: Heat Flux Model Curves vs. Experimental Data for 8 Layer MLI Blanket at -75° CBT

The heat flux prediction results of investigated models for 8 layer MLI blanket at -75°C cold boundary temperature is shown above in Figure 5.30 with experimental heat flux results. As illustrated in Figure 5.30, The Layer by Layer

equation overestimates the heat flux predictions at increasing warm boundary temperatures. Even though the Layer by Layer equation gives satisfactory results at the warm boundary temperatures up to 330 K, the model error is increasing above 330 K due to its curve trend. Therefore, the use of Doenecke Equation becomes more favorable. The discrepancy of heat flux results of all three models with respect to experimental data is shown in Table 5-24.

Table 5-24: Comparison of Heat Flux Results of Investigated Models for 8 Layer MLI Blanket at -75°C

Warm Boundary Temperature (K)	**Layer by Layer Model Heat Flux (W/m^2)**	**Doenecke Equation Heat Flux (W/m^2)**	**Lockheed Equation Heat Flux (W/m^2)**	**Experimental Heat Flux (W/m^2)**
265.7	6.57	5.88	3.58	5.73
310.9	14.25	11.77	6.5	11.02
324.1	17.07	13.87	7.40	14.09

6. CONCLUSIONS

MLI blankets are passive thermal control elements used as insulation material in spacecraft applications and cryogenic pipelines. MLI blankets prevent excessive heat loss in spacecraft components which lost heat against deep space temperature which is around 4K. It also prevents excessive heat gain of cryogenic tanks and pipelines used in various industry which exposures direct sunlight and environmental heat.

In order to utilize the MLI concept in industry, it is important to predict and measure the thermal performance of MLI blankets. In literature, there are several research governing MLI blankets experimentally and numerically. Based on literature review, three different equations were selected to predict the heat flux of existing in-house experimental results of 8 and 22 layer MLI blankets.

Layer by Layer equation, Doenecke equation and Modified Lockheed equation were used to predict the heat flux of MLI blankets. In order to utilize these equations, a numerical calculation program were used and the parameters required by these equations were defined. Heat flux prediction of these equations were compared with the MLI blankets to discuss the validity of these equations.

In section 5.1, the Layer by Layer Model was investigated. Heat flux predictions of Layer by Layer model showed that the equation has a good agreement with experimental results for 8 layer MLI blanket at -127°C and 22 layer MLI blanket at -75°C with and average error of 5.5%. However, the equation overestimates the heat flux of 8 layer MLI blanket at -75°C cold boundary temperature with an average error around 21.6%. On the contrary, the equation underestimates the the heat flux of 22 layer MLI blanket at 127°C cold boundary temperature with an average error around 20.3%. Overall inspection of heat fluxes determined by Layer by Layer model shows that this model can be used to predict the heat fluxes of MLI blankets at these cold and warm boundary temperatures.

In section 5.2, the Doenecke equation was investigated. Heat flux predictions of Doenecke equation showed that the equation has a good agreement with

experimental results for both MLI blankets at 75°C cold boundary temperature with an average error of 3.9%. The equation also has a good agreement for 8 layer MLI blanket at -127°C with a slight overestimation. On the other hand, the equation has underestimated heat flux values for 22 layer MLI blanket at -127°C compared with experimental heat flux values. The average error of the equation with the experimental results are 19.6%. Overall inspection of heat fluxes determined by Doenecke equation shows that this model can be used to predict the heat fluxes of MLI blankets at these cold and warm boundary temperatures as well as Layer by Layer model.

In section 5.3, the Modified Lockheed equation was investigated. Heat flux predictions of Modified Lockheed equation showed that the equation is unable to predict the trend of heat fluxes at this boundary temperatures. The equation also strongly underestimates the heat fluxes which are experimentally obtained. Modified Lockheed equation predicts a linear heat flux for all warm boundary temperatures unlike the other investigated models.

For the future work, it is concluded that several studies can be done in order to broaden the knowledge of investigated equations and behavior of thermal performance of MLI blankets under different circumstances.

- The coefficient in Modified Lockheed equation can be optimized to obtain successful heat flux prediction of MLI blankets at these cold and warm boundary temperatures.
- Increasing the steady state experimental heat flux values for different boundary temperature conditions to enlarge the validity of investigated equations.

7. REFERENCES

[1] Gilmore, D., 2002, *Spacecraft Thermal Control Handbook, Volume I: Fundamental Technologies*, American Institute of Aeronautics and Astronautics, Inc., Washington, DC.

[2] Elchert, J. P., 2018, “Cryogenic Multilayer Insulation Theory and An Analysis of Seams Under a Variety of Assumptions,” undefined.

[3] Tien, C. L., and Cunnington, G. R., 1973, “Cryogenic Insulation Heat Transfer,” *Advances in Heat Transfer*, T.F. Irvine, and J.P. Hartnett, eds., Elsevier, pp. 349–417.

[4] Jacob, S., 1993, “Multilayer insulation in cryoequipment - a study of reference literature” [Online]. Available: https://publikationen.bibliothek.kit.edu/270033662. [Accessed: 11-May-2021].

[5] Miyakita, T., Hatakenaka, R., Sugita, H., Saitoh, M., and Hirai, T., 2015, “Evaluation of Thermal Insulation Performance of a New Multi-Layer Insulation with Non-Interlayer-Contact Spacer.”

[6] Hedayat, A., Hastings, L., and Brown, T., 2001, “Analytical Models for Variable Density Multilayer Insulation Used in Cryogenic Storage.”

[7] “Moeini, E., Karimian, S. M., Najafi, H. R., and Esfahani, A. G., ‘Thermal Performance Evaluation of a Fabricated Multilayer Insulation Blanket and Validity of Cunnington-Tien Correlation for This MLI,’ p. 7.”

[8] Krishnaprakas, C. K., Badari Narayana, K., and Dutta, P., 2000, “Heat Transfer Correlations for Multilayer Insulation Systems,” Cryogenics, **40**(7), pp. 431–435.

[9] Spradley, I. E., Nast, T. C., and Frank, D. J., 1990, “Experimental Studies of MLI Systems at Very Low Boundary Temperatures,” *Advances in Cryogenic Engineering: Part A & B*, R.W. Fast, ed., Springer US, Boston, MA, pp. 477–486.

[10] Holmes, V. L., McCRARY, L. E., and Krause, D. R., 1972, “Measurement of Apparent Thermal Conductivity of Multilayer Insulations at Low-Compressive Loads,” J. Spacecr. Rockets, **9**(11), pp. 791–795.

[11] Johnson, W., Frank, D., Nast, T., and Fesmire, J., 2015, “Thermal Performance Testing of Cryogenic Multilayer Insulation with Silk Net Spacers,” IOP Conf. Ser. Mater. Sci. Eng., **101**, p. 012018.

[12] Deng, B., Yang, S., Xie, X., Wu, D., Pan, W., Li, X., and Li, Q., 2019, “Experimental Research of Perforation Rate for Multilayer Insulation Used in Cryogenic Transfer Lines,” IOP Conf. Ser. Mater. Sci. Eng., **502**, p. 012118.

[13] Deng, B., Yang, S., Xie, X., Wang, Y., Bian, X., Gong, L., and Li, Q., 2019, “Study of the Thermal Performance of Multilayer Insulation Used in Cryogenic Transfer Lines,” Cryogenics, **100**, pp. 114–122.

[14] Johnson, W. L., Heckle, K. W., and Hurd, J., 2014, “Thermal Coupon Testing of Load-Bearing Multilayer Insulation,” AIP Conf. Proc., **1573**(1), pp. 725–731.

[15] Johnson, W. L., Vanderlaan, M., Wood, J. J., Rhys, N. O., Guo, W., Sciver, S. V., and Chato, D. J., 2017, “Repeatability of Cryogenic Multilayer Insulation,” IOP Conf. Ser. Mater. Sci. Eng., **278**, p. 012196.

[16] Wang, L. S., and Tien, C. L., 1967, “A Study of Various Limits in Radiation Heat-Transfer Problems,” Int. J. Heat Mass Transf., **10**(10), pp. 1327–1338.

[17] 1974, “Radiation Heat Transfer in Multilayer Insulation Having Perforated Shields,” *Thermophysics and Spacecraft Thermal Control*, American Institute of Aeronautics and Astronautics, pp. 65–74.

[18] *“NASA Technical Reports Server (NTRS)” [Online]. Available: Https://Ntrs.Nasa.Gov/Citations/19740014451. [Accessed: 18-Oct-2020].*

[19] Ross, R. G., 2015, “Quantifying MLI Thermal Conduction in Cryogenic Applications from Experimental Data,” IOP Conf. Ser. Mater. Sci. Eng., **101**, p. 012017.

[20] Doenecke, J., 1993, *Survey and Evaluation of Multilayer Insulation Heat Transfer Measurements*, 932117, SAE International, Warrendale, PA.

[21] McIntosh, G. E., 1994, “Layer by Layer MLI Calculation Using a Separated Mode Equation,” *Advances in Cryogenic Engineering*, P. Kittel, ed., Springer US, Boston, MA, pp. 1683–1690.

[22] Gu, L., 2003, “Generalized Equation for Thermal Conductivity of MLI at Temperatures From 20K to 300K.”

[23] Li, P., and Cheng, H., 2006, “Thermal Analysis and Performance Study for Multilayer Perforated Insulation Material Used in Space,” Appl. Therm. Eng., **26**(16), pp. 2020–2026.

[24] Flynn, T. M., 2004, *Cryogenic Engineering: Second Edition, Revised and Expanded*.

[25] Timmerhaus, K. D., and Reed, R. P., 2007, *Cryogenic Engineering Fifty Years of Progress*, Springer, New York; London.

[26] Kropschot, R. H., 1961, “Multiple Layer Insulation for Cryogenicapplications,” Cryogenics, **1**(3), pp. 171–177.

[27] “ECSS-E-HB-31-01 Part 7A – Thermal Design Handbook – Part 7: Insulations (5 December 2011) | European Cooperation for Space Standardization” [Online]. Available: https://ecss.nl/hbstms/ecss-e-hb-31-01-part-7a-thermal-design-handbook-part-7-insulations-5-december-2011/. [Accessed: 04-Jul-2021].

[28] “Multi-Layer Insulation Films and Tapes from DUNMORE Protect ESA’s Rosetta Mission for Over 10 Years in Space,” PRWeb [Online]. Available: https://www.prweb.com/releases/mli-film/esa-rosetta/prweb12316545.htm. [Accessed: 04-Jul-2021].

[29] “ASTM C740 / C740M-13(2019), Standard Guide for Evacuated Reflective Insulation In Cryogenic Service, ASTM International, West Conshohocken, PA, 2019, Www.Astm.Org.”

[30] “Custom Textile Gallery | Knitted Fabric and Textiles,” Apex Mills.

[31] “Polyethylene Terephthalate - Online Catalogue Source - Supplier of Research Materials in Small Quantities - Goodfellow” [Online]. Available: http://www.goodfellow.com/E/Polyethylene-terephthalate.html. [Accessed: 23-May-2021].

[32] “Nomex® Fiber - STERN EWS” [Online]. Available: https://www.sternandstern.com/fibers/nomex-fiber/. [Accessed: 23-May-2021].

[33] Yamaguchi, H., Ho, M. T., Matsuda, Y., Niimi, T., and Graur, I., 2017, “Conductive Heat Transfer in a Gas Confined between Two Concentric Spheres: From Free-Molecular to Continuum Flow Regime,” Int. J. Heat Mass Transf., **108**, pp. 1527–1534.

[34] “Accommodation Coefficient - an Overview | ScienceDirect Topics” [Online]. Available:

https://www.sciencedirect.com/topics/chemistry/accommodation-coefficient. [Accessed: 03-Sep-2021].

[35] Corruccini, R. J., 1959, “Gaseous Heat Conduction at Low Pressures and Temperatures,” Vacuum, **7–8**, pp. 19–29.

[36] Keller, C. W., 1971, *Thermal Performance of Multilayer Insulations Final Report*, LMSC-A974469.

[37] Kuchnir, M., 1980, “Apparatus to Measure Thermal Conductance,” Cryogenics, **20**(4), pp. 203–207.

[38] Johnson, W., 2010, “Thermal Performance Of Cryogenic Multilayer Insulation At Various Layer Spacings,” Electron. Theses Diss. 2004-2019.

[39] “Radiative Heat Transfer - 3rd Edition” [Online]. Available: https://www.elsevier.com/books/radiative-heat-transfer/modest/978-0-12-386944-9. [Accessed: 26-Aug-2021].

[40] *MATLAB Release 2016a The MathWorks, Inc., Natick, Massachusetts, United States.*

8. APPENDIX

8.1 Appendix 1 – Layer-by-Layer Model 22 Layer MLI Blanket at Cold Boundary Layer at -127°C MATLAB Code

```
%% 22 Layer MLI Blanket at Cold Boundary Layer at -127°C %%
clc
clear all

A=0.52*0.52*2; %Surface Area
T(1)=-127+273.15; % Average temperature at cold boundary layer
j=1;
N=23; % Number of Reflector Layer

delx= 0.000202; % Actual seperator thickness in m obtained by
measuring
f= 0.1193; % Seperator density obtained by netting density/solid
dacron density

sigma= 5.670*10^-8; % Stefan-boltzmann constant

for temp= 200:1:350 %Warm boundary temperature sweep

T(N)=temp; % Temperature at warm boundary layer sweep

delT=(T(N)-T(1))/(N-1); % Initial temperature distrubition between
each layer

for i=1:1:(N-1)

T(i+1)=T(i)+delT;

end

T; % Initial temperature distrubition

for k=1:1:20 % Iteration number
for i=1:1:(N-1)

% Solid conduction term
Tc(i)=(T(i+1)+T(i))/2;
c2(i)= 0.008*(-0.20056703+3.2843027*10^-5*(Tc(i)^2)); % Dacron
constant
ks(i)= 0.017+7*10^-6*(800-Tc(i))+0.0228*log(Tc(i)); % Temperature
dependent dacron conductivity
Ks(i)=c2(i)*f*ks(i)/delx; % Conductance of solid conduction term
qs(i)=Ks(i)*((T(i+1))-(T(i))); % Heat flow due to conduction

% Radiative heat transfer term
em(i)=(0.011823+6.17562*10^-5*(T(i))); % Temperature dependent
emissivity of DAM
Kr(i)=(em(i)/(2-em(i))).*sigma*
((T(i+1))^2+(T(i))^2)*((T(i+1))+(T(i))); % Conductance due radiaiton
qr(i)=Kr(i)*(((T(i+1))-(T(i)))); % Heat flow due to radiation
%

% Gaseous conduction term
```

```
C1=1.1666; %Gas constant for air
p=0.0005; % Interstitial pressure by Pascal
alpha= 0.9; % Accomodation coefficient for air
Kg(i)= C1*p*alpha; % Gaseous conductance
qg=Kg*(((T(i+1))-(T(i)))); % Heat flow due to gaseous conduction

KT=Ks+Kg+Kr; % Sum of conductances at layer i
RT=KT.^-1; % Thermal resistance at layer i

end

for i=1:1:(N-1)

totalReal=sum(RT); % Total thermal resistance for 22 Layer  MLI
blanket
Real=sum(RT(1:i)); % Thermal resistance between layer 1 to i
T(i+1)=T(1)+(Real/totalReal)*(T(N)-T(1)); % New temperature
distribution considering thermal resistances
end
q=qr(1)+qs(1)+qg(1); % Total heat flow across MLI blanket
end

qtotal(j)=q; % Heat Flux W/m^2
j=j+1;

end
T % Temperature distrubition after iteration

N=1:1:N;
totalpower=qr+qg+qs % Heat Fluxes between each alternating layer pair
temp=200:1:350;
figure(1)
plot(temp,qtotal,'lineWidth',2)
hold on
plot(265.7,3.01/A,'r*') % Experimental Values (Yeni)
plot(289.4,4.578/A,'r*') % Experimental Values (Yeni)
plot(322.2,6.80/A,'r*') % Experimental Values (Yeni)
grid on
xlabel('Warm Boundary Temperature (K)','Fontsize',14)
ylabel('Heat Flux (W/m^2)','Fontsize',14)
legend('Prediction Results','Experimental Results')
title('Experimental and Numerical Results for 22 layer MLI Blanket at
-127°C Cold Boundary Temperature','Fontsize',14)
set(gca,'FontSize',14)
```

8.2 Appendix 2 – Layer-by-Layer Model 8 Layer MLI Blanket at Cold Boundary Layer at -127°C MATLAB Code

```
%% 8 Layer MLI Blanket at Cold Boundary Layer at -127°C %%
clc
clear all

A=0.52*0.52*2; %Surface Area
T(1)=-127+273.15; % Average temperature at cold boundary layer
j=1;
N=9; % Number of Reflector Layer

delx= 0.000282; % Actual seperator thickness in m obtained by
measuring
f= 0.1193; % Seperator density obtained by netting density/solid
dacron density

sigma= 5.670*10^-8; % Stefan-boltzmann constant

for temp= 200:1:350 % Warm boundary temperature sweep

T(N)=temp; % Temperature at warm boundary layer sweep

delT=(T(N)-T(1))/(N-1); % Initial temperature distrubition between
each layer

for i=1:1:(N-1)

T(i+1)=T(i)+delT;

end

T; % Initial temperature distrubition

for k=1:1:20 % Iteration number
for i=1:1:(N-1)

% Solid conduction term
Tc(i)=(T(i+1)+T(i))/2;
c2(i)= 0.008*(-0.20056703+3.2843027*10^-5*(Tc(i)^2)); % Dacron
constant
ks(i)= 0.017+7*10^-6*(800-Tc(i))+0.0228*log(Tc(i)); % Temperature
dependent dacron conductivity
Ks(i)=c2(i)*f*ks(i)/delx; % Conductance of solid conduction term
qs(i)=Ks(i)*((T(i+1))-(T(i))); % Heat flow due to conduction

% Radiative heat transfer term
em(i)=(0.011823+6.17562*10^-5*(T(i))); % Temperature dependent
emissivity of DAM
Kr(i)=(em(i)/(2-em(i))).*sigma*
((T(i+1))^2+(T(i))^2)*((T(i+1))+(T(i))); % Conductance due radiaiton
qr(i)=Kr(i)*(((T(i+1))-(T(i)))); % Heat flow due to radiation
%

% Gaseous conduction term
C1=1.1666; % Gas constant for air
p=0.0005; % Interstitial pressure by Pascal
alpha= 0.9; % Accomodation coefficient for air
```

```
Kg(i)= C1*p*alpha; % Gaseous conductance
qg=Kg*(((T(i+1))-(T(i)))); % Heat flow due to gaseous conduction

KT=Ks+Kg+Kr; % Sum of conductances at layer i
RT=KT.^-1; % Thermal resistance at layer i

end

for i=1:1:(N-1)

totalReal=sum(RT); % Total thermal resistance for 22 Layer  MLI
blanket
Real=sum(RT(1:i)); % Thermal resistance between layer 1 to i
T(i+1)=T(1)+(Real/totalReal)*(T(N)-T(1)); % New temperature
distribution considering thermal resistances
end
q=qr(1)+qs(1)+qg(1); % Total heat flow across MLI blanket
end

qtotal(j)=q; % Heat Flux W/m^2
j=j+1;

end
T % Temperature distrubition after iteration

N=1:1:N;
totalpower=qr+qg+qs % Heat Fluxes between each alternating layer pair
temp=200:1:350;
figure()
plot(temp,qtotal,'lineWidth',2)
hold on

plot(254,4.599/A,'r*') % Experimental Values 8 layer (Yeni)
plot(281,6.024/A,'r*') % Experimental Values 8 layer (Yeni)
plot(303.7,8.578/A,'r*') % Experimental Values 8 layer (Yeni)
grid on
xlabel('Warm Boundary Temperature (K)','Fontsize',14)
ylabel('Heat Flux (W/m^2)','Fontsize',14)
legend('Prediction Results','Experimental Results')
title('Experimental and Numerical Results for 8 layer MLI Blanket at -
127°C Cold Boundary Temperature','Fontsize',14)
set(gca,'FontSize',14)
```

8.3 Appendix 3 – Layer by Layer Model 22 Layer MLI Blanket at Cold Boundary Layer at -75°C MATLAB Code

```
%% 22 Layer MLI Blanket at Cold Boundary Layer at -75°C %%
clc
clear all

A=0.52*0.52*2; %Surface Area
T(1)=-75+273.15; % Average temperature at cold boundary layer
j=1;
N=23; % Number of Reflector Layer

delx= 0.000202; % Actual seperator thickness in m obtained by
measuring
f= 0.1193; % Seperator density obtained by netting density/solid
dacron density

sigma= 5.670*10^-8; % Stefan-boltzmann constant

for temp= 250:1:350 % Warm boundary temperature sweep

T(N)=temp; % Temperature at warm boundary layer sweep

delT=(T(N)-T(1))/(N-1); % Initial temperature distrubition between
each layer

for i=1:1:(N-1)

T(i+1)=T(i)+delT;

end
T; %Initial temperature distrubition
for k=1:1:20 % Iteration number
for i=1:1:(N-1)

% Solid conduction term
Tc(i)=(T(i+1)+T(i))/2;
c2(i)= 0.008*(-0.20056703+3.2843027*10^-5*(Tc(i)^2)); %Dacron constant
ks(i)= 0.017+7*10^-6*(800-Tc(i))+0.0228*log(Tc(i)); % Temperature
dependent dacron conductivity
Ks(i)=c2(i)*f*ks(i)/delx; % Conductance of solid conduction term
qs(i)=Ks(i)*((T(i+1))-(T(i))); % Heat flow due to conduction

% Radiative heat transfer term
em(i)=(0.011823+6.17562*10^-5*(T(i)));  % Temperature dependent
emissivity of DAM
Kr(i)=(em(i)/(2-em(i))).*sigma*
((T(i+1))^2+(T(i))^2)*((T(i+1))+(T(i))); % Conductance due radiaiton
qr(i)=Kr(i)*(((T(i+1))-(T(i)))); % Heat flow due to radiation
%

% Gaseous conduction term
C1=1.1666; %Gas constant for air
p=0.0005; % Interstitial pressure by Pascal
alpha= 0.9; % Accomodation coefficient for air
Kg(i)= C1*p*alpha; % Gaseous conductance
qg=Kg*(((T(i+1))-(T(i)))); % Heat flow due to gaseous conduction
```

```
KT=Ks+Kg+Kr; % Sum of conductances at layer i
RT=KT.^-1; % Thermal resistance at layer i

end
%
for i=1:1:(N-1)

totalReal=sum(RT); % Total thermal resistance for 8 Layer  MLI blanket
Real=sum(RT(1:i)); % Thermal resistance between layer 1 to i
T(i+1)=T(1)+(Real/totalReal)*(T(N)-T(1)); % New temperature
distribution considering thermal resistances
end
q=qr(1)+qs(1)+qg(1); % Total heat flow across MLI blanket
end

qtotal(j)=q; % Heat Flux w/m^2
j=j+1;

end
T %temperature distrubition after iteration

N=1:1:N;
totalpower=qr+qg+qs % Heat Fluxes between each alternating layer pair
temp=250:1:350;
figure()
plot(temp,qtotal,'lineWidth',2)
hold on

plot(262.1,1.736/A,'r*') % Experimental Values 22 layer (Yeni)
plot(323.1,4.515/A,'r*') % Experimental Values 22 layer (Yeni)
plot(335.8,5.685/A,'r*') % Experimental Values 22 layer (Yeni)
grid on
xlabel('Warm Boundary Temperature (K)','Fontsize',14)
ylabel('Heat Flux (W/m^2)','Fontsize',14)
legend('Prediction Results','Experimental Results')
title('Experimental and Numerical Results for 22 layer MLI Blanket at
-75°C Cold Boundary Temperature','Fontsize',14)
set(gca,'FontSize',14)
```

8.4 Appendix 4 – Layer by Layer Model 8 Layer MLI Blanket at Cold Boundary Layer at -75°C MATLAB Code

```
%% 8 Layer MLI Blanket at Cold Boundary Layer at -75°C %%
clc
clear all

A=0.52*0.52*2; %Surface Area
T(1)=-75+273.15; % Average temperature at cold boundary layer
j=1;
N=9; % Number of Reflector Layer

delx= 0.000282; % Actual seperator thickness in m obtained by
measuring
f= 0.1193; % Seperator density obtained by netting density/solid
dacron density

sigma= 5.670*10^-8; % Stefan-boltzmann constant

for temp= 250:1:350 % Warm boundary temperature sweep

T(N)=temp; % Temperature at warm boundary layer sweep

delT=(T(N)-T(1))/(N-1); % Initial temperature distrubition between
each layer

for i=1:1:(N-1)

T(i+1)=T(i)+delT;

end
T; %Initial temperature distrubition
for k=1:1:20 % Iteration number
for i=1:1:(N-1)

% Solid conduction term
Tc(i)=(T(i+1)+T(i))/2;
c2(i)= 0.008*(-0.20056703+3.2843027*10^-5*(Tc(i)^2)); %Dacron constant
ks(i)= 0.017+7*10^-6*(800-Tc(i))+0.0228*log(Tc(i)); % Temperature
dependent dacron conductivity
Ks(i)=c2(i)*f*ks(i)/delx; % Conductance of solid conduction term
qs(i)=Ks(i)*((T(i+1))-(T(i))); % Heat flow due to conduction

% Radiative heat transfer term
em(i)=(0.011823+6.17562*10^-5*(T(i)));  % Temperature dependent
emissivity of DAM
Kr(i)=(em(i)/(2-em(i))).*sigma*
((T(i+1))^2+(T(i))^2)*((T(i+1))+(T(i))); % Conductance due radiaiton
qr(i)=Kr(i)*(((T(i+1))-(T(i)))); % Heat flow due to radiation
%

% Gaseous conduction term
C1=1.1666; %Gas constant for air
p=0.0005; % Interstitial pressure by Pascal
alpha= 0.9; % Accomodation coefficient for air
Kg(i)= C1*p*alpha; % Gaseous conductance
```

```
qg=Kg*(((T(i+1))-(T(i)))); % Heat flow due to gaseous conduction

KT=Ks+Kg+Kr; % Sum of conductances at layer i
RT=KT.^-1; % Thermal resistance at layer i

end
%
for i=1:1:(N-1)

totalReal=sum(RT); % Total thermal resistance for 8 Layer  MLI blanket
Real=sum(RT(1:i)); % Thermal resistance between layer 1 to i
T(i+1)=T(1)+(Real/totalReal)*(T(N)-T(1)); % New temperature
distribution considering thermal resistances
end
q=qr(1)+qs(1)+qg(1); % Total heat flow across MLI blanket
end

qtotal(j)=q; % Heat Flux w/m^2
j=j+1;

end
T %temperature distrubition after iteration

N=1:1:N;
totalpower=qr+qg+qs % Heat Fluxes between each alternating layer pair
temp=250:1:350;
figure()
plot(temp,qtotal,'lineWidth',2)
hold on

plot(265.7,3.096/A,'r*') % Experimental Values (Yeni)
plot(310.9,5.957/A,'r*') % Experimental Values (Yeni)
plot(324.1,7.62/A,'r*') % Experimental Values (Yeni)


grid on
xlabel('Warm Boundary Temperature (K)','Fontsize',14)
ylabel('Heat Flux (W/m^2)','Fontsize',14)
legend('Prediction Results','Experimental Results')
title('Experimental and Numerical Results for 8 layer MLI Blanket at -
75°C Cold Boundary Temperature','Fontsize',14)
set(gca,'FontSize',14)
```

8.5 Appendix 5 – Doenecke Method 22 Layer MLI Blanket at Cold Boundary Layer at -127°C MATLAB Code

```
%% 22 Layer MLI Blanket at Cold Boundary Layer at -127°C with Heat
Transfer Mode Percentages%%
clc
clear all

sigma= 5.675*10^-8; % Stefan-boltzmann constant
A=0.52*0.52*2; % MLI blanket surface area
fn=0.9530; % Blanket number of layer parameter
fp=0.9491; % Blanket perforatiion parameter
fa= (1/10)^(0.373*log10(A)); % Blanket area parameter

Tc= -127+273.15; %Cold Boundary Temperature
Th=200:1:350;
Tm=nthroot(((Th.^2+Tc.^2).*(Tc+Th))./4,3); % Mean temperature

qc=(0.000136.*(1./(4.*sigma.*Tm.^2)).*fn.*fa.*fp).*sigma.*(Th.^4-
Tc.^4); % Solid Conduction Heat Flux
qr=((0.000121.*Tm.^0.667).*fn.*fa.*fp).*sigma.*(Th.^4-Tc.^4); %
Thermal Radiation Heat Flux
qt=qc+qr;

qcp=qc./qt*100; % Solid Conduction Percentage
qrp=qr./qt*100; % Thermal Radiation Percentage

figure(1)
plot(Th,qcp)
hold on
plot(Th,qrp)

xlabel('Warm Boundary Temperature (K)','Fontsize',14, 'FontWeight',
'bold')
ylabel('Heat Flux Percentages (%)','Fontsize',14, 'FontWeight',
'bold')
legend('Solid Conduction','Thermal Radiation')
title('Percentages of Heat Transfer Modes for 22 layer MLI at -127°C
Cold Boundary Temperature','Fontsize',14)
set(gca,'FontSize',14)

figure(2)
plot(Th,qt,'lineWidth',2)
title('Experimental and Numerical Results for 22 layer MLI Blanket at
-127°C Cold Boundary Temperature','Fontsize',14)
hold on
grid on

plot(265.7,3.01/A,'r*') % Experimental Values
plot(289.4,4.578/A,'r*') % Experimental Values
plot(322.2,6.80/A,'r*') % Experimental Values
xlabel('Warm Boundary Temperature (K)','Fontsize',14, 'FontWeight',
'bold')
ylabel('Heat Flux (W/m^2)','Fontsize',14, 'FontWeight', 'bold')
set(gca,'FontSize',14)

legend('Prediction Results','Experimental Results')
```

8.6 Appendix 6 – Doenecke Method 8 Layer MLI Blanket at Cold Boundary Layer at -127°C MATLAB Code

```
%% 8 Layer MLI Blanket at Cold Boundary Layer at -127°C with Heat
Transfer Mode Percentages%%
clc
clear all

sigma= 5.675*10^-8; % Stefan-boltzmann constant
A=0.52*0.52*2; % MLI blanket surface area
fn=1.6023; % Blanket number of layer parameter
fp=0.9491; % Blanket perforatiion parameter
fa= (1/10)^(0.373*log10(A)); % Blanket area parameter

Tc= -127+273.15;
Th=200:1:350;
Tm=nthroot(((Th.^2+Tc.^2).*(Tc+Th))./4,3); % Mean temperature

qc=(0.000136.*(1./(4.*sigma.*Tm.^2)).*fn.*fa.*fp).*sigma.*(Th.^4-
Tc.^4); % Solid Conduction Heat Flux
qr=((0.000121.*Tm.^0.667).*fn.*fa.*fp).*sigma.*(Th.^4-Tc.^4); %
Thermal Radiation Heat Flux
qt=qc+qr;

qcp=qc./qt*100; % Solid Conduction Percentage
qrp=qr./qt*100; % Thermal Radiation Percentage

figure(1)
plot(Th,qcp)
hold on
plot(Th,qrp)

xlabel('Warm Boundary Temperature (K)','Fontsize',14, 'FontWeight',
'bold')
ylabel('Heat Flux Percentages (%)','Fontsize',14, 'FontWeight',
'bold')
legend('Solid Conduction','Thermal Radiation')
title('Percentages of Heat Transfer Modes for 8 layer MLI at -127°C
Cold Boundary Temperature','Fontsize',14)
set(gca,'FontSize',14)

figure(2)
plot(Th,qt,'lineWidth',2)
title('Experimental and Numerical Results for 8 layer MLI Blanket at -
127°C Cold Boundary Temperature','Fontsize',14)
hold on
grid on

plot(254,4.599/A,'r*') % Experimental Values 8 layer
plot(281,6.024/A,'r*') % Experimental Values 8 layer
plot(303.7,8.578/A,'r*') % Experimental Values 8 layer
xlabel('Warm Boundary Temperature (K)','Fontsize',14, 'FontWeight',
'bold')
ylabel('Heat Flux (W/m^2)','Fontsize',14, 'FontWeight', 'bold')
set(gca,'FontSize',14)

legend('Prediction Results','Experimental Results')
```

8.7 Appendix 7 – Doenecke Method 22 Layer MLI Blanket at Cold Boundary Layer at -75°C MATLAB Code

```
%% 22 Layer MLI Blanket at Cold Boundary Layer at -75°C with Heat
Transfer Mode Percentages%%
clc
clear all

sigma= 5.675*10^-8; % Stefan-boltzmann constant
A=0.52*0.52*2; % MLI blanket surface area
fn=0.9530; % Blanket number of layer parameter
fp=0.9491; % Blanket perforatiion parameter
fa= (1/10)^(0.373*log10(A)); % Blanket area parameter

Tc= -75+273.15;
Th=250:1:350;
Tm=nthroot(((Th.^2+Tc.^2).*(Tc+Th))./4,3); % Mean temperature

qc=(0.000136.*(1./(4.*sigma.*Tm.^2)).*fn.*fa.*fp).*sigma.*(Th.^4-
Tc.^4); % Solid Conduction Heat Flux
qr=((0.000121.*Tm.^0.667).*fn.*fa.*fp).*sigma.*(Th.^4-Tc.^4); %
Thermal Radiation Heat Flux
qt=qc+qr;

qcp=qc./qt*100; % Solid Conduction Percentage
qrp=qr./qt*100; % Thermal Radiation Percentage

figure(1)
plot(Th,qcp)
hold on
plot(Th,qrp)

xlabel('Warm Boundary Temperature (K)','Fontsize',14, 'FontWeight',
'bold')
ylabel('Heat Flux Percentages (%)','Fontsize',14, 'FontWeight',
'bold')
legend('Solid Conduction','Thermal Radiation')
title('Percentages of Heat Transfer Modes for 22 layer MLI at -75°C
Cold Boundary Temperature','Fontsize',14)
set(gca,'FontSize',14)

figure(2)
plot(Th,qt,'lineWidth',2)
title('Experimental and Numerical Results for 22 layer MLI Blanket at
-75°C Cold Boundary Temperature','Fontsize',14)
hold on
grid on

xlabel('Warm Boundary Temperature (K)','Fontsize',14, 'FontWeight',
'bold')
ylabel('Heat Flux (W/m^2)','Fontsize',14, 'FontWeight', 'bold')
plot(262.1,1.736/A,'r*') % Experimental Values 22 layer
plot(323.1,4.515/A,'r*') % Experimental Values 22 layer
plot(335.8,5.685/A,'r*') % Experimental Values 22 layer
set(gca,'FontSize',14)

legend('Prediction Results','Experimental Results')
```

8.8 Appendix 8 – Doenecke Method 8 Layer MLI Blanket at Cold Boundary Layer at -75°C MATLAB Code

```
%% 8 Layer MLI Blanket at Cold Boundary Layer at -75°C with Heat
Transfer Mode Percentages%%
clc
clear all

sigma= 5.675*10^-8; % Stefan-boltzmann constant
A=0.52*0.52*2; % MLI blanket surface area
fn=1.6023; % Blanket number of layer parameter
fp=0.9491; % Blanket perforatiion parameter
fa= (1/10)^(0.373*log10(A)); % Blanket area parameter

Tc= -75+273.15;
Th=250:1:350;
Tm=nthroot(((Th.^2+Tc.^2).*(Tc+Th))./4,3); % Mean temperature

qc=(0.000136.*(1./(4.*sigma.*Tm.^2)).*fn.*fa.*fp).*sigma.*(Th.^4-
Tc.^4); % Solid Conduction Heat Flux
qr=((0.000121.*Tm.^0.667).*fn.*fa.*fp).*sigma.*(Th.^4-Tc.^4); %
Thermal Radiation Heat Flux
qt=qc+qr;

qcp=qc./qt*100; % Solid Conduction Percentage
qrp=qr./qt*100; % Thermal Radiation Percentage

figure(1)
plot(Th,qcp)
hold on
plot(Th,qrp)

xlabel('Warm Boundary Temperature (K)','Fontsize',14, 'FontWeight',
'bold')
ylabel('Heat Flux Percentages (%)','Fontsize',14, 'FontWeight',
'bold')
legend('Solid Conduction','Thermal Radiation')
title('Percentages of Heat Transfer Modes for 8 layer MLI at -75°C
Cold Boundary Temperature','Fontsize',14)
set(gca,'FontSize',14)

figure(2)
plot(Th,qt,'lineWidth',2)
title('Experimental and Numerical Results for 8 layer MLI Blanket at -
75°C Cold Boundary Temperature','Fontsize',14)
hold on
grid on

plot(265.7,3.096/A,'r*') % Experimental Values
plot(310.9,5.957/A,'r*') % Experimental Values
plot(324.1,7.62/A,'r*') % Experimental Values
xlabel('Warm Boundary Temperature (K)','Fontsize',14, 'FontWeight',
'bold')
ylabel('Heat Flux (W/m^2)','Fontsize',14, 'FontWeight', 'bold')
set(gca,'FontSize',14)

legend('Prediction Results','Experimental Results')
```

8.9 Appendix 9 – Modified Lockheed Model for 22 layer MLI blanket at -127°C MATLAB Code

```
%% Modified Lockheed Model for 22 layer MLI blanket at -127°C with
Heat Transfer Mode Percentages%%
clc
clear all

Tc=-127+273.15; % Cold Boundary Temperature
Th= 200:1:350;
Tm=(Th+Tc)/2; % Mean Temperature

Ns=22; % Number of layer
N=49.50; % Layer density (layer/cm)
e=0.035; % Emissivity of reflector
A=0.52*0.52*2; % Blanket surface area

qc= (2.4*10^-4.*(0.017+7*10.^-6.*(800-
Tm)+0.0228.*log(Tm))*N.^2.63.*(Th-Tc))./Ns; % Conductive heat flux
qr= (6.864*10^-10.*e.*(Th.^4.67-Tc.^4.67))./Ns; % Radiative heat flux

qt=(qc+qr); % Total Heat Flux
qcp=qc./qt*100; % Solid Conduction Percentage
qrp=qr./qt*100; % Thermal Radiation Percentage

figure(1)
plot(Th,qcp)
hold on
plot(Th,qrp)

xlabel('Warm Boundary Temperature (K)','Fontsize',14, 'FontWeight',
'bold')
ylabel('Heat Flux Percentages (%)','Fontsize',14, 'FontWeight',
'bold')
legend('Solid Conduction','Thermal Radiation')
title('Percentages of Heat Transfer Modes for 22 layer MLI at -127°C
Cold Boundary Temperature','Fontsize',14)
set(gca,'FontSize',14)

figure(2)
plot(Th,qt,'lineWidth',2)
hold on
plot(265.7,3.01/A,'r*') % Experimental Values
plot(289.4,4.578/A,'r*') % Experimental Values
plot(322.2,6.80/A,'r*') % Experimental Values

grid on
xlabel('Warm Boundary Temperature (K)','Fontsize',14, 'FontWeight',
'bold')
ylabel('Heat Flux (W/m^2)','Fontsize',14, 'FontWeight', 'bold')
legend('Prediction Results','Experimental Results')
title('Experimental and Numerical Results for 22 layer MLI Blanket at
-127°C Cold Boundary Temperature','Fontsize',14)

set(gca,'FontSize',14)
```

8.10 Appendix 10 – Modified Lockheed Model for 8 layer MLI blanket at -127°C MATLAB Code

```
%% Modified Lockheed Model for 8 layer MLI blanket at -127°C with Heat
Transfer Mode Percentages%%
clc
clear all

Tc=-127+273.15; % Cold Boundary Temperature
Th= 200:1:350;
Tm=(Th+Tc)/2; % Mean Temperature

Ns=8; % Number of layer
N=35.47; % Layer density (layer/cm)
e=0.035; %Emissivity of reflector
A=0.52*0.52*2; % Blanket surface area

qc= (2.4*10^-4.*(0.017+7*10.^-6.*(800-
Tm)+0.0228.*log(Tm))*N.^2.63.*(Th-Tc))./Ns; % Conductive heat flux
qr= (6.864*10^-10.*e.*(Th.^4.67-Tc.^4.67))./Ns; % Radiative heat flux

qt=(qc+qr); % Total Heat Flux
qcp=qc./qt*100; % Solid Conduction Percentage
qrp=qr./qt*100; % Thermal Radiation Percentage

figure(1)
plot(Th,qcp)
hold on
plot(Th,qrp)

xlabel('Warm Boundary Temperature (K)','Fontsize',14, 'FontWeight',
'bold')
ylabel('Heat Flux Percentages (%)','Fontsize',14, 'FontWeight',
'bold')
legend('Solid Conduction','Thermal Radiation')
title('Percentages of Heat Transfer Modes for 8 layer MLI at -127°C
Cold Boundary Temperature','Fontsize',14)
set(gca,'FontSize',14)

figure(2)
plot(Th,qt,'lineWidth',2)
hold on

plot(254,4.599/A,'r*') % Experimental Values 8 layer
plot(281,6.024/A,'r*') % Experimental Values 8 layer
plot(303.7,8.578/A,'r*') % Experimental Values 8 layer
grid on
xlabel('Warm Boundary Temperature (K)','Fontsize',14, 'FontWeight',
'bold')
ylabel('Heat Flux (W/m^2)','Fontsize',14, 'FontWeight', 'bold')
legend('Prediction Results','Experimental Results')
title('Experimental and Numerical Results for 8 layer MLI Blanket at -
127°C Cold Boundary Temperature','Fontsize',14)

set(gca,'FontSize',14)
```

8.11 Appendix 11 – Modified Lockheed Model for 22 layer MLI blanket at-75°C MATLAB Code

```
%% Modified Lockheed Model 22 layer -75°C with Heat Transfer Mode
Percentages%%
clc
clear all

Tc=-75+273.15; % Cold Boundary Temperature
Th= 200:1:350;
Tm=(Th+Tc)/2; % Mean Temperature

Ns=22; % Number of layer
N=49.50; % layer density (layer/cm)
e=0.035; % Emissivity of reflector
A=0.52*0.52*2; % Blanket surface area

qc= (2.4*10^-4.*(0.017+7*10.^-6.*(800-
Tm)+0.0228.*log(Tm))*N.^2.63.*(Th-Tc))./Ns; % Conductive heat flux
qr= (6.864*10^-10.*e.*(Th.^4.67-Tc.^4.67))./Ns; % radiative heat flux

qt=(qc+qr); % Total Heat Flux
qcp=qc./qt*100; % Solid Conduction Percentage
qrp=qr./qt*100; % Thermal Radiation Percentage

figure(1)
plot(Th,qcp)
hold on
plot(Th,qrp)

xlabel('Warm Boundary Temperature (K)','Fontsize',14, 'FontWeight',
'bold')
ylabel('Heat Flux Percentages (%)','Fontsize',14, 'FontWeight',
'bold')
legend('Solid Conduction','Thermal Radiation')
title('Percentages of Heat Transfer Modes for 22 layer MLI at -75°C
Cold Boundary Temperature','Fontsize',14)
set(gca,'FontSize',14)

figure(2)
plot(Th,qt,'lineWidth',2)
hold on
plot(262.1,1.736/A,'r*') % Experimental Values 22 layer
plot(323.1,4.515/A,'r*') % Experimental Values 22 layer
plot(335.8,5.685/A,'r*') % Experimental Values 22 layer
grid on

xlabel('Warm Boundary Temperature (K)','Fontsize',14, 'FontWeight',
'bold')
ylabel('Heat Flux (W/m^2)','Fontsize',14, 'FontWeight', 'bold')
legend('Prediction Results','Experimental Results')
title('Experimental and Numerical Results for 22 layer MLI Blanket at
-75°C Cold Boundary Temperature','Fontsize',14)

set(gca,'FontSize',14)
```

8.12 Appendix 12 – Modified Lockheed Model 8 layer MLI blanket at -75°C MATLAB Code

```
%% Modified Lockheed Model 8 layer -75°C with Heat Transfer Mode
Percentages %%
clc
clear all

Tc=-75+273.15; % Cold Boundary Temperature
Th= 200:1:350;
Tm=(Th+Tc)/2; % Mean Temperature

Ns=8; % Number of layer
N=35.47; % Layer density (layer/cm)
e=0.035; % Emissivity of reflector
A=0.52*0.52*2; % Blanket surface area

qc= (2.4*10^-4.*(0.017+7*10.^-6.*(800-
Tm)+0.0228.*log(Tm))*N.^2.63.*(Th-Tc))./Ns; % Conductive heat flux
qr= (6.864*10^-10.*e.*(Th.^4.67-Tc.^4.67))./Ns; % Radiative heat flux

qt=(qc+qr); % Total Heat Flux
qcp=qc./qt*100; % Solid Conduction Percentage
qrp=qr./qt*100; % Thermal Radiation Percentage

figure(1)
plot(Th,qcp)
hold on
plot(Th,qrp)

xlabel('Warm Boundary Temperature (K)','Fontsize',14, 'FontWeight',
'bold')
ylabel('Heat Flux Percentages (%)','Fontsize',14, 'FontWeight',
'bold')
legend('Solid Conduction','Thermal Radiation')
title('Percentages of Heat Transfer Modes for 8 layer MLI at -75°C
Cold Boundary Temperature','Fontsize',14)
set(gca,'FontSize',14)

figure(2)
plot(Th,qt,'lineWidth',2)

hold on
plot(265.7,3.096/A,'r*') % Experimental Values
plot(310.9,5.957/A,'r*') % Experimental Values
plot(324.1,7.62/A,'r*') % Experimental Values
grid on

xlabel('Warm Boundary Temperature (K)','Fontsize',14, 'FontWeight',
'bold')
ylabel('Heat Flux (W/m^2)','Fontsize',14, 'FontWeight', 'bold')
legend('Prediction Results','Experimental Results')
title('Experimental and Numerical Results for 8 layer MLI Blanket at -
75°C Cold Boundary Temperature','Fontsize',14)

set(gca,'FontSize',14)
```